Title
AN ANALYSIS OF n+, n-, AND n| PHOTOPRODUCTION FROM THE FIRST THROUGH THE THIRD RESONANCE REGION

Authors
Moorhouse, R.G.
Oberlack, H.
Rosenfeld, A.H.

Publication Date
1973-07-01

Submitted to Physical Review D

LBL-1590
Preprint

AN ANALYSIS OF π^+, π^-, AND π^0 PHOTOPRODUCTION FROM THE FIRST THROUGH THE THIRD RESONANCE REGION

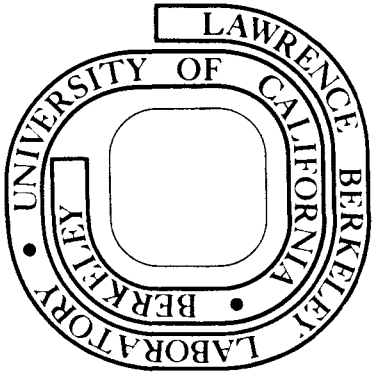

R. G. Moorhouse, H. Oberlack
and A. H. Rosenfeld

July 1973

Prepared for the U.S. Atomic Energy Commission
under Contract W-7405-ENG-48

DISCLAIMER

AN ANALYSIS OF π^+, π^-, AND π^0 PHOTOPRODUCTION FROM THE FIRST THROUGH THE THIRD RESONANCE REGION*

R. G. Moorhouse
Department of Natural Philosophy
Glasgow University, Glasgow, Scotland

and

H. Oberlack and A. H. Rosenfeld
Lawrence Berkeley Laboratory, University of California
Berkeley, California 94720

July 1973

ABSTRACT

A continuous-energy partial-wave analysis of 4148 data points on the processes $\gamma p \to \pi^+ p$, $\gamma p \to \pi^0 p$ and $\gamma n \to \pi^- p$ in the range of center-of-mass energy from 1160 to 1780 MeV, has been made. The method used is parameterization of resonances and background in the imaginary parts of the amplitudes, with the real parts being calculated from fixed-t dispersion relations, thus ensuring a proper treatment of the Born terms. It is found that the imaginary parts of the amplitudes are resonance dominated, though not resonance saturated. Many $N^*N\gamma$ couplings (of both isospin 1/2 and isospin 3/2 resonances, N^*) are determined for the first time. A comparison of the signs and magnitudes of the various resonance formation partial-wave amplitudes (depending on the product of the $N^*N\gamma$ and $N^*N\pi$ couplings) is made to the predictions of the essentially parameterless naive quark model. The critical comparison of the signs is found to be extremely favorable to that model, while there is an overall qualitative agreement in magnitude.

1. INTRODUCTION

Over the last few years pion photoproduction has been playing an increasingly important part in resonance systematics. The photon has spin 1 and isospin 0 or 1, so that it has two independent couplings to isospin 3/2 resonances ($N^*_{3/2}$) and four independent couplings to isospin 1/2 resonances ($N^*_{1/2}$); moreover, these couplings can be determined relative to the Born approximation in sign as well as magnitude. This contrasts to the determination of πN couplings from πN elastic scattering where for each of these resonances we can only determine the magnitude of one number. Thus, from photoproduction we obtain knowledge of numbers associated with each resonance which can be a test of, or a guide to, theories of elementary particle structure. None of the numbers are predicted by SU3 alone because, since γ belongs to a different SU3 multiplet than π, the process $\gamma + N \rightarrow \pi + N$ is "SU3 inelastic."[1] More particularly, SU3 together with the F/D ratio and vector dominance photon couplings (with, for example, quark model signs) only predicts the ratio of the two isospin couplings of any one isospin 1/2 resonance in any one helicity transition. Much more powerfully, a quark model will predict every number in magnitude and sign.[1-5] These predictions may be compared with the numbers obtained from a partial-wave analysis of the data.[5]

To improve our knowledge of these numbers, an experiment on pion photoproduction, by polarized photons on hydrogen and deuterium in the resonances region, is underway in the 82"-bubble chamber at SLAC, which will furnish a considerable increase in the world data of polarized events in photoproduction. As a preparation for analyzing the new world data set, which will result from this and other forthcoming experiments, and also because there have been new experimental results since the previous photoproduction[3, 6-8] analyses, we have undertaken a partial-wave analysis of existing data. The analysis includes most existing data from 250 MeV/c to 1200 MeV/c photon laboratory energy in the reactions (i) $\gamma p \rightarrow \pi^+ n$, (ii) $\gamma p \rightarrow \pi^0 p$, and (iii) $\gamma n \rightarrow \pi^- p$. The method and results are interesting enough to report in full, a short report containing our preliminary results having already been made.[5]

The difficulty with the analysis of photoproduction is that for each process (i)-(iii) there are four independent complex amplitudes at each energy and angle, giving seven independent real quantities apart from the overall phase, and thus to make an independent determination at one energy and angle we need to make at least seven experimental measuremetns--say one differential cross section and six measurements involving polarization of one or more particles. Meanwhile the experimental situation within our energy range is that the coverage of differential cross sections is barely adequate in quantity and quality, while the total number of data points on all measured polarization quantities is less than the number of differential cross-section data points.

There is a similar though less severe problem in the analysis of pion-nucleon elastic scattering where, if for simplicity we illustrate by the isospin 3/2 reaction $\pi^+ p \rightarrow \pi^+ p$, there are two independent complex amplitudes at each energy and angle giving three independent real quantities in addition to the overall phase. Experimentally, over much of the resonance region there is differential cross section and one polarization measurement. The problem of finding the scattering amplitudes is resolved firstly by including only a limited number of partial waves in the fit to the data (which among other things resolves the overall phase indeterminancy) and secondly, by making strong use of the

continuity in energy of the amplitudes.

We can make use of these same means in the analysis of pion photoproduction, but because of the relatively much worse data situation, we would not expect to be successful without further input. Fortunately such input exists, because from the pion-nucleon partial-wave analysis we already have a list of the s-channel resonances which are active in photoproduction through the processes $\gamma N \rightarrow N^* \rightarrow \pi N$ and thus, so far as these processes are concerned, the only unknowns to be determined from the photoproduction data are the $(N^* N\gamma)$ couplings. Moreover, there are indications from existing data and analyses[3,6-8] that resonances dominate the imaginary parts of the amplitudes and, to the extent that this is true, the energy variation of the imaginary parts of the partial-wave amplitudes will be largely predetermined and the analysis of pion photoproduction correspondingly simplified.

In choosing a method of analysis, there is a further important feature of the data to be considered. It is well established that the real part of the amplitudes is important–in particular, the pion exchange in charged pion photoproduction that can be expressed gauge-invariantly by the Born approximation.[3, 6]

It seemed clear to us that the combination of poor data with a knowledge of energy dependence indicated analysis by a continuous energy parameterization of the amplitudes. Also the presumed resonance dominance of the imaginary (but not the real) parts of the photoproduction amplitudes led us to parameterize the imaginary parts (in terms of resonances and background), but to calculate the real parts from these imaginary parts by fixed-t dispersion relations. The parameters are then determined by fitting the resulting complex amplitudes to experiment. A further advantage of this method is that by definition,

the fixed-t dispersion relations include the Born terms in the real parts. This neatly solves the problem of double counting of the Born terms, which may occur when real parts of background and resonances are added to the explicit Born or pion pole terms in more naive resonance or isobar models such as those of Refs. 6 and 7. Of course the fixed-t dispersion relation approach raises some problems, for example, that of the parameterization of the high-energy imaginary parts outside the range of detailed experimentation. Such points are discussed in Section 2 below.

We should briefly distinguish our method from previous uses of fixed-t dispersion relations in pion photoproduction phenomenology, which has been mainly in the first resonance region.[9, 10] One line of work[9] has been to project the fixed-t dispersion relations into multipole amplitudes, obtaining a set of coupled integral equations which can then be solved self-consistently in principle without reference to the photoproduction data except for the useful assumption of the dominance of the M_1 multipole of the p_{33} (1230) resonance. These theoretical calculations are in the large successful, but are necessarily approximate, and adjustments to the calculations are made from time to time to give better agreement with outcoming data. Alternatively, stronger assumptions on the dominant M_1 multiple of p_{33} (1230) can be made.[10] Recently, over an energy region similar to ours, Devenish, Lyth, and Rankin,[11] in a series of papers, have used imaginary parts from previously existing[3, 7, 8] partial-wave analyses in fixed-t dispersion relations and have inspected the resulting fits to data; they have examined what adjustments to these preexisting imaginary parts are necessary to fit the data better. Unlike our parameters their imaginary parts were not in a computer minimization loop.

In our approach using fixed-t dispersion relations we determine the imaginary parts, which are our only variables, by fitting to the experiments and we are enabled to do this by our extensive data range and the use of all three measured charge channels simultaneously.

2. THE INVARIANT AMPLITUDES AND THEIR PARAMETERIZATION; THE DISPERSION RELATIONS

In this section we explain in detail the K-matrix formalism for the imaginary part of the amplitudes, and the variable parameters used therein; we also formulate the construction of the imaginary part of the invariant amplitudes from the K-matrices and our use of the fixed-t dispersion relations for generating the real parts of the invariant amplitudes. We also give explicitly all other necessary parts of the formalism, such as the isospin structure, and the connection of the invariant with the helicity amplitudes.

2.1. The Expression of Invariant in Terms of Helicity Amplitudes

The T-matrix for any single pion photoproduction process such as $\gamma p \to \pi^+ n$ may be written (in the Pauli metric) as

$$T = [\tfrac{1}{2} i \gamma_5 \gamma_\mu \gamma_\nu A_1(s,t) + 2i\gamma_5 P_\mu (q - \tfrac{1}{2} k)_\nu A_2(s,t) + \gamma_5 \gamma_\mu q_\nu A_3(s,t) + \gamma_5 \gamma_\mu (2P_\nu - iM\gamma_\nu) A_4(s,t)] (\epsilon_\mu k_\nu - \epsilon_\nu k_\mu) \tag{2.1}$$

where q_μ, k_μ are the four-momenta of the pion and photon respectively, $P_\mu = \frac{1}{2}(p_{1\mu} + p_{2\mu})$ being the average of the four-momenta of the initial and final nucleon, ϵ_μ being the photon polarization, and where $A_i(s,t)(i = 1, 2, 3, 4)$ are invariant functions of the usual Mandelstam invariants s and t. The nucleon mass is M.

The transition matrix elements are obtained by sandwiching Eq. (2.1) between initial and final state spinors. For the calculation of experimental quantities it is usual and easier to work in the center-of-mass system and reduce the T-matrix to a form $\mathfrak{T}$ where

$$\bar{u}(p_2)\, T\, u(p_1) \equiv \frac{4\pi E}{M}\, \chi_f^{\dagger}\, \mathfrak{F}\, \chi_i \tag{2.2}$$

where χ_f, χ_i are the Pauli two-component spinors of the initial and final states quantized along the z axis. The factor $4\pi E/M$ is a conventional normalization, with E being the center-of-mass energy. Using projection operators to express Dirac spinors in terms of Pauli spinors one finds the standard expression

$$\mathfrak{F} = i\underset{\sim}{\sigma}\cdot\underset{\sim}{\epsilon}\, \mathfrak{F}_1 + (\underset{\sim}{\sigma}\cdot\underset{\sim}{q})\underset{\sim}{\sigma}\cdot(\underset{\sim}{k}\times\underset{\sim}{\epsilon})\, \mathfrak{F}_2 + i(\underset{\sim}{\sigma}\cdot\underset{\sim}{k})(\underset{\sim}{q}\cdot\underset{\sim}{\epsilon})\, \mathfrak{F}_3 + i(\underset{\sim}{\sigma}\cdot\underset{\sim}{q})(\underset{\sim}{q}\cdot\underset{\sim}{\epsilon})\, \mathfrak{F}_4 \tag{2.3}$$

where $\underset{\sim}{k}, \underset{\sim}{q}$ are the center-of-mass three-momenta, and $\underset{\sim}{\epsilon}$ the polarization of the photon in the radiation gauge. The normalization of the T-matrix is such that the differential cross section from an initial nucleon spinor χ_i to a final nucleon spinor χ_f is

$$\frac{d\sigma}{d\Omega} = \frac{q}{k}\, |\langle \chi_f | \mathfrak{F} | \chi_i \rangle|^2. \tag{2.4}$$

The relationship between the A_i and $\mathfrak{F}_i$ is

$$\mathfrak{F}_1 = \frac{E-M}{8\pi E}(D_1 D_2)^{\frac{1}{2}}\left[A_1 + (E-M)A_4 - \frac{k_0 q_0 - \underset{\sim}{k}\cdot\underset{\sim}{q}}{E-M}(A_3 - A_4)\right]$$

$$\mathfrak{F}_2 = \frac{E-M}{8\pi E}\left(\frac{D_2}{D_1}\right)^{\frac{1}{2}} q\left[-A_1 + (E+M)A_4 + \frac{k_0 q_0 - \underset{\sim}{k}\cdot\underset{\sim}{q}}{E+M}(A_3 - A_4)\right]$$

$$\mathfrak{F}_3 = \frac{E-M}{8\pi E}(D_1 D_2)^{\frac{1}{2}}\, q\left[(E-M)A_2 + A_3 - A_4\right]$$

$$\mathfrak{F}_4 = \frac{E-M}{8\pi E}\left(\frac{D_2}{D_1}\right)^{\frac{1}{2}} q^2\left[-(E+M)A_2 + A_3 - A_4\right]$$

and

$$D_1 = (M^2 + \underset{\sim}{k}^2)^{\frac{1}{2}} + M, \quad D_2 = (M^2 + \underset{\sim}{q}^2)^{\frac{1}{2}} + M. \tag{2.5}$$

From Eqs. (2.3) and (2.4) one can readily deduce the expressions for the experimental quantities in terms of the $\mathfrak{F}_i$ as given for example in Ref. 9. However, we prefer rather to work in terms of helicity amplitudes which are given by writing in the center-of-mass system

$$A_{\mu\lambda}(\theta,\phi) = \frac{M}{4\pi E}\,\bar{u}(p_2,\lambda_2)\, T(\lambda_\gamma)\, u(p_1,\lambda_1) \tag{2.6a}$$

$$= \chi_2^{+}(\lambda_2)\, \mathfrak{F}(\lambda_\gamma)\, \chi(\lambda_1) \tag{2.6b}$$

$$\lambda = \lambda_\gamma - \lambda_1, \qquad \mu = -\lambda_2 \tag{2.7}$$

where $u(p_i, \lambda_i)$ is a spinor representing a nucleon of four-momentum p_i, helicity λ_i, $T(\lambda_\gamma)$ is such that in Eq. (2.1) the photon has helicity λ_γ, and $\chi_i(\lambda_i)$, $\mathfrak{F}(\lambda_\gamma)$ are the corresponding quantities in the two-component spinor expression. Equation (2.7) defines the initial state helicity λ and the final state helicity μ. In Eqs. (2.6) we have conventionally omitted functional dependence on energy of the helicity amplitudes.

There are four independent helicity amplitudes; the dependence of the other four being expressed through the relationship

$$A_{-\mu,-\lambda}(\theta,\phi) = -e^{i(\lambda-\mu)(\pi-2\phi)} A_{\mu\lambda}(\theta,\phi). \tag{2.8}$$

We choose the four independent amplitudes to be those with $\lambda_\gamma = +1$ and by separating the phase factor $e^{i(\lambda-\mu)\phi}$ we define amplitudes $H_N(\theta)$, $H_{SF}(\theta)$ $H_{SA}(\theta)$, $H_D(\theta)$ (where the suffixes refer in an obvious way[12] to the helicity-flip properties of the amplitudes) through:

$$H_N(\theta) \equiv A_{1/2,\,1/2}(\theta,\phi) = \sqrt{2}\cos\tfrac{1}{2}\theta[(\mathfrak{I}_2 - \mathfrak{I}_1) + \tfrac{1}{2}(1-\cos\theta)(\mathfrak{I}_3 - \mathfrak{I}_4)] \quad (2.9a)$$

$$H_{SP}(\theta) \equiv e^{-i\phi}A_{1/2,\,3/2}(\theta,\phi) = -1/\sqrt{2}\sin\tfrac{1}{2}\theta[(1+\cos\theta)(\mathfrak{I}_3 + \mathfrak{I}_4] \quad (2.9b)$$

$$H_{SA}(\theta) \equiv e^{-i\phi}A_{-1/2,\,1/2}(\theta,\phi) = \sqrt{2}\sin\tfrac{1}{2}\theta[(\mathfrak{I}_1 + \mathfrak{I}_2) + \tfrac{1}{2}(1+\cos\theta)(\mathfrak{I}_3 + \mathfrak{I}_4)] \quad (2.9c)$$

$$H_D(\theta) \equiv e^{-2i\phi}A_{-1/2,\,3/2}(\theta,\phi) = 1/\sqrt{2}\cos\tfrac{1}{2}\theta[(1-\cos\theta)(\mathfrak{I}_3 - \mathfrak{I}_4)]. \quad (2.9d)$$

Experimental quantities can be expressed in terms of the H_N, H_{SP}, H_{SA}, H_D as described and given in Appendix A. For example the differential cross section is

$$\frac{d\sigma}{d\Omega} = \frac{1}{2}\frac{q}{k}\left(|H_N|^2 + |H_D|^2 + |H_{SP}|^2 + |H_{SA}|^2\right) \quad (2.10)$$

2.2. The Expression of Helicity Amplitudes in Terms of Partial-Wave Amplitudes

The helicity amplitudes have the expansion

$$A_{\mu\lambda}(\theta,\phi) = \sum_j A^j_{\mu\lambda}(2j+1)\,d^j_{\lambda\mu}(\theta)\,e^{i(\lambda-\mu)\phi} \quad (2.11)$$

where $A^j_{\mu\lambda}$ comprise four independent amplitudes of total angular momentum j, which can be combined into four independent partial-wave amplitudes (proportional to $A^j_{\mu\lambda} \pm A^j_{-\mu\lambda}$) of good parity and total angular momentum j. For these latter we employ the normalization and notation as used by Walker.[7] The notation $A_{\ell+}$, $B_{\ell+}$ is used for partial waves with $j = \ell + 1/2$ and parity $(-1)^\ell$ and $A_{(\ell+1)-}$, $B_{(\ell+1)-}$ for $j = \ell + 1/2$ and parity $(-1)^{\ell+1}$. Thus the integer suffix ℓ or $\ell+1$ is the orbital angular momentum of the πN system. The amplitudes A, B have initial total photon-nucleon helicity [λ in (2.11)] of 1/2 and 3/2 respectively. Equation (2.11) can be rewritten in terms of the amplitudes H_N, H_{SP}, H_{SA}, H_D defined by Eq. (2.9) on the left-hand side, and the amplitudes A, B

instead of the amplitudes $A^j_{\mu\lambda}$ on the right-hand side:

$$\begin{aligned}
H_N(\theta) &= \sqrt{2}\cos\tfrac{1}{2}\theta\sum_{\ell=0}^{\infty}(A_{\ell+} - A_{(\ell+1)-})(P'_\ell - P'_{\ell+1}) \\
H_{SP}(\theta) &= \frac{1}{\sqrt{2}}\sin\tfrac{1}{2}\theta(1+\cos\theta)\sum_{\ell=1}^{\infty}(B_{\ell+} - B_{(\ell+1)-})(P''_\ell - P''_{\ell+1}) \\
H_{SA}(\theta) &= \sqrt{2}\sin\tfrac{1}{2}\theta\sum_{\ell=0}^{\infty}(A_{\ell+} + A_{(\ell+1)-})(P'_\ell + P'_{\ell+1}) \\
H_D(\theta) &= \frac{1}{\sqrt{2}}\cos\tfrac{1}{2}\theta(1-\cos\theta)\sum_{\ell=1}^{\infty}(B_{\ell+} + B_{(\ell+1)-})(P''_\ell + P''_{\ell+1})
\end{aligned} \quad (2.12)$$

2.3. Charge and Isospin Amplitudes

The formalism of sections 2.1 and 2.2 applies to amplitudes for any of the processes $\gamma p \to \pi^+ n$, $\gamma n \to \pi^- p$, $\gamma p \to \pi^0 p$. For none of these amplitudes is isospin a good quantum number, but the πN interaction conserves isospin, and πN resonances are in states of definite isospin. Consequently it is necessary to distinguish the isospin properties of the amplitudes. If we consider the amplitude A_i as referring to the emission of a pion of isospin index α, then

$$A_i = A_i^{(+)}\delta_{\alpha 3} + A_i^{(-)}\tfrac{1}{2}[\tau_\alpha, \tau_3] + A_i^{(0)}\tau_\alpha. \quad (2.13)$$

Equation (2.13) only assumes that the photon interaction with hadrons occurs through isoscalar and isovector parts, so that $A^{(0)}$ is an isoscalar amplitude and $A^{(+)}$, $A^{(-)}$ are isovector amplitudes. By taking pion-nucleon final states of definite isospin we find that the combinations $A_i^{(+)} + 2A_i^{(-)}$, $A_i^{(+)} + A_i^{(-)}$ lead to isospins in the final state of 1/2, 3/2 respectively and we define

$$A^S = -(3)^{\frac{1}{2}} A^{(0)} \qquad \text{(isoscalar amplitude)}$$

$$A^{V1} = (1/3)^{\frac{1}{2}} (A_i^{(+)} + 2A_i^{(-)}) \qquad \text{(isovector amplitude leading to isospin 1/2 in } \pi N) \qquad (2.14)$$

$$A^{V3} = (2/3)^{\frac{1}{2}} (A_i^{(+)} - A_i^{(-)}) \qquad \text{(isovector amplitude leading to isospin 3/2 in } \pi N).$$

The expressions for the transitions $\gamma p \to \pi^+ n$, $\gamma n \to \pi^- p$, $\gamma p \to \pi^0 p$ and $\gamma n \to \pi^0 n$ in terms of the isoscalar and isovector amplitudes Eq. (2.14) are from Eq. (2.13):

$$A_{i+} \equiv \langle \pi^+ n | A_i | \gamma p \rangle = -(1/3)^{\frac{1}{2}} A^{V3} + (2/3)^{\frac{1}{2}} (A^{V1} - A^S)$$

$$A_{i0} \equiv \langle \pi^0 p | A_i | \gamma p \rangle = (2/3)^{\frac{1}{2}} A^{V3} + (1/3)^{\frac{1}{2}} (A^{V1} - A^S)$$

$$A_{i-} \equiv \langle \pi^- p | A_i | \gamma n \rangle = (1/3)^{\frac{1}{2}} A^{V3} - (2/3)^{\frac{1}{2}} (A^{V1} + A^S)$$

$$A_{in0} \equiv \langle \pi^0 n | A_i | \gamma n \rangle = (2/3)^{\frac{1}{2}} A^{V3} + (1/3)^{\frac{1}{2}} (A^{V1} + A^S). \qquad (2.15)$$

Exactly corresponding linear relations to Eq. (2.15) hold between helicity amplitudes and partial-wave amplitudes with corresponding isospin properties, and in what follows we will use the indices of the left- or right-hand sides of Eq. (2.15) for any amplitudes without further explanation. (We have no further use for the amplitudes $A_i^{(+)}$, $A_i^{(-)}$ and $A_i^{(0)}$ of Eq. (2.13), so no confusion will arise).

2.4. The Parameterization of the Partial-Wave Amplitudes

Having formulated isospin we can proceed with our constructive approach and explain the parameterization of the imaginary parts of

$$A^{V3}_{\ell\pm},\ B^{V3}_{\ell\pm},\ A^{V1}_{\ell\pm},\ B^{V1}_{\ell\pm},\ A^{S}_{\ell\pm},\ B^{S}_{\ell\pm} \qquad (2.16)$$

for insertion into Eq. (2.12). Any of Eq. (2.16) can be regarded as a partial T-matrix (which we shall just denote by T without any indices

where no confusion can arise), which may be constructed from a K-matrix by the formula

$$T^{-1} = K^{-1} - iq \qquad (2.17)$$

where q denotes the diagonal matrix of center-of-mass momenta. In principle T and K are of dimensions to include all the open channels, but that is impracticable and a suitable approximation is to take three channels, two being strong interaction channels and one being a γN channel. Of the strong interaction channels, one is the πN channel, and the other is a pseudochannel representing all the other energetically possible strong interaction states; we will call this pseudochannel the inelastic channel. By the nature of our amplitudes (2.16) both the πN and the inelastic channel correspond to eigenstates of isospin.

Our notation is

πN : channel 1

inelastic: channel 2

γN : channel 3

and we write the K-matrix as a sum of factorizable poles

$$K_{ij}(E) = \sum_{r=1}^{R} \xi_r \frac{\gamma_i^{(r)} \gamma_j^{(r)}}{E_r - E}, \qquad (i, j = 1, 2, 3). \qquad (2.18)$$

In Eq. (2.18), E is the center-of-mass energy and E_r is a parameter which may take on any value and the corresponding pole in (2.18) would only necessarily be a resonance if it lay in or near the physical region where we analyze the data. In particular, the poles such that E_r is in the unphysical left-hand region of the E-plane do not correspond to resonances and are a representation of the singularities in that region. $\xi_r = \pm 1$ for poles in the left-hand region, while $\xi_r = +1$ for poles in the

physical region, from causality. For an isolated resonance pole $(\gamma_i^{(r)})^2$ is proportional to the partial width for decay into channel i.

There are motivations for the use of factorization in Eq. (2.18). Firstly, the factorizable form is economical in parameter. Secondly, it ensures that the zeros of the T-matrix denominator derived through Eq. (2.17), are given by an equation of order R in E where R is the number of poles. Without factorization of the K-matrix, the order in E is greater than R, thus giving extra poles in the T-matrix.[13]

Our partial waves contain barrier factors as follows:

$$\gamma_i^{(r)} = \gamma_i^{(r)'} \frac{B_i(E)}{B_i(E_p)} \quad , \qquad E < E_p \tag{2.19a}$$

$$\gamma_i^{(r)} = \gamma_i^{(r)'} \quad , \qquad E > E_p, \tag{2.19b}$$

where $\gamma_i^{(r)'}$ are constants and E_p is the position of the lowest energy resonance pole in the sum (2.18).

$$B_i(E) = (q_i r)^{\ell}/[D_{\ell_i}(q_i r)]^{\frac{1}{2}} \tag{2.20}$$

where q_i is the c.m. momentum in channel i, and ℓ_i the orbital angular momentum in channel i, r is a parameter in the range 0.5 to 1.5 fe and may be different for different partial waves. $D_\ell(qr)$ is the Blatt-Weisskopf denominator factor[14] so that, e.g., $D_0(x) = 1$, $D_1(x) = 1 + x^2$, $D_2(x) = 9 + 3x^2 + x^4$.

There is a problem in the definition of ℓ_3, the orbital angular momentum of the γN system since our partial waves are not eigenstates of the total γN orbital angular momentum. $A_{\ell+}$, $B_{\ell+}$ both involve photon orbital angular momenta, $\ell_\gamma = \ell$ and $\ell+2$, while $A_{\ell-}$, $B_{\ell-}$ both involve photon orbital angular momenta, $\ell_\gamma = \ell$ and $\ell-2$ (with the

obvious exception of $\ell = 1$). We have always taken the lowest possible value for ℓ_3:

$$\begin{aligned} &(\ell_\gamma = \ell, \ell+2) \quad A_{\ell+}, B_{\ell+} \quad : \quad \ell_3 = \ell \\ &(\ell_\gamma = \ell, \ell-2) \quad A_{\ell-}, B_{\ell-} \quad : \quad \ell_3 = \ell-2 \\ &(\ell_\gamma = 1) \qquad A_{1-} \qquad : \quad \ell_3 = 1 . \end{aligned} \tag{2.21}$$

In connection with a possible inadequacy of this choice we may note: (i) at center-of-mass energy 1403 MeV, k is already 0.58 GeV/c compared to k = 1.08 GeV/c at the third resonance energy of 1705 MeV so that for those partial waves, namely $d_{3/2}$ and upward, which are only important above 1400 MeV, the choice of ℓ_3 is not critical; (ii) the value of ℓ_3 is exact for the $p_{1/2}$ wave (A_{1-}) and for the dominant M1 multipole of the $p_{3/2}$ wave. This leaves just the lower energy $s_{1/2}$ wave and the (small) E2 part of the $p_{3/2}$ wave as possibly being critically affected by the choice of ℓ_3 in the part of our energy range from 1160 to about 1240 MeV center-of-mass energy. We see from Eq. (2.21) that our prescription for $s_{1/2}$ waves is $\ell_3 = 0$, but in our preliminary work[5] (Table Va below) we had chosen $\ell_3 = 1$; we obtained a significant improvement in the fit to the lowest energy region in changing to $\ell_3 = 0$.

We return now to the consideration of the form (2.18) of the K-matrix where we see that the $\gamma_3^{(r)'}$ s, which when (r) corresponds to a resonance state is an $N\gamma$ partial width, are the only parameters pertaining peculiarly to the $N\gamma$ system. We determine the $\gamma_1^{(r)}$, $\gamma_2^{(r)}$, E_r and ξ_r by fitting the pion-nucleon elastic scattering partial waves (in the energy range where we will use the photoproduction data) using the purely hadronic part of the K-matrix (2.18).[15] This fit determines the N^* resonances and background terms which appear in our parameteri-

zation (2.18). The variable parameters to be determined by a fit to the photoproduction experiments are the $\gamma_3^{(r)'}$.

We must now construct the proper charge amplitudes, using the isospin properties. As shown in section 2.3, there are three independent amplitudes (2.14) and so correspondingly there are three types of photon couplings $\gamma_3^{(r)}$, which we denote $\gamma_{V3}^{(r)}$, $\gamma_{V1}^{(r)}$, $\gamma_S^{(r)}$:

$$\gamma_3^{(r)} \rightarrow \gamma_{V3}^{(r)}, \gamma_{V1}^{(r)}, \gamma_S^{(r)}. \tag{2.22}$$

For the isovector photon coupling to isospin 3/2 resonances, $\gamma_{V3}^{(r)}$, (r) must be an isospin 3/2 resonance (or background term) while for the isovector and isoscalar photon couplings to isospin 1/2 resonances, $\gamma_{V1}^{(r)}$ and $\gamma_S^{(r)}$, (r) must be an isospin 1/2 resonance (or background term).

Consequently for a given J^P and total γN helicity, λ (1/2 or 3/2) we define three different K-matrices:

$$K_{ij}^{V3} = \sum_{r(I=3/2)} \frac{\gamma_i^{(r)}\gamma_j^{(r)}}{E_r - E}, \qquad \gamma_3^{(r)} = \gamma_{V3}^{(r)} \tag{2.23a}$$

$$K_{ij}^{V1} = \sum_{r(I=1/2)} \frac{\gamma_i^{(r)}\gamma_j^{(r)}}{E_r - E}, \qquad \gamma_3^{(r)} = \gamma_{V1}^{(r)} \tag{2.23b}$$

$$K_{ij}^{S} = \sum_{r(I=1/2} \frac{\gamma_i^{(r)}\gamma_j^{(r)}}{E_r - E}, \qquad \gamma_3^{(r)} = \gamma_S^{(r)} \tag{2.23c}$$

which, through the relation $T^{-1} = K^{-1} - iq$ construct the corresponding T-matrices:

$$T_{ij}^{V3}, \quad T_{ij}^{V1}, \quad T_{ij}^{S}. \tag{2.24}$$

We only require the T_{13} elements of these matrices, and using Eq. (2.15) we can form the photoproduction T-matrix elements, for a given J^P and total γN helicity λ for $\gamma p \rightarrow \pi^+ n$, $\gamma p \rightarrow \pi^0 p$, $\gamma n \rightarrow \pi^- p$.

$$\gamma p \rightarrow \pi^+ n: \quad T_{13}^{+} = -(1/3)^{\frac{1}{2}} T_{13}^{V3} + (2/3)^{\frac{1}{2}} (T_{13}^{V1} - T_{13}^{S}) \tag{2.25a}$$

$$\gamma p \rightarrow \pi^0 p: \quad T_{13}^{0} = (2/3)^{\frac{1}{2}} T_{13}^{V3} + (1/3)^{\frac{1}{2}} (T_{13}^{V1} - T_{13}^{S}) \tag{2.25b}$$

$$\gamma n \rightarrow \pi^- p: \quad T_{13}^{-} = (1/3)^{\frac{1}{2}} T_{13}^{V3} - (2/3)^{\frac{1}{2}} (T_{13}^{V1} - T_{13}^{S}). \tag{2.25c}$$

Since we are working to first order in the electromagnetic coupling constant, T^{V3} is a linear function of $\gamma_{V3}^{(r)}$ and T^{V1}, T^S are linear functions of $\gamma_{V1}^{(r)}$, $\gamma_S^{(r)}$ with the same coefficient for a given (r). Consequently, instead of $\gamma_{V3}^{(r)}$, $\gamma_{V1}^{(r)}$, $\gamma_S^{(r)}$ we can define the couplings

$$\begin{aligned} \gamma^{V3(r)} &\equiv \gamma_{V3}^{(r)} && \text{(isospin of r = 3/2)} \\ \gamma^{P(r)} &\equiv (2/3)^{\frac{1}{2}} (\gamma_{V1}^{(r)} - \gamma_S^{(r)}) && \text{(isospin of r = 1/2)} \\ \gamma^{N(r)} &\equiv -(2/3)^{\frac{1}{2}} (\gamma_{V1}^{(r)} + \gamma_S^{(r)}) && \text{(isospin of r = 1/2)} \end{aligned} \tag{2.26}$$

the last two being couplings of positive and neutral isospin 1/2 states respectively. It is more meaningful to use these couplings, which are more directly connected with experimental processes, and so lead to fewer questions of error correlation.

2.5. The Fixed-t Dispersion Relations and the Real Parts of the Amplitudes

Having constructed the imaginary parts of the amplitudes in terms of (fixed) parameters determined from pion-nucleon elastic scattering and variable γN-couplings, we can proceed to construct the real parts of the amplitudes using the fixed-t dispersion relations for the

invariant amplitudes. These can be written, for the amplitudes A_{i+}, A_{i-}, A_{i0} (corresponding to $\gamma p \to \pi^+ n$, $\gamma n \to \pi^- p$, and $\gamma p \to \pi^0 p$ respectively) as

$$\text{Re } A_{i\pm,0}(s,t) = B_{i\pm,0}(s,t) + \int_{(M+m)^2}^{\infty} ds' \left(\frac{\text{Im } A_{i\pm,0}(s',t)}{s'-s} + \xi_i \frac{\text{Im } A_{i\mp,0}(s',t)}{s'-u}\right) \tag{2.27}$$

where the Born terms are given by:

$$B_{1+}(s,t) = \sqrt{2}\, G\, S, \quad B_{2+}(s,t) = -\sqrt{2}\, G\, S\, T,$$

$$B_{3+}(s,t) = -\frac{\sqrt{2}\, G}{2M}(\mu_P' S - \mu_N' U), \quad B_{4+}(s,t) = -\frac{\sqrt{2}\, G}{2M}(\mu_P' S + \mu_N' U)$$

$$B_{i-}(s,t) = \xi_i B_{i+}(u,t) \qquad (i = 1, 2, 3, 4) \tag{2.28}$$

$$B_{10}(s,t) = \frac{1}{2} G (S+U), \quad B_{20}(s,t) = -\frac{1}{2} G(S+U)T$$

$$B_{30}(s,t) = -\frac{1}{2} G \frac{\mu_P' - \mu_N'}{2M}(S-U), \quad B_{40}(s,t) = -\frac{1}{2} G \frac{\mu_P' + \mu_N'}{2M}(S+U).$$

Where $G = ge/4\pi$, $S = 1/(s-M^2)$, $U = 1/(u-M^2)$, $T = 1/(t-m^2)$ and μ_P', μ_N' are the proton and neutron anomalous magnetic moments respectively. We take $g^2/4\pi = 14.7$, $e^2/4\pi = 1/137$, $\mu_P' = 1.793$, $\mu_N' = -1.913$. In Eqs.(2.27) and (2.28) $\xi_i = +1$ if $i = 1, 2, 4$, and $\xi_i = -1$ if $i = 3$.

For practical application we divide the range of integration in Eq. (2.27) into two parts so that

$$\text{Re } A_{i\pm,0}(s,t) = B_{i\pm,0}(s,t) + \int_{(M+m)^2}^{\Lambda^2} ds' \left(\frac{\text{Im } A_{i\pm,0}(s',t)}{s'-s} + \xi_i \frac{\text{Im } A_{i\mp,0}(s',t)}{s'-u}\right)$$

$$+ \int_{\Lambda^2}^{\infty} ds' \left(\frac{\text{Im } A_{i\pm,0}(s',t)}{s'-s} + \xi_i \frac{\text{Im } A_{i\mp,0}(s',t)}{s'-u}\right) \tag{2.29}$$

where $E = \Lambda$ is the upper limit of the energy range in which we are fitting the photoproduction data (or slightly greater than that upper limit)

so that in the first integrand of Eq. (2.29) we already have a parameterized form of $\text{Im } A_{i\pm,0}(s',t)$ through the following steps:

(i) According to section 2.4, construct the imaginary parts of the T-matrix elements $\text{Im } T_{13}^+$, $\text{Im } T_{13}^0$ and $\text{Im } T_{13}^-$ corresponding respectively to the processes $\gamma p \to \pi^+ n$, $\gamma p \to \pi^0 p$ and $\gamma n \to \pi^- p$. There is a T-matrix element for each J^P and photon-nucleon helicity $\lambda (= 1/2, 3/2)$ and each element is a linear function of the photon couplings-three for each J^P, λ, and r, namely $\gamma_{V3}^{(r)}$, $\gamma_{V1}^{(r)}$, $\gamma_S^{(r)}$

(ii) To construct for example the invariant amplitudes $\text{Im } A_{i+}(s,t)$ we make the following substitution in Eq. (2.12)

$$A_{\ell+} = \text{Im } T_{13}^+ (J = \ell + 1/2,\ P = (-1)^\ell,\ \lambda = 1/2)$$

$$A_{(\ell+1)-} = \text{Im } T_{13}^+ (J = \ell + 1/2,\ P = (-1)^{\ell+1},\ \lambda = 1/2)$$

$$B_{\ell+} = \text{Im } T_{13}^+ (J = \ell + 1/2,\ P = (-1)^\ell,\ \lambda = 3/2)$$

$$B_{(\ell+1)-} = \text{Im } T_{13}^+ (J = \ell + 1/2,\ P = (-1)^{\ell+1},\ \lambda = 3/2)$$

to find $H_{\text{flip}}(\theta)$ (flip = N, D, SP, SA). By inverting Eqs. (2.5) and (2.9) we readily construct the required $\text{Im } A_{i+}(s,t)$ $(i = 1, 2, 3, 4)$. Similarly for A_{i-} and A_{i0}.

Two points of fundamental difficulty arise:

We have formed $\text{Im } A_{i\pm,0}(s',t)$ for $(M+m)^2 < s' < \Lambda^2$, in terms of our parameters, as the sum of a partial-wave series, cut off at some upper limit of angular momentum. However, the convergence of the partial-wave series is not proved except for certain processes within certain regions (the Lehman ellipse of convergence in the $\cos\theta$ plane). Nevertheless, convergence can hold outside this region and it is possible that a cut-off series provides a good approximation in a considerably extended region. Devenish, Lyth, and Rankin[11] have argued on

the basis of the Mandelstam double-spectral representation that the cut-off series for $\mathrm{Im}A_i(s,t)$ is good for $-t \leq 1.0\,(\mathrm{GeV/c})^2$ in $\pi^\pm$ photoproduction and $-t \lesssim 1.5\,(\mathrm{GeV/c})^2$ in π^0 photoproduction.

The troublesome region is that of larger $|\cos\theta|$, that is small s and large t. The most likely source of trouble at smaller s is in the $p_{33}(1230)$ resonance region, since the p_{33} makes a big contribution to $\mathrm{Im}A_i$ linearly proportional to $(\cos\theta)$. To take account of possible nonconvergence we have added to the partial wave series a term nonzero only for $|t| > 0.8$. The form adopted is given by

$$\mathrm{Im}\,A_{i\pm,0}(s,t) = (\text{partial-wave series}) + C_{i\pm,0}\,\theta(t-t_0)(t-t_0)\,\delta(s-s_\Delta) \qquad (2.30)$$

where $C_{I\pm,0}$ are 12 parameters to be determined by the fit to experiment, $t_0 = -0.8$ and $s_\Delta = (1.23)^2$. The extra term in Eq. (2.30) is only nonzero in the unphysical region so that its only contribution in the physical region is to the real part via the integral (2.29). Consequently the use of a δ-function in s rather than a Breit-Wigner or other more spreadout form is not greatly significant. The form (2.30) is not general enough to correct for all possible difficulties, this is not possible without introducing too many parameters to be meaningful.

The other point of fundamental difficulty is that the second, high-energy integral of Eq. (2.29) contains parameters referring to the amplitude outside the data region. Obviously, without direct data restriction on the high-energy imaginary part we cannot hope to determine these, in principle infinitely many, parameters. The problem is to find an adequate parameterization involving a minimum number of parameters; the smaller the contribution to $\mathrm{Re}A_i$ from the high-energy integral in Eq. (2.29), the more satisfactory is the fixed-t dispersion relation analysis. We did not adopt in the present work a

Regge parameterization for large s, $\mathrm{Im}A_i(s,t) \propto s^{\alpha_i(t)-1}$ where $\alpha_i(t)$ might a priori be taken as the ρ-ω-A_2 trajectory, partly because the high-energy data suggest $\alpha_{\mathrm{eff}} \approx 0$ for $0 < -t < 1.5\,(\mathrm{GeV/c})^2$. However, recent work[16] with fixed-t dispersion relations at high energy seems able to resolve this seeming contradiction by successfully using the ρ-ω-A_2 trajectory (though it may well leave some fundamental questions about the significance of α_{eff} unanswered) and it may be that future low-energy analyses will be done with a ρ-ω-A_2 Regge parameterization for large s.

In the present work we have dealt with the problem rather arbitrarily by representing $\mathrm{Im}A_{i\pm0}(s,t)$ for $s > \Lambda^2$ as a sum over a few pseudoresonances, and we do not give physical significane to the values of the parameters of these pseudoresonances, but regard them as parameterizing the whole contribution to the high-energy integral. An exception to this nonsignificance is the $f_{37}(1950)$ which gives a large enough contribution to the real part, through the dispersion integral, in the upper end of our data region that the δ-function parameters D of Eq. (2.31) below can be regarded as estimating the couplings of this resonance. To a lesser extent we will also consider giving weight to the corresponding $f_{35}(1890)$ parameters. The general form of our parameterization is to add to the imaginary parts of the partial-wave amplitudes of Eq. (2.12) for each charge state a contribution given by

$$\mathrm{Im}\,A_{l\pm} = D_{l\pm}^{\lambda=1/2}\,\delta(s-s_{l\pm}^{1/2})$$

$$\mathrm{Im}\,B_{l\pm} = D_{l\pm}^{\lambda\,3/2}\,\delta(s-s_{l\pm}^{3/2}) \qquad (2.31)$$

where $s_{l\pm}^{\lambda} > \Lambda^2$ and $D_{l\pm}^{\lambda}$ are constants. In practice we do not use more than 8 parameters D in parameterizing the high-energy

imaginary part.

This completes the construction of $\mathrm{Re}\,A_{i\pm,0}(s,t)$ (and incidentally of $\mathrm{Im}\,A_{i\pm,0}(s,t)$), using Eq. (2.29). The variable parameters used are the photon couplings and the C and D parameters of Eqs. (2.30) and (2.31). Using Eqs. (2.5) and (2.9) we then find the experimental quantities of Appendix A as a function of our parameters, and vary the parameters to find the best least-squares fit to experiment. Our "theoretical" expression also contains parameters such as the resonance or background energies E_r found from a fit to pion-nucleon elastic scattering data. We will hold ourselves free to vary such parameters (by a small percentage) in our fitting procedure.

3. DATA USED

We have based our data collection on the compilation by Spillantini and Valente.[17] Amendments and experiment points not yet contained in that compilation have been added. In an effort to select data which are in fair agreement with each other, we have excluded some experimental data which were included in previous analyses. We have not used any data points which are quoted in the form of graphs only. The data references list[18] contains the selected data which were used for this analysis, together with the energy range for which the data were selected. A total of 4148 data points was used in the analysis.

Some special treatment has been given to the data in the course of the fitting process:

a) The data on differential cross section are so abundant that they tend to outweigh the information on asymmetries and polarizations. To increase the weight of the asymmetry and polarization data, their errors have been artificially decreased by a factor of 2.5.

b) If experimental data are given in the literature only with their statistical errors systematic errors as quoted by the authors or as estimated by us have been added quadratically.

c) In some cases results are quoted up to an overall uncertainty in absolute magnitude. In these cases the data have been varied within the quoted range.

4. TECHNIQUE AND PHYSICS OF DATA FITTING

In this section we shall deal with some details and technicalities of the fitting procedure and some questions concerning the uniqueness of the fits achieved.

4.1. Program Technique and Physical Assumptions

The aim of this analysis is to measure the $(N^*N\gamma)$ couplings and not to hunt for resonances. We therefore have to impose a reasonable set of πN parameters, i.e. poles and couplings to channels 1 and 2 in the K-matrix formalism described in section 2. A precursor analysis of 2 channels (πN and the pseudochannel containing all other hadronic final states) was undertaken[15] using elastic phase-shift data from various analyses[19] in the energy range between threshold and 2100 MeV as restricting data. Variables in such fits were the pole energies, the couplings γ_1 and γ_2 in the πN and pseudochannel, and the masses representing the pseudo two-body final state. Such masses were restricted to lie between the masses of the nucleon and the p_{33} (1236) for the final baryon and between the masses of the pion and the ρ meson for the final meson. Within bounds the interaction radius was treated as a free parameter for each partial wave. The K-matrix parameters, as obtained as an average of such analyses and as imposed as starting

values on the pion-photoproduction analysis, are listed in Table I. These parameters were treated as constants for most of the γN-analysis and were varied within bounds of a few percent only after all photon couplings of any importance had been varied.

The minimization of the χ^2 function (as defined in section 2) was done under control of the minimizer VAO4A[20]—very efficient in using conjugate direction techniques without the need for calculating derivatives with respect to variable parameters.

Our variables X appearing in VAO4A are not directly physical parameters like $P = \gamma_3$'s, but are related to these through

$$P = A + B \frac{X}{1+|X|} .$$

We thus have a control over the range in which parameter P can vary, namely $P \in [A-B/2, A + B/2]$.

Each χ^2 evaluation involves the calculation of the helicity amplitudes for all 4148 data points, therefore efficient organization of the calculations is advisable. Figure 1 illustrates the approach taken here. The imaginary parts of the helicity amplitudes $\tilde{H}$ (defined in Appendix A) are calculated at each grid point spanned in the plane of energy and t, by a total of 55 energy points and 9 t-dispersion integral points. They lead to the integration points in the fixed-t dispersion relations and thus form the basis for the real parts of $\tilde{H}$. These real parts do not contain the Born terms yet and since the partial waves employed in this analysis are restricted to $F_{7/2}$ waves, the angular dependence at a fixed energy can be at most of order $\cos^3\theta$ in Im $\tilde{H}$ and terms of higher order in Re $\tilde{H}$ are small corrections. In addition, the strongest energy variations are governed by narrow resonance structures like the s_{11} (1540) with a width of ~60 MeV in our parameterization.

The energy spacing is chosen as 20 MeV in laboratory photon energy (~10 MeV in total c.m. energy). To evaluate $\tilde{H}$ at the energy and angle of an experimental point we are thus lead to a simultaneous interpolation which is quadratic both in energy and t. We then add in the Born terms which are precalculated at the exact energy and angle of the experimental point and apply the missing angular factors to arrive at the full helicity amplitudes H. Isospins have been combined such that we are left with helicity amplitudes appropriate for π^+n, π^0p and π^-p final states.

To ensure the right phases and the appropriate low-energy behavior, we add two additional contributions to χ^2. Firstly, we calculate the phases of the $s_{1/2}$, $p_{1/2}$, and $p_{3/2}$ waves in three isospin combinations and compare those with phases which are derived from elastic πN-scattering.[21] Secondly, the low-energy behavior of the real parts of s and p waves is compared to the corresponding real parts from other low-energy analyses.[22] Both contributions are calculated at four energies, the highest being E_{lab} = 450 MeV. These phases and real parts as well as the errors adopted here are listed in Table II.

4.2. Data Fitting and Physical Assumptions

So far we have described our model, based on reasonable general physical assumptions, in sections 1 and 2, and 4.1, and have described its implementation in a program in the immediately preceding section 4.1. In using the program we are faced with the problem of how many and which photon coupling parameters, γ_3 (and other parameters) to vary to obtain a fit to the data. "All simultaneously" is not a good answer because the great extent of the parameter space leads to well-known fundamental difficulties as well as more mundane difficulties of

computer-time limitation.

Rather we choose to vary a first-batch of parameters and make a partial χ^2 minimization, then to vary both a second batch of parameters and the first-batch and make a partial χ^2 minimization, then to vary both a third batch and the second and first batches, and so on until the varying of further parameters leads to negligible further fall in χ^2. Obviously the choice of batches and their order can have a large influence on the speed of the minimization and possibly also on the final χ^2 and final values of the parameters as discussed below. The choice of the first batch is particularly important and we are fortunate in having some definite knowledge to guide us.

In the choice of the first batch of variable parameters we use the following facts:

(i) the p_{33} (1230) is important in photoproduction right up to 600 MeV in photon laboratory energy, and its photon couplings are known to at least 20% accuracy.

(ii) the d_{13} (1520) and f_{15} (1690) are important resonances in their energy regions (particularly in their helicity 3/2 couplings).

We, therefore, always use as our first batch of variable parameters, the photon couplings of p_{33} (1230), d_{13} (1520) and f_{15} (1690) and, moreover, we always limit the p_{33} (1230) couplings to lie within ~20% of their "known" values. Having made a partial minimization, we then vary them along with further batches. The different choices of further batches generate our various good or bad fits to the data. In the first variation of a new batch we notice whether or not there is a considerable overall decrease in χ^2 or a strong local effect. The number of variations possible in relative order of introduction of parameters is so large that we certainly may have missed different good fits to the data.

Nevertheless it should be noted that first variation of certain parameters, for instance these of the d_{33} (1635) + s_{31} (1620) and the D parameters of section 2.5, always leads to a huge decrease in χ^2 while the first variation of other parameters, for instance the C parameters of section 2.5, never makes any significant difference. We sometimes find that branches end up at the same χ^2, and nearly the same final parameter values, when they correspond to equivalent parameters which have been added in different orders.

5. RESULTS

Having gone through these obviously very subjective ways of obtaining fits to the data, we ended up with a total of 11 basically different fits out of which 3 (set B) are eminently better than the remaining 8 (set A) as judged by the overall χ^2/data point of ~3.5 as opposed to 5.0 - 9.0. We therefore report in this section on these 3 fits (set B) as our best results, and comment in section 6 below on the significance to be given to set A.

Tables III (a)-(c) display the fixed and fitted parameters of those three accepted fits which will henceforth be identified as I, II, and III. The number of free parameters of type γ_3, C, and D are 56, 68, and 74 respectively—one of the major differences being that no parameters of type C are excited for fit I, thus accounting for 12 parameters less.

We next point to some of the features of ($N^*N\gamma$) resonance couplings which turn out to be common between the three fits. ($N^*N\gamma$) resonance couplings correspond to total γ-nucleon helicity, λ, where

$$\lambda = 1/2,\ 3/2.$$

Also, according to section 2.4 [for example Eq. (2.26)] we express the $N^*N\gamma$ couplings of isospin 3/2 resonances as γ'^{V3}_{λ} and the two independent

($N^*N\gamma$) charge state couplings of isospin 1/2 resonances as $\gamma_\lambda'^{P}$ (corresponding to $N^{*+} \to \gamma p$) and $\gamma_\lambda'^{N}$ (corresponding to $N^{*0} \to \gamma n$). As explained in section 2.4, the primes on the couplings denote that these are reduced widths, without kinematical energy dependence.

The following couplings are in agreement between the 3 fits of set B to better than 15%:

$s_{31}(1620)$: $\gamma_{1/2}'^{V3}$; $p_{33}(1230)$: $\gamma_{1/2}'^{V3}$, $\gamma_{3/2}'^{V3}$; $s_{11}(1545)$: $\gamma_{1/2}'^{P}$;

$s_{11}(1700)$: $\gamma_{1/2}'^{P}$; $p_{11}(1470)$: $\gamma_{1/2}'^{P}$; $d_{13}(1520)$: $\gamma_{3/2}'^{P}$, $\gamma_{1/2}'^{N}$,

$\gamma_{3/2}'^{N}$; $d_{15}(1670)$: $\gamma_{3/2}'^{N}$; $f_{15}(1690)$: $\gamma_{3/2}'^{P}$.

In all fits the following couplings are found to be weak:

$d_{13}(1520)$: $\gamma_{1/2}'^{P}$; $d_{15}(1670)$: $\gamma_{1/2}'^{P}$, $\gamma_{3/2}'^{P}$, $\gamma_{1/2}'^{N}$;

$f_{15}(1690)$: $\gamma_{1/2}'^{P}$, $\gamma_{1/2}'^{N}$, $\gamma_{3/2}'^{N}$.

The 3 fits agree to within 30% on the strong couplings to s_{11}^0 (1545) and $s_{11}^0(1700)$, and the weak, but non-negligible coupling to p_{11}^0 (1450). Furthermore, all fits agree on the necessity for background excitation in s- and p-waves in all isospin states, although the relative amount of background is considerably at variance among the three solutions.

There are two places of major disagreement among the three solutions: $d_{33}(1670)$ and $p_{11}(1750)$. While fits II and III agree very well on a strong helicity 1/2 and weak helicity 3/2 coupling for the d_{33} resonance, solution I finds the opposite relation to be favorable. The $p_{11}(1750)$ resonance is found by both fits II and III to be excited in equal amounts off protons as off neutrons (i.e., to be predominantly isoscalar),

while fit I finds it entirely produced off neutrons with almost no coupling to protons.

For those K-matrix poles outside the data range, not restrained by experimental data, the fitted parameters are not necessarily expected to be very similar for different fits and, indeed, for some couplings (e.g. to $p_{13}(1840)$) Table III exhibits large discrepancies among the three fits. However, it is remarkable that the coupling to $p_{31}(1910)$ is found with the same sign and similarly large magnitude in all three solutions, a notable result in view of the large ρN couplings found in an isobar model analysis of $\pi N \to \pi\pi N$.[23]

We comment now on the parameters of type D (introduced in section 2.5) which represent a parameterization of the high-energy contributions to the dispersion integrals. The δ-functions in energy were chosen to represent poles in the f_{35} and f_{37} partial waves at an energy of 1950 MeV and in the g_{17} partial wave at 2200 MeV. These resonances are suspected to have strong γN-coupling. In addition both the f_{35} and f_{37} resonances are coupled to the γN-system as K-matrix poles and thus contribute to the imaginary parts of the helicity amplitudes as well. We could measure the strength of the resonance coupling in many different ways. In these fits, the sign of equivalent couplings to the resonance poles and the high-energy poles are constrained to be the same. Since in the energy region where data are tested we are more than a full width away from the resonance energy, the real part dominates the imaginary, and we therefore estimate the resonance couplings from the real part in the higher-energy portion of our data region. The f_{37} estimates are to be found in Table Vd, and are discussed in section 6 below; none of the parameters of Table III are to be interpreted as being these resonance couplings. Of course these real parts in the data

region are mostly due to the parameters D of Table III. We find a remarkable agreement among the three fits for the D parameters corresponding to the f_{37} resonance and also, to a lesser extent, for the f_{35}. Not surprisingly, the contribution from the g_{17} resonance is found to vary both in sign and magnitude in these solutions. These latter parameters seem to compensate for the effects of several strongly coupled partial waves at higher energies. We tried to artificially constrain the signs of both f_{35} and f_{37} couplings in other constellations, but in each case encountered a large decrease in the fit quality.

Parameters of type C (introduced in section 2.5) are meant to compensate for a possible nonconvergence of the partial wave expansion for large and small s. Such parameters are found not to influence the quality of the fits by any large amount; fit I does not even need any such parameters and the fitted C parameters disagree between fit II and III. Somewhat surprisingly, we do not find a considerable difference in the magnitude of these parameters for the three different reactions while the above mentioned findings of Ref. 11 would suggest a stronger influence on the charged pion channels than on the $\pi^0 p$ final state. Concluding the comparison of our three fits we remark that we find a definite need for a modest, but non-negligible amount of nonresonant contributions to low (s and p) partial waves. There is an almost unanimous agreement among the three fits on the sign of such backgrounds, and magnitudes agree to within factors of 2. In Table IV we collect the contributions to χ^2 from the three different reactions and the various types of experimental quantities separately for the three fits. The information is contained in the number of data points employed in each fit and in the individual χ^2/data point as averaged over energy and angle. It is obvious from Table IV that we fit cross sections for the $\gamma p \to \pi^+ n$

reaction (i) better than those for the other two reactions, this is to a large extent being due to inconsistencies among various experiments for $\gamma p \to \pi^0 p$ (ii) and $\gamma n \to \pi^- p$ (iii). The measurements of asymmetries and polarizations are on the whole fitted satisfactorily except for the measurements of the polarization of the final state nucleon in the reaction $\gamma p \to \pi^+ n$, these representing the measurements of one experiment at energies between the first and second resonance region.

In comparing the resulting χ^2/data point of our three fits we find fit III to be better by approximately 10% and we shall use this fit to now compare our results to the data in the form of figures.

In Figs. 2 and 5 we present the results and the experimental points for the differential cross sections of reaction (i) at eight energies between 330 and 1130 MeV. We notice the generally excellent interpretation of the data exhibiting the strong forward peak at lower energies which is due to the contribution of the pion pole. Off the forward direction our fits follow very systematically the development of the strong angular dependence due to the resonances in the second and third region.

Data on the differential cross sections for the other two reactions (ii) and (iii), as shown on Figs. 3, 4, 6, and 7, is seen to be by no means of such good quality as that on $\gamma p \to \pi^+ n$. In the case of $\gamma p \to \pi^0 p$ there are difficulties of detection of the final-state particles, and for $\gamma n \to \pi^- p$ there are the kinematical and dynamical difficulties associated with a deuterium target. In such a situation, a continuous energy parameterization of the amplitudes, such as ours, will resist following incorrect excursions of the data. Nevertheless, we may identify one or two places where our fitted cross sections, given as solid lines, maybe incorrect; one such place occurs for large angle $\gamma p \to \pi^0 p$ at and above

1150 MeV/c, near the end of our data range (Figs. 3 and 6).

In Figs. 8-13 we present all three of our fits to polarization-type data. The data is sparse and the figures illustrate how further data can discriminate between different fits to the present data.

In the final part of this section we present the results of our fits in a form easily comparable to quark model predictions of photon couplings. We introduce the resonance couplings $A_{1/2}$ and $A_{3/2}$ in the convention first used by Copley, Kark, and Obryk[2] and subsequently used for comparisons to quark model predictions.[3-5] We relate $A_{1/2}$, $A_{3/2}$ to the fit parameters given in Table III by:

$$\left.\begin{aligned} A^{P,N}_{1/2} &= \pm \left(\tfrac{3}{2}\right)^{\frac{1}{2}} a_1 \quad \gamma'^{P,N}_{1/2} \\ A^{P,N}_{3/2} &= \mp \left(\tfrac{3}{2}\right)^{\frac{1}{2}} a_3 \quad \gamma'^{P,N}_{3/2} \end{aligned}\right\} \quad I = 1/2 \qquad (5.1)$$

$$\left.\begin{aligned} A^{V3}_{1/2} &= \mp \quad a_1 \quad \gamma'^{V3}_{1/2} \\ A^{V3}_{3/2} &= \pm \quad a_3 \quad \gamma'^{V3}_{3/2} \end{aligned}\right\} \quad I = 3/2 \qquad (5.2)$$

where $a_1 = 2\left[\frac{E_r}{M}\frac{\pi}{k}(2j+1)\right]^{\frac{1}{2}}$, $a_3 = a_1\left[\frac{(2j-1)(2j+3)}{16}\right]^{\frac{1}{2}}$.

The superscripts for the I = 1/2 resonances refer to the positive and neutral charge state of the resonance. The amplitudes are then measured in $GeV^{-1/2}$.

To arrive at this formulation we have defined the elastic width of a resonance (one of the K-matrix poles) by $\Gamma_{\pi N}$ where

$$\Gamma_{\pi N}/2 = \gamma_1^2 \, q_1(E_r) \qquad (5.3)$$

and its total width by Γ where

$$\Gamma/2 = \gamma_1^2 q_1(E_r) + \gamma_2^2 \, q_2(E_r) \qquad (5.4)$$

where q_1 and q_2 denote the c.m. momenta at the resonance energy E_r in the elastic and inelastic channels. In this approximation the free parameters employed in this analysis are related to Walker's[7] amplitudes at resonance $A_{\ell\pm}(E_r)$, $B_{\ell\pm}(E_r)$ through

$$A(E_r) = 2\gamma_1\gamma'_{1/2}/\Gamma\,; \quad B(E_r) = 2\gamma_1\gamma'_{3/2}/\Gamma\,. \qquad (5.5)$$

In Table Va,b we present again some of our preliminary results obtained from an average over seven fits as published previously.[5] The "experimental" couplings are compared to the predictions calculated using the FKR[4] quark model. We found a generally good agreement between the pion-photoproduction analysis and the predictions from this quark model especially for the signs of the prominent resonances. While the spread in the couplings found was rather large in some cases, our new solutions (with a much improved fit of the data) display a much more consistent picture, as marked above. Therefore, in Table Vc,d we present the results of these three fits, opposing them again to the quark model predictions. We shall evaluate the agreement between quark model and pion-photoproduction results in the next section. We conclude this part by pointing out that the new results, on the whole, are within the spread of values given in Table Va,b. The results of these three fits display a much smaller spread than those previously observed.

6. DISCUSSION AND CONCLUSION

6.1. General Features and Comparison with Previous Analyses. The most important previous analysis is that of Walker,[7,3] since it is the only one covering all charge states from the first through the third resonance region. Most of the Walker analysis was performed in 1966-67,[7] but it was modified and updated in some respects for comparison with the quark model in 1969.[3] Our analysis contains a good deal more data (section 3) and employs the entirely different method outlined in section 2; these two features help us to determine real photon couplings of many more resonances than the Walker analysis. There is one other most important difference: in the present state of the data–and for the foreseeable future–no single fit, with its resulting helicity amplitudes and its resonance parameters, is the unique best fit. In this paper we have presented the reader with several fits to the data and the range, over these various fits, of any given resonance parameter, which gives a quantitative indication of the error in the determination of that parameter. We regard this as a more realistic determination of errors than a deduction from the error matrix or finding the real error,[8] in any one given fit.

As explained in section 2, in all our waves we have the possibility of background in the imaginary parts, as well as resonance contributions. In our fitting procedure (section 4) we do allow an excitation of this imaginary background in nearly all waves, and the fitting program indeed finds some background. However, in general this background is small compared to the resonance contribution. Consequently, we can say that we have resonance dominance of the imaginary part though not resonance saturation. The only waves where imaginary background

makes a contribution comparable to the resonance contribution are the low-angular momentum waves, s_{11}, p_{11}, and p_{13}. The analysis of Walker[3,7] also found resonance dominance of the imaginary part but there was a strong constraint in the fitting procedure in favor of resonance dominance; consequently our evidence is somewhat stronger. As we would expect from the importance of the Born terms, (and inter alia the partial-wave projections of the dispersion integral over the p_{33} resonance) the real parts are not resonance dominated.

We now comment on those real photon resonance couplings which have been determined for the first time in the present analysis. The most important, in view of the quark model as discussed below and also most remarkable in view of the fact that we do not fit data in that resonance region, is the f_{37} (1950). The determination comes from the important contribution to the real part via the dispersion integral. Devenish, Lyth, and Rankin[11] in their dispersion relation investigations based on previous analyses[3,7,8] have also obtained values of these couplings in qualitative agreement with our values.

We could also obtain a value for the f_{35} (1890) couplings by the same means, but we place less reliance on these because (i) the partial wave is of smaller magnitude and consequently somewhat less well determined from interference with other amplitudes, and (ii) there may well be two f_{35} resonances at not dissimilar energies; if so, we would be observing, at our low energies, the combined effect of both. (A reason for suspecting a further f_{35} resonance is that the existence of the f_{17} (~2000) N^* resonance and some other observations suggests that the {70} $L = 2^+$ quark model multiplet exists and this contains an f_{35} in addition to the normal f_{35} usually assigned to the {56} $L = 2^+$ multiplet.)

As far as the principal resonances other than the f_{37} go, namely the

$d_{13}(1520)$ and $f_{15}(1690)$, we determine for the first time the d^0_{13} (1520), $\lambda = 1/2$, and f^0_{15}, $\lambda = 1/2$ amplitudes. We also have determined, quite well enough to indicate the sign (and the very approximate magnitude) the couplings of the $d^0_{15}(1670)$, $s_{11}(1690)$, $p_{11}(1750)$, $p^0_{11}(1450)$, $s_{31}(1620)$, and $d_{33}(1660)$. The theoretical significance of these couplings is discussed below, in section 6.2.

The other resonance couplings have been studied in previous analyses; before comparing our values to previous ones we should say something about our various solutions. They are in two classes: (A) eight solutions, seven of which were reported previously by Moorhouse and Oberlack[5] having $9 > \chi^2/(\text{data point}) > 5$ and (B) three new solutions having $4 > \chi^2/(\text{data point}) > 3$. The markedly better χ^2 per data point was due partly to a revision of the $\gamma p \to \pi^0 p$ Wolverton data[18] and mostly to a change from the threshold behavior adopted by Walker[7] to the threshold behavior described above in section 2.4. In fact our eight preliminary solutions are a reasonable qualitative fit to the data and in a situation of sometimes inconsistent data, subject to large systematic error, we would not advise the reader to completely ignore these solutions. We will refer to the solutions as our set A and B of solutions.

Generally, we have qualitative agreement with those resonance couplings found by Walker, with some exceptions which we note below along with other comments:

(i) $d_{13}(1520)$. The big couplings here are the $A^P_{3/2}$ and $A^N_{3/2}$ and our $A^P_{3/2}$ appears 10% bigger than Walkers and our $A^N_{3/2}$ 10% smaller, so that this helicity 3/2 amplitude no longer appears to be nearly pure isovector. The range of variation of the $A^P_{3/2}$ parameter found by us is approximately 15% and this 'error' is somewhat less than that

suggested by the 'real error' found by Moorhouse and Rankin.[8] Arai et al.[24] in an analysis of their and other data following Walker, find a value of $A^P_{3/2}$ between our average and the value of Walker.

(ii) $s_{11}(1530)$. Our value for both couplings is significantly less than those of Walker, perhaps by as much as 50%, but of course there is agreement in sign.

(iii) $p_{11}(1470)$. We have a considerable proton coupling, $A^P_{1/2}$, of the same order or larger as the s_{11} couplings and a smaller, perhaps small, neutron coupling.

6.2. Comparison with the Quark Model.

Over the past several years the developing agreement between the quark model predictions[2-4] for the $(N^*N\gamma)$ couplings and the results of partial-wave analysis of experiment,[3, 6-8] has been a major impetus behind interest in the L-excitation quark model. In making the comparison in the present work, we could use either the traditional nonrelativistic quark model as used and developed in the papers of Refs. 2 and 3, or the model of Feynman, Kislinger, and Ravndal which, though it solves none of the fundamental relativistic difficulties, has some relativistic features. Among these features is the inclusion, in a way definitely prescribed by the formalism, of terms corresponding to 'recoil' terms in the nonrelativistic model. Though the nonrelativistic quark model (using the most elementary and natural formulation of recoil terms),[25] returns very similar numerical answers to the model of Feynman, Kislinger, and Ravndal, it is the model of these latter authors which we use here.

We first compare the signs of the theoretical and partial-wave analysis amplitudes, as given in Tables Va-d. The signs of the partial-wave analysis amplitudes, are determined relative to the gauge

invariant Born terms (pole terms) in the fixed-t dispersion relation (Eq. 2.30); so, also are the signs of the quark model calculation, since the quark model coupling constants appear in the quark model calculation of the pole terms. Thus we are not free to multiply all the theoretical signs in Tables Va-d by a minus sign; the sign given is determined and is compared with the similarly determined 'experimental' sign.

The theoretical sign is a product of the resonance decay amplitudes[1] into πN and γN in which the arbitrary sign of the intermediate state drops out. It has been previously emphasized[5, 26] that the resulting signs are non-trival and do not follow from SU3. The most vital comparisons are those in which the quark model prediction does not involve recoil and non recoil terms of opposite sign in either of the matrix elements; the consequent prediction cannot depend on details of the quark model wave functions; the wrong sign here would either be a failure of the quark model or an indication of strong mixing of states.

In fact, out of 13 starred signs in the Tables, three are undetermined and 10 out of 10 of the determined signs agree. This factor of 10 to 1 in favor of the quark model seems very strong; it should be emphasized that these agreements are obtained without variable parameters. The agreements depend on the existence of both the recoil and nonrecoil terms and therefore verify the dynamical assumptions of the quark model. The symmetry $SU6_W$ fails completely, for example predicting the large $A^P_{3/2}$ and $A^N_{3/2}$ amplitudes of the $d_{13}(1520)$ to be zero. A broken version[27] of this symmetry can succeed, but at the expense of introducing arbitrary couplings in each multiplet, and even with these extra arbitrary couplings, this phenomenological theory appears till now, to have no phenomenological advantage over the quark model.

Of the unstarred signs, we find nine which are reasonably determined [we have included $p_{11}(1470)$ but excluded $p_{11}(1750)$ in this count]. Of these, six agree and three disagree, the disagreeing ones being $p_{11}(1470)\ A^P_{1/2}$, $A^N_{1/2}$ and $s_{11}(1690)\ A^N_{1/2}$. Since cancellations between recoil and nonrecoil terms of different sign are involved, we cannot say for sure that this is not a consequence of such details of the model. However, none of the cancellations are very fine, and in view of this and the six agreements, we prefer to attribute the disagreements to configuration mixing. In the case of the $s_{11}(1690)$ belonging to the [8, 4] of the {70} $L = 1^-$, mixing with the $s_{11}(1545)$ belonging to the [8, 2] of the {70} $L = 1^-$, seems indicated by the nonzero signal observed in the $A^P_{1/2}$ amplitude of the $s_{11}(1690)$, where the quark model predicts zero. Also the comparative nearness of these states would make such a mixing certainly possible, and the strong quark model photon coupling of $s_{11}(1545)$ would give a large effect for a mixing angle of ~40°. Mixing is also possible between the $p_{11}(1470)$ and the $p_{11}(1750)$, and there is still some doubt about the primary assignment of these states to quark model multiplets.[28] While on the subject of mixing, we should remark that the smallness of the πN width of $d_{13}(1700)$ makes considerable mixing between $d_{13}(1520)$ and $d_{13}(1700)$ extremely unlikely; consequently, the force of our (unmixed) successful predictions for $d_{13}(1520)$ is undiminished.

The six unstarred agreements are noteworthy, especially for the unmixed resonances $d_{13}(1520)$, $s_{31}(1630)$, and $d_{33}(1660)$. We see in it a preliminary indication that even the approximate relative magnitudes of recoil and nonrecoil terms may be given correctly by the quark model. It is interesting that the sign of the $s_{31}(1630)$ depends on the recoil–nonrecoil balance in the πN decay.[25]

We see that the agreement for magnitudes is qualitative, even bearing in mind that the uncertainty in the πN decay width should be multiplied into the partial wave analysis uncertainty in the numbers given. When a large amplitude is predicted a large amplitude always occurs; also that the actual large amplitude is always greater than the predicted 'large' amplitude; these are all starred cases.

A special case of magnitude comparisons is when the quark model predicts zero as in the proton couplings of the [8, 4] of the {70} $L = 1^-$ and $A^N_{3/2}$ coupling of the [8, 2] of the {56} $L = 2^+$. A valid comparison may be made for the $d^+_{15}(1670)$ and $f_{15}(1690)$ $A^N_{3/2}$ where little mixing is expected. The values in our set A were in all these cases compatible with zero. In set B, the d^+_{15} couplings are still small even though nonzero, but the f_{15}, $A^N_{3/2}$ coupling has become considerable. If this latter trend is supported in future work and if the $f_{15}(1690)$ is unmixed, this amplitude should be very revealing for refinement and reform of the quark model.

ACKNOWLEDGMENTS

We are grateful for the assistance of the programming group of LBL's group A, especially B. Pardoe and W. Koellner, and in particular acknowledge, with appreciation, the dedicated help of P. Cook.

One of us (R. G. M.) would like to acknowledge the hospitality and support of the Lawrence Berkeley Laboratory.

APPENDIX A

To express experimental quantities in terms of the $H_i(\theta)$ we write the differential cross section in the center-of-mass as

$$\frac{d\sigma}{d\Omega} = \frac{q}{k} \sum \left| \langle \chi_f | \mathfrak{F} | \chi_i \rangle \right|^2 , \qquad (A.1)$$

where χ_1, χ_f are two component spinors appropriate to the polarization of the initial and final nucleon and $\mathfrak{F}$ contains the polarization of the γ according to Eq. (2.3); the summation (or average where appropriate) is taken over unobserved spins. The matrix elements in (A. 1) can be trivially expressed as superpositions of the helicity matrix elements (2.6) and via (2.9) in terms of the $H_{flip}(\theta)$ and ϕ. One readily obtains the following expressions which we need for the existing data:

(i) differential cross section, $\sigma(\theta)$:

$$\sigma(\theta) = \frac{q}{k} \left[|H_N(\theta)|^2 + |H_D(\theta)|^2 + |H_{SP}(\theta)|^2 + |H_{SA}(\theta)|^2 \right] \qquad (A.2)$$

(ii) differential cross sections for photons polarized perpendicular and parallel to the production plane:

$$\sigma_\perp(\theta) = \frac{1}{2}\frac{q}{k} \left[|H_{SP}(\theta) + H_{SA}(\theta)|^2 + |H_N(\theta) - H_D(\theta)|^2 \right] \qquad (A.3)$$

$$\sigma_\parallel(\theta) = \frac{1}{2}\frac{q}{k} \left[|H_{SP}(\theta) - H_{SA}(\theta)|^2 + |H_N(\theta) + H_D(\theta)|^2 \right] \qquad (A.4)$$

(iii) polarized photon asymmetry [from (ii)], $\Sigma(\theta)$:

$$\Sigma(\theta)\,\sigma(\theta) \equiv (\sigma_\perp - \sigma_\parallel) = \frac{q}{k} \mathrm{Re}\left[H_{SP}(\theta) H^*_{SA}(\theta) - H_N(\theta) H^*_D(\theta) \right] \qquad (A.5)$$

(iv) polarization of the final nucleon in the direction $\underset{\sim}{k} \times \underset{\sim}{q}$, $P(\theta)$:

$$P(\theta)\,\sigma(\theta) = -\frac{q}{k} \mathrm{Im}\left[H_{SP}(\theta) H^*_D(\theta) + H_N(\theta) H^*_{SA}(\theta) \right] \qquad (A.6)$$

(v) polarized target asymmetry, where σ_+ and σ_- are the cross sections for nucleons polarized parallel and antiparallel respectively to $\underset{\sim}{k} \times \underset{\sim}{q}$, $T(\theta)$:

$$T(\theta)\,\sigma(\theta) \equiv (\sigma_+ - \sigma_-) = \frac{q}{k}\,\mathrm{Im}[\,H_{SP}(\theta) H_N^*(\theta) + H_D(\theta)\,H_{SA}^*(\theta)]. \quad \text{(A. 7)}$$

It can be convenient to work in terms of amplitudes $\tilde{H}$ defined by

$$\begin{aligned} H_N(\theta) &= \cos\tfrac{1}{2}\theta \quad \tilde{H}_N(\cos\theta) \\ H_{SP}(\theta) &= \tfrac{1}{2}(1+\cos\theta)\sin\tfrac{1}{2}\theta\ \tilde{H}_{SP}(\cos\theta) \\ H_{SA}(\theta) &= \sin\tfrac{1}{2}(\theta)\ \tilde{H}_{SA}(\cos\theta) \\ H_D(\theta) &= \tfrac{1}{2}(1-\cos\theta)\cos\tfrac{1}{2}\theta\,\tilde{H}_D(\cos\theta) \end{aligned} \quad \text{(A. 8)}$$

where it can be seen from Eqs. (2.5), (2.9), and (2.27) that the $\tilde{H}$ are functions of $\cos\theta$ only without poles in the physical region. (In fact, from (2.12) the $\tilde{H}$ are polynomial functions of $\cos\theta$ if only a finite number of partial waves contribute and indeed, even taking account of the pion pole explicitly exhibited in Eqs. (2.27), (2.28) the partial-wave series is convergent so that some polynomial functions of $\cos\theta$ give a representation of the $\tilde{H}$ to any desired accuracy).

It is enlightening to display the experimental quantities in terms of the $\tilde{H}$, thus explicitly exhibiting some necessary angular characteristics of the experimental quantities:

$$\begin{aligned} \sigma(\theta) &= \tfrac{1}{2}\tfrac{q}{k}[\,|\tilde{H}_N|^2 c^2 + |\tilde{H}_D|^2 c^2 s^4 + |\tilde{H}_{SP}|^2 s^2 c^4 + |\tilde{H}_{SA}|^2 s^2 \\ \sigma_\perp(\theta) &= \tfrac{1}{2}\tfrac{q}{k}[\,|\tilde{H}_N - \tilde{H}_D s^2|^2 c^2 + |\tilde{H}_{SA} + \tilde{H}_{SP} c^2|^2 s^2] \\ \sigma_\parallel(\theta) &= \tfrac{1}{2}\tfrac{q}{k}[\,|H_N + H_D s^2|^2 c^2 + |H_{SA} + H_{SP} c^2|^2 s^2] \\ \Sigma(\theta)\,\sigma(\theta) &= \tfrac{q}{k}[\,\mathrm{Re}\,(\tilde{H}_{SP}\tilde{H}_{SA}^* - \tilde{H}_N \tilde{H}_D^*)]\, s^2 c^2 \\ P(\theta)\,\sigma(\theta) &= \tfrac{q}{k}[\,\mathrm{Im}\,(\tilde{H}_{SP}\tilde{H}_D^* s^2 c^2 + \tilde{H}_N \tilde{H}_{SA}^*)]\, sc \\ T(\theta)\,\sigma(\theta) &= \tfrac{q}{k}[\,\mathrm{Im}\,(\tilde{H}_{SP}\tilde{H}_N c^2 + \tilde{H}_D \tilde{H}_{SA} s^2)]\, sc \end{aligned} \quad \text{(A. 9)}$$

where in (A9) $s = \sin\frac{1}{2}\theta$ and $c = \cos\frac{1}{2}\theta$ so that at $\theta = 0°$: $s = 0$, $c = 1$ and at $\theta = 180°$: $s = 1$, $c = 0$.

APPENDIX B

In this section we define and introduce the partial-wave amplitudes as given in Table VI. We make use of the standard expressions to resurrect the helicity coefficients $A^j_{\mu\lambda}$ defined in the partial-wave expansion (2.11) from the helicity amplitudes $\tilde{H}_N$, $\tilde{H}_{SA}$, $\tilde{H}_{SP}$, H_D of Eq. (2.12):

$$A^j_{\mu\lambda} = \frac{1}{4\pi}\int d\Omega\, A_{\mu\lambda}(\theta,\phi)\; d_{\lambda\mu}(\theta)\; e^{-i(\lambda-\mu)\phi} . \qquad (B.1)$$

Since the amplitudes $A_{\ell\pm}$, $B_{\ell\pm}$ (introduced in section 2.2) are linear functions of the $A^j_{\mu\lambda}$, we may combine expressions of type (B.1) to arrive at the following projection formulae

$$A_{\ell+} = \frac{1}{4(\ell+1)}\int_{-1}^{1} dz \Big\{ \tilde{H}_{SA}(z)(1-z)\,(P'_{\ell+1}(z) + P'_{\ell}(z)) - \tilde{H}_N(z)\,(1+z)\,(P'_{\ell+1}(z) - P'_{\ell}(z)) \Big\} \qquad (B.2)$$

$$A_{\ell-} = \frac{1}{4\ell}\int_{-1}^{1} dz \Big\{ \tilde{H}_{SA}(z)\,(1-z)\,(P'_{\ell}(z) + P'_{\ell-1}(z)) + \tilde{H}_N(z)\,(1+z)\,(P'_{\ell}(z) - P'_{\ell-1}(z)) \Big\} \qquad (B.3)$$

$$B_{\ell+} = \frac{1}{4\ell(\ell+1)(\ell+2)}\int_{-1}^{1} dz(1-z)^2 \Big\{ \tilde{H}_D(z)\,(1-z)\,(P''_{\ell+1}(z) + P''_{\ell}(z)) - \tilde{H}_{SD}(z)(1+z)\,(P''_{\ell+1}(z) - P''_{\ell}(z)) \Big\} \qquad (B.4)$$

$$B_{\ell-} = \frac{1}{4(\ell-1)\ell(\ell+1)}\int_{-1}^{1} dz\,(1-z)^2 \Big\{ \tilde{H}_D(z)\,(1-z)\,(P''_{\ell}(z) + P''_{\ell-1}(z)) + \tilde{H}_{SP}(z)\,(1+z)\,(P''_{\ell}(z) - P''_{\ell-1}(z)) \Big\} \qquad (B.5)$$

where the $\tilde{H}$ are defined in Appendix A, and $z = \cos\theta$.

The isospin convention is given in section 2.3 and we define amplitudes A^P and A^N as

$$A^P = (2/3)^{\frac{1}{2}}\,(A^{V1} - A^S)$$

$$A^N = -(2/3)^{\frac{1}{2}}\,(A^{V1} + A^S) \qquad (B.5)$$

For completeness we give the amplitudes for the physical processes [(cf. Eqs. (2.15), (2.25), (2.26)]

$$A^+ = -(1/3)^{\frac{1}{2}} A^{V3} + A^P$$

$$A^0 = (2/3)^{\frac{1}{2}}\, A^{V3} + (1/\sqrt{2})\, A^P$$

$$A^- = (1/3)^{\frac{1}{2}}\, A^{V3} + A^N \qquad (B.6)$$

$$A^{n\pi^0} = (2/3)^{\frac{1}{2}}\, A^{V3} - (1/\sqrt{2})\, A^N$$

The partial-wave amplitudes are then given in dimensionless "Argand units" and are for practical purposes multiplied by a factor 100. The quantities G(PROTON, NEUTRON, V3) listed in Table VI are therefore related to A^P, A^N, and A^{V3} by

$$G = 100\,(q\,k)^{\frac{1}{2}}\, A \qquad (B.7)$$

with q and k the c.m. momenta in the πN and γN systems.

The helicity amplitudes H_N, H_{SP}, H_{SA}, H_D as defined in Eq. (2.12) are not contained in this publication, but can be obtained as Ref. (29).

Footnote and References

*Work done under the auspices of the Atomic Energy Commission.

1. R. G. Moorhouse and N. Parsons, Nucl. Phys. (to be published).

2. C. Becchi and G. Morpurgo, Phys. Letters 17, 352 (1965); R. H. Dalitz and D. G. Sutherland, Phys. Rev. 146, 1180 (1966); R. G. Moorhouse, Phys. Rev. Letters 16, 771 (1966); L. A. Copley, G. Karl, and E. Obryk, Phys. Letters 29B, 117 (1969) and Nucl. Phys. B13, 303 (1969); D. Faiman and A. W. Hendry, Phys. Rev. 180, 1572 (1968).

3. R. L. Walker, Proceedings of the Daresbury Conference on Electron and Photon Interactions at High Energy, edited by D. Braben, Daresbury Laboratory, 1969.

4. R. P. Feynman, M. Kislinger, and F. Ravndal, Phys. Rev. D3, 1706 (1971).

5. R. G. Moorhouse and H. Oberlack, Phys. Letters 43B, 44 (1973).

6. Y. C. Chau, N. Dombey, and R. G. Moorhouse, Phys. Rev. 163, 1632 (1967).

7. R. L. Walker, Phys. Rev. 182, 1729 (1969); some of the results of this paper are revised in Ref. 3.

8. R. G. Moorhouse and W. A. Rankin, Nucl. Phys. B23, 181 (1970); W. A. Rankin, Ph. D. thesis (Glasgow University, 1970).

9. F. A. Berends, A. Donnachie, and D. L. Weaver, Nucl. Phys. B4, 1 (1967) and B4, 54 (1967).

10. J. Engels, A. Müllensiefen, and W. Schmidt, Phys. Rev. 175, 1951 (1968).

11. R. L. E. Devenish, D. H. Lyth, and W. A. Rankin, Daresbury report DNPL/P 109 (1972).

12. H_N and H_D are nonflip and double-flip amplitudes; H_{SP} and H_{SA} are single-flip amplitudes with the initial photon and nucleon having spins parallel and antiparallel respectively. The amplitudes are just the $H_1(\theta)$, $H_2(\theta)$, $H_3(\theta)$, $H_4(\theta)$ defined in Ref. 7 with the correspondence $H_1 = H_{SP}$, $H_2 = H_N$, $H_3 = H_D$, $H_4 = H_{SA}$.

13. E. P. Wigner and L. Eisenbud [Phys. Rev. 72, 29 (1947)] in the different situation of potential scattering with sharp boundary conditions have derived a factorizable pole-form like Eq. (2.18) for the M-matrix. However, in elementary particle scattering, K has left-hand singularities other than poles, and for the left-hand singularities Eq. (2.18) is certainly an approximation.

14. J. M. Blatt and V. F. Weisskopf, Theoretical Nuclear Physics (John Wiley and Sons, New York, 1952) p. 358 ff.

15. H. Oberlack, Group A Physics Note 772, 1973 (unpublished).

16. E. N. Argyres, A. P. Contogouris, J. P. Holden, and M. Svec "The structure of Amplitudes of Neutral Pion Photoproduction" McGill preprint; I. Barbour and R. G. Moorhouse, CERN preprint (and to be published); M. Hontebeyrie et al. (Bordeaux preprint, December 1972). These preceding high-energy photoproduction papers take high-energy imaginary parts approximately proportional to $s^{\alpha(t)-1}$, where $\alpha(t)$ is the ρ-ω-A_2 trajectory, and low-energy imaginary parts approximately from existing partial wave analysis of photoproduction[3,7] and deduce also the high-energy real parts from fixed-t dispersion relations, and obtain a fit to the high-energy experiments. This approach to high-energy photoproduction was motivated by the success of the same approach in high-energy pion-nucleon charge-exchange scattering (G. Ghandour and R. G. Moorhouse, Phys. Rev. D 6, 856 (1972); E. N. Argyres and A. P. Contogouris, Phys. Rev. D6, 2018 (1972);

M. Coirier, J. Guillaume, Y. Leroyer, and P. Salin, Nucl. Phys. B44, 157 (1972), the whole approach being an extension of some of the ideas of the dual absorptive model (H. Harari, Phys. Rev. Letters 26, 1400 (1971).

17. P. Spillantini and V. Valente, CERN/HERA 70-1 (1970).

18. Data set used in this analysis. The symbols in parentheses at the end of each reference identify the data in the legend of the figures.

$\gamma p \rightarrow \pi^+ n, \sigma(\theta)$

M. Beneventano, G. Bernardini, D. Lee, G. Stoppini, and L. Tau, Nuovo Cimento, 4, 323 (1956). (ILLI-56)

A. J. Lazarus, W. K. H. Panofsky, and F. R. Tangherlini, Phys. Rev., 113, 1330 (1958). (STAN-58)

J. R. Kilner, Ph. D. Thesis (Cal. Inst. of Technology, 1962). (CALT-62)

E. A. Knapp, R. W. Kenney, and V. Perez-Mendez, Phys. Rev., 114, 605 (1963). (UCRL-63)

D. W. G. S. Leith, R. Little, and E. M. Lawson, Phys. Letters, 8, 355 (1964). (GLAS-64)

R. A. Alvarez, Phys. Rev., 142, 957 (1965). (STAN-65)

D. Freytag, W. J. Schwille, and R. J. Wedemeyer, Z. Physik, 186, 1 (1965). (BONN-65)

C. Schaerf, Nuovo Cimento, 44, 504 (1966). (STAN-66)

Yu. M. Aleksandrov, V. F. Grushin, V. A. Zapevalon, and E. M. Leikin, Sov. Phys.—JETP, 22, 39 (1966). (MOSC-66)

G. Buschhorn, J. Carrol, R. D. Eandi, P. Heide, R. Hubner, W. Kern, U. Kotz, P. Schmuser, and J. Skronn, Phys. Rev. Letters, 19, 1027 (1966). (DESY-66)

Yu. M. Aleksandrov, V. F. Grushin, and E. M. Leikin, Phys. Letters, 25B, 372 (1967). (MOSC-67)

G. Buschhorn, J. Carrol, R. D. Eandi, P. Heide, R. Hubner, W. Kern, U. Kotz, P. Schmuser, and H. J. Skronn, Phys. Rev. Letters, 18, 571 (1967). (DESY-67)

S. D. Ecklund and R. L. Walker, Phys. Rev., 159, 1195 (1967). (CALT-67)

H. A. Thiessen, Phys. Rev., 155, 1488 (1967). (CALT-67)

R. A. Alvarez, G. Cooperstein, K. Kalata, R. C. Lanza, and D. Luckey, Phys. Rev. Letters, 21, 1019 (1968). (MIT-68)

C. Betourne, J. C. Bizot, J. Perez -y- Jorba, and D. Treille, Phys. Rev., 172, 1343 (1968). (ORSA-68)

B. d'Almagne, Ph. D. Thesis, Orsay, Linear Accelerator Laboratory Report No. LAL 1239, 1970). (ORSA-70)

G. Fischer, H. Fischer, M. Heuel, G. v. Holtey, G. Knop, and J. Stumpfig, Nucl. Phys. B16, 119 (1970). (BONN-70)

T. Fujii, H. Okuno, S. Orito, H. Sasaki, T. Nozaki, F. Takasaki, K. Takikawa, K. Amako, I. Endo, K. Yoshida, M. Higuchi, M. Sato, and Y. Sumi, Phys. Rev. Letters 26, 1672 (1971). (TOKY-71)

$\gamma p \rightarrow \pi^+ n, P(\theta)$

K. H. Althoff, H. Piel, W. Wallraff, and G. Wessels, Phys. Letters, 26B, 640 (1968). (BONN-68)

U. Hahn, H. Heinrichs, and W. Wallraff, preprint Bonn Univ. PI1-143 (1971). (BONN-71)

$\gamma p \rightarrow \pi^+ n, \Sigma(\theta)$

R. E. Taylor and R. F. Mozley, Phys. Rev. 117, 835 (1960). (STAN-60)

R. C. Smith and R. F. Mozley, Phys. Rev., 130, 2429 (1963). (STAN-64)

F. F. Liu, D. J. Drickey, and R. F. Mozley, Phys. Rev., 136, B 1183 (1964). (STAN-64)

F. F. Liu and S. Vitale, Phys. Rev., 144, 1093 (1966). (STAN-66)

M. Grilli, P. Spillantini, F. Soso, M. Nigro, E. Schiavuta, and V. Valente, Nuovo Cimento, 54A, 877 (1968). (FRAS-68)

J. Alspector, D. Fox, D. Luckey, C. Nelson, L. S. Osborne, G. Tarnopolsky, Z. Bar-Yam, J. de Pagter, J. Dowd, W. Kern, and S. M. Matin, Phys. Rev. Letters 28, 1403 (1972) (MIT-71)

$\gamma p \rightarrow \pi^+ n, T(\theta)$

S. Arai, S. Fukui, N. Horikawa, R. Kajikawa, T. Kasuga, H. Kobayakawa, A. Masaike, T. Matsuda, T. Nakanishi, T. Ohshima, M. Saito, S. Sugimoto, and T. Yamaki, Phys. Letters B40, 426 (1972). (TOKY-72)

K. H. Althoff, P. Feller, H. Herr, W. Hoffmann, V. Kadansky, D. Menze, U. Opara, F. J. Schittko, W. Schulz and W. T. Schwille, Nucl. Phys. B 53, 9 (1973). (BONN-73)

$\gamma p \rightarrow \pi^0 p, \sigma(\theta)$

R. L. Walker, D. C. Oakley, and A. V. Tollestrup, Phys. Rev., 97, 1279 (1954). (CALT-54)

W. S. McDonald, V. Z. Peterson, and D. R. Corson, Phys. Rev., 107, 577 (1957). (CALT-57)

H. H. Bingham and A. B. Clegg, Phys. Rev., 112, 2053 (1958). (CALT-58)

V. L. Highland and J. W. Dewire, Phys. Rev., 132, 1293 (1963). (CALT-63)

R. E. Diebold Ph. D. Thesis (Calif. Inst. of Technology, 1963). (CALT-63)

R. M. Talman, Ph. D. Thesis (Calif. Inst. of Technology, 1963). (CALT-63)

H. De Staebler, E. F. Erickson, A. C. Hearn, and C. Schaerf, Phys. Rev., 140, B 336 (1965). (STAN-65)

G. L. Hatch, Ph. D. Thesis (Calif. Inst. of Technology, 1966). (CALT-66)

M. Braunschweig, D. Husmann, K. Lubelsmeyer, and D. Schmitz, Phys. Letters, 22, 705 (1966). (DESY-66)

C. Bacci, G. Penso, G. Salvini, C. Mencuccini, A. Reale, V. Silvestrini, M. Spinetti, and B. Stella, Phys. Rev., 159, 1124 (1967). (FRAS-67)

M. Croissiaux, E. B. Dally, R. Morand, J. P. Pahin, and W. Schmidt, Phys. Rev., 164, 1623 (1967). (ORSA-67)

R. Morand, E. F. Erikson, J. P. Pahin, and M. G. Croissiaux, Phys. Rev., 180, 1299 (1969). (ORSA-68)

G. Sauvage, Thesis, Orsay, Linear Accelerator Laboratory Report No. LAL 1207 (1969). (ORSA-69)

G. Fischer, H. Fischer, G. v. Holtey, H. Kampgen, G. Knop, P. Schulz, H. Wessels, W. Braunschweig, H. Genzel and R. Wedemeyer, Nucl. Phys. B 16, 93 (1970). (BONN-70)

P. S. L. Booth, M. F. Butler, L. J. Carroll, J. R. Holt, J. N. Jackson, W. H. Range, E. G. H. Williams, and J. R. Wormald, DNPL/P 95, (1971). (LIVE-71)

F. B. Wolverton, Ph. D. Thesis (Calif. Inst. of Technology, 1968), revised data as private communication from R. L. Walker (1972). (CALT-72)

Y. Hemmi, T. Inagaki, Y. Inagaki, A. Maki, K. Miyake, T. Nakamura, N. Tamura, J. Tsukamoto, N. Yamashita, H. Itoh, S. Kobayashi, S. Yasumi, and H. Yoshida, Phys. Letters B 43 (1973). (TOKY-73)

$\gamma p \rightarrow \pi^0 p, P(\theta)$

P. C. Stein, Phys. Rev. Letters, 2, 473 (1959). (CORN-59)

R. Querzoli, G. Salvini, and A. Silverman, Nuovo Cimento, 19, 53 (1961). (FRAS-61)

L. Bertanza, L. Mannelli, S. Santulli, G. V. Silvestrini, and V. Z. Peterson, Nuovo Cimento, 24, 734 (1962). (FRAS-62)

C. Mencuccini, R. Querzoli, and G. Salvini, Phys. Rev., 126, 1181 (1962). (FRAS-62)

J. O. Maloy, V. Z. Peterson, G. A. Salaudin, F. Waldner, A. Manfredini, J. I. Friedman, and H. Kendall, Phys. Rev., 139, B 733 (1965). (STAN-65)

K. H. Althoff, K. Kramp, H. Matthay, and H. Piel, Z. Physik, 194, 135 (1966). (BONN-66)

K. H. Althoff, K. Kramp, H. Matthey, and H. Piel, Z. Physik, 194, 144 (1966). (BONN-66)

K. H. Althoff, D. Finlen, N. Minatti, H. Piel, D. Trines, and M. Unger, in Proceedings of 1967 Stanford Conference. (BONN-67)

E. D. Bloom, C. A. Heusch, C. Y. Prescott, and L. S. Rochester, Phys. Rev. Letters, 19, 671 (1967). (CALT-67)

D. E. Lundquist, R. L. Anderson, J. V. Allaby, and D. M. Ritson, Phys. Rev., 168, 1527 (1968). (STAN-68)

S. Hayakawa, N. Horikawa, R. Kajikawa, K. Kikuchi, H. Kobayakawa, A. Masaike, K. Mori, H. Obayashi, and K. Ukai, J. Phys. Soc. Japan, 25, 307 (1968).

M. N. Prentice, R. Railton, J. G. Rutherglen, K. M. Smith, G. R. Brookes, P. J. Bussey, F. H. Combley, G. H. Eaton, W. Galbraith, and J. E. Shaw, Nucl. Phys. B41, 353 (1972). (GLAS-71)

D. Trines, Ph. D. Thesis, PIB 1-160 (Bonn University, 1972). (BONN-72)

$\gamma p \rightarrow \pi^0 p, \Sigma(\theta)$

D. J. Drickey and R. F. Mozley, Phys. Rev., 136, B 543 (1964). (STAN-64)

G. Barbiellini, G. Bologna, C. Capon, J. De Wire, G. De Zorzi, G. Diambrini, F. L. Fabbri, G. P. Murtas, and G. Sette, Phys. Rev., 184, 1402 (1969). (FRAS-69)

J. Alspector, D. Fox, D. Luckey, C. Nelson, L. S. Osborne, G. Tarnopolsky, Z. Bar-Yam, J. de Pagter, J. Dowd, W. Kern, and S. M. Matin, Phys. Rev. Letters 28, 1403 (1972). (MIT-71)

$\gamma n \rightarrow \pi^- p, \sigma(\theta)$

T. Fujii, H. Okuno, S. Orito, H. Sasaki, T. Nozaki, F. Takasaki, K. Takikawa, K. Amako, I. Endo, K. Yoshida, M. Higuchi, M. Sato, and Y. Sumi, Phys. Rev. Letters 26, 1672 (1971). (TOKY-71)

P. E. Scheffler and P. L. Walden, private communication (1971). (CALT-71)

Aachen-Bonn-Hamburg-Heidelberg-München Collaboration, private communication by G. Knies (1972). (DESY-72)

$\gamma n \rightarrow \pi^- p, P(\theta)$

J. R. Kenemuth and P. C. Stein, Phys. Rev., 129, 2259 (1963). (CORN-63)

$\gamma n \rightarrow \pi^- p, \Sigma(\theta)$

F. F. Liu, D. J. Drickey, and R. F. Mozley, Phys. Rev., 136, B 1183 (1964). (STAN-64)

T. Nishikawa, S. Hiramatsu, Y. Kimura, M. Kobayashi, K. Kondo, S. Okumura, T. Suzuki, K. Takikawa, T. Tsuru, and H. Yoshida, Phys. Rev. Letters, 21, 1288 (1968). (TOKY-68)

J. Alspector, D. Fox, D. Luckey, C. Nelson, L. S. Osborne, G. Tarnopolsky, Z. Bar-Yam, J. de Pagter, J. Dowd, W. Kern, and S. M. Matin, Phys. Rev. Letters 28, 1403 (1972). (MIT-71)

19. A. Donnachie, R. G. Kirsopp, and C. Lovelace, Phys. Letters B 26, 161 (1968); C. H. Johnson, Jr., Lawrence Radiation Laboratory Report UCRL-17683 (1967); L. D. Roper and R. M. Wright, Phys. Rev. 138, B 921 (1965); P. Bareyre, C. Bricman, and G. Villet, Phys. Rev. 165, 1730 (1968); A. T. Davies, Nucl. Phys. B 21, 359 (1970); S. Almehed and C. Lovelace, Nucl. Phys. B 40, 157 (1972).

20. M. J. D. Powell, Computer Journal 7, 155 (1964).

21. L. D. Roper, R. M. Wright, and B. T. Feld, Phys. Rev. 138, B190 (1965).

22. P. Noelle, W. Pfeil, and D. Schwela, Nucl. Phys. B26, 461 (1971); P. Noelle and W. Pfeil, Nucl. Phys. B 31, 1 (1971).

23. D. J. Herndon et al., XVI International Conference on High-Energy Physics, Chicago 1972.

24. S. Arai, S. Fukui, N. Horikawa, R. Kajikawa, T. Kasuya, H. Kobayakawa, A. Masuike, T. Matsuda, T. Nakanashi, T. Ohshima, M. Saito, S. Sugimoto, T. Yamaki, K. Amako, and K. Yoshida, Nucl. Phys. B 48, 397 (1972).

25. In the nonrelativistic quark model, recoil terms have always been included in the electromagnetic interaction, as used in the papers of Ref. 2. However, some extensive investigations of resonance decays into pseudoscalar mesons [D. Faiman and A. W. Hendry, Phys. Rev. 173, 1720 (1968)] do not include recoil terms. Not only does this

exclusion seem inconsistent, but the evidence presented in this paper on the signs of the pion photoproduction amplitudes with formation of $s_{31}(1630)$ and $s_{11}(1530)$ shows that the inclusion of recoil terms in resonance decays into pseudoscalar mesons is phenomenologically necessary.

26. R. G. Moorhouse, Proceedings of the XVI International Conference on High-Energy Physics at Batavia, edited by J. D. Jackson and A. Roberts, National Accelerator Laboratory, Batavia, 1973, Vol. 1, p. 182.

27. E. W. Colglazier and J. L. Rosner, Nucl. Phys. B 27, 349 (1971); D. Faiman and D. Plane, Phys. Letters 39B, 358 (1972); Nucl. Phys. B 50, 379 (1972).

28. This doubt is connected with the current absence of any p_{33} partner to the $p_{11}(1470)$ in the $\{56\}_2$ $L = 0^+$ multiplet in πN elastic partial-wave analysis. (See, for example, R. G. Moorhouse, Proceedings of the Purdue Conference on Baryon Resonances, 1973.)

29. R. G. Moorhouse, H. Oberlack, and A. H. Rosenfeld, UCID-3629 (1973) (unpublished).

TABLE I. Initial values for the parameters of the hadronic part of the K-matrix.[a]

Wave	E_r (MeV)	γ_1'	γ_2'	ξ	$\Gamma/2$ (MeV)	m_2 (MeV)	M_2 (MeV)
			Part a				
s_{31}	1617	0.295	0.363	+	105	350	940
	1950	0.365	-0.743	+			
	2988	1.748	-0.712	-			
p_{31}	1925	0.244	0.357	+	117	568	948
	2145	0.357	-0.394	+			
	684	1.153	-0.740	+			
p_{33}	1235	0.525	0.0	+	63	333	1223
	2356	0.597	0.880	+			
d_{33}	1658	0.181	0.542	+	125	138	1218
	2092	0.094	-0.578	+			
	-2649	0.885	-1.030	+			
d_{35}	2327	0.235	0.706	+	476	414	1092
	-1938	0.765	-1.480	+			
f_{35}	1869	0.147	0.362	+	86	137	1196
	-1610	0.427	-1.057	+			
f_{37}	1955	0.257	0.296	+	104	540	940
	3247	0.649	-0.343	+			
	- 201	0.655	-1.114	+			

TABLE I. (cont.)

Wave	E_r (MeV)	γ_1'	γ_2'	ξ	$\Gamma/2$ (MeV)	m_2 (MeV)	M_2 (MeV)
			Part b				
s_{11}	1507	0.199	0.329	+	30	548	943
	1772	0.520	-0.465	+	271		
	- 858	0.352	1.048	+			
p_{11}	1474	0.491	0.412	+	165	281	940
	1792	0.358	-0.404	+	182		
	2285	0.658	0.389	+			
	1004	0.556	-0.028	+			
p_{13}	1841	0.251	0.525	+	176	615	940
	2136	0.193	-0.495	+			
	311	0.947	-0.108	+			
d_{13}	1511	0.271	-0.289	+	66	301	940
	2547	0.538	0.946	+			
	966	0.410	0.666	+			
d_{15}	1674	0.232	-0.249	+	60	269	1009
	2395	0.378	0.671	+			
	- 358	0.520	1.476	+			
f_{15}	1681	0.264	0.232	+	65	400	940
	2042	0.249	-0.471	+			
	422	0.505	-0.754	+			

[a]These values were obtained from a two-channel elastic, inelastic fit to elastic πN partial-wave amplitudes for a) isospin 3/2, b) isospin 1/2 waves. E_r denotes the pole positions in the K-matrix, γ_1' and γ_2' the (dimensionless) couplings to the elastic and inelastic channel respectively, ξ a sign factor multiplying the pole term in the K-matrix sum. M_2 and m_2 are pseudomasses describing the inelastic channel. Γ is the total width of a resonance in the approximation $\frac{\Gamma}{2} = \gamma_1'^2\, q_1(E_r) + \gamma_2'^2\, q_2(E_r)$ where q_1, q_2 are the c.m. momenta in the two channels.

TABLE II. Real parts and phase angles for s and p wave amplitudes as used to constrain the fitted amplitudes by testing the phase prediction through the Watson theorem and the low-energy continuity of the real parts.[a]

Wave	λ	Real part	Angle	Real part	Angle
		E = 250 MeV		E = 290 MeV	
s_{11}	1/2	5.6 ± 0.07	8.4 ± 0.4	4.20 ± 0.07	9.6 ± 0.4
p_{11}	1/2	-	-2.0 ± 0.8	-	0.1 ± 0.8
p_{13}	1/2	0.7 ± 0.60	-0.9 ± 0.4	0.70 ± 0.60	1.6 ± 0.4
p_{13}	3/2	2.35 ± 0.10	-0.9 ± 0.4	2.35 ± 0.10	1.6 ± 0.4
s_{31}	1/2	-11.0 ± 0.70	-8.5 ± 0.4	-10.0 ± 0.70	12.2 ± 0.4
p_{31}	1/2	-	-1.9 ± 0.4	-	-3.3 ± 0.4
p_{33}	1/2	5.9 ± 0.60	21.9 ± 0.8	7.0 ± 0.60	44.8 ± 0.8
p_{33}	3/2	-18.75 ± 0.40	21.9 ± 0.8	-16.7 ± 0.40	44.8 ± 0.8
		E = 350 MeV		E = 450 MeV	
s_{11}	1/2	4.2 ± 0.07	10.7 ± 0.4	-	13.7 ± 0.4
p_{11}	1/2	-	4.0 ± 0.8	-	18.6 ± 0.8
p_{13}	1/2	0.7 ± 0.60	2.2 ± 0.4	-	-3.6 ± 0.4
p_{13}	3/2	2.35± 0.10	2.2 ± 0.4	-	-3.6 ± 0.4
s_{31}	1/2	-7.0 ± 0.70	-15.6 ± 0.4	-	-21.1 ± 0.4
p_{31}	1/2	-	-4.7 ± 0.4	-	7.2 ± 0.4
p_{33}	1/2	0.0 ± 0.60	94.5 ± 0.8	-	134.2 ± 0.8
p_{33}	3/2	0.0 ± 0.10	94.5 ± 0.8	-	134.2 ± 0.8

[a] λ denotes the total helicity of the γN-system. Real parts are in units of $(GeV^{-1} \times 10^{-2})$, phase angles in degrees. The isospin 1/2 amplitudes are related to the amplitudes defined in Eq. (2.25a) by $(1/3)^{\frac{1}{2}} (T^{V1} - T^{S})$, isospin 3.2 amplitudes by $(3/2)^{\frac{1}{2}} T^{V3}$.

TABLE III. Parameters resulting from the three best fits I - III.

Wave	r	E_r(MeV)	γ_1'	γ_2'	$\gamma_{1/2}^{V3}$	$\gamma_{3/2}^{V3}$
			Part a[a]			
s_{31}	1	1598	0.320	0.394	-119	
		1593	0.327	0.399	-131	
		1605	0.349	0.400	-115	
	2	X	X	X	X	
		X	X	X	X	
		[1950]	[0.365]	[-0.743]	11	
	3	2992	1.744	-0.724	443	
		3002	1.735	-0.733	404	
		3051	1.725	-0.756	466	
p_{31}	1	[1925]	[0.244]	[0.357]	-173	
		1911	0.272	0.402	- 81	
		1925	0.244	0.357	- 60	
p_{33}	1	1231	0.534	[0]	126	-268
		1231	0.532	[0]	126	-266
		1231	0.532	[0]	125	-267
	2	[2356]	[0.597]	[0.880]	- 86	-165
		[2356]	[0.597	[0.880]	-105	-180
		[2356]	[0.597]	[0.880]	-130	-179
d_{33}	1	1673	0.172	0.556	15	- 56
		1678	0.164	0.589	59	3
		1676	0.147	0.619	66	- 28
d_{35}	1	[2327]	[0.235]	[0.706]	48	7
		[2327]	[0.235]	[0.706]	73	- 24
		[2327]	[0.235]	[0.706]	53	- 10
f_{35}	1	[1869]	[0.147]	[0.362]	17	11
		[1869]	[0.147]	0.362	16	9
		[1869]	[0.147]	0.362	18	6
f_{37}	1	[1955]	[0.257]	[0.296]	27	- 17
		[1955]	[0.257]	[0.296]	31	- 14
		[1955]	[0.257]	[0.296]	9	- 1

TABLE III. (cont.)

Wave	r	E_r(MeV)	γ_1'	γ_2'	$\gamma_{1/2}'^P$	$\gamma_{3/2}'^P$	$\gamma_{1/2}'^N$	$\gamma_{3/2}'^N$
				Part b[a]				
s_{11}	1	1546	0.281	0.412	42		- 38	
		1548	0.262	0.417	45		- 22	
		1548	0.262	0.417	47		- 40	
	2	1707	0.527	-0.434	75		- 128	
		1674	0.563	-0.417	72		- 112	
		1676	0.595	-0.421	66		- 82	
	3	- 773	0.352	0.982	-607		2111	
		- 780	0.337	1.071	-848		2307	
		- 637	0.327	0.988	-797		2181	
p_{11}	1	1439	0.476	0.388	106		- 56	
		1467	0.431	0.474	107		- 24	
		1446	0.426	0.469	102		- 38	
	2	1787	0.386	-0.390	12		- 106	
		1783	0.392	-0.362	- 38		- 64	
		1777	0.344	-0.348	- 37		- 57	
	3	X	X	X	X		X	
		X	X	X	X		X	
		[2285]	[0.658]	[0.389]	- 41		- 66	
	4	1004	[0.556]	[-0.028]	21		12	
		1009	0.548	0.045	- 94		170	
		977	0.606	-0.001	- 55		139	
p_{13}	1	[1841]	[0.251]	[0.525]	13	10	42	13
		1846	0.227	447	- 29	- 34	- 12	119
		[1841]	[0.251]	[0.525]	- 17	- 54	- 23	110
	3	311	[0.947]	[-0.108]	-132	-171	158	-166
		311	[0.947]	[-0.108]	- 69	-170	17	52
		311	[0.947]	[-0.108]	- 55	-150	13	55
d_{13}	1	1513	0.310	-0.291	- 5	182	83	-146
		1518	0.357	-0.266	5	173	78	-108
		1519	0.347	-0.252	2	175	71	-110
	2	X	X	X	X	X	X	X
		X	X	X	X	X	X	X
		1678	0.129	0.281	- 22	38	14	30
d_{15}	1	1664	0.219	-0.259	14	- 9	- 15	25
		1669	0.178	-0.276	20	- 7	- 15	28
		1669	0.178	-0.276	9	- 9	- 10	25
f_{15}	1	1681	0.263	0.226	13	78	- 15	- 20
		1691	0.211	0.271	10	82	- 18	- 23
		1691	0.211	0.271	8	76	- 21	- 23

TABLE III. (cont.)

	C_1	C_2	C_3	C_4
		Part c^b		
$\gamma p \to \pi^+ n$	X 0.042 0.146	X 0.044 -0.141	X 0.046 0.154	X -0.023 0.122
$\gamma p \to \pi^\circ p$	X 0.057 0.132	X -0.008 -0.122	X 0.053 0.151	X 0.051 0.125
$\gamma n \to \pi^- p$	X -0.038 -0.140	X -0.050 0.140	X 0.039 0.153	X 0.055 -0.109

TABLE III. (cont.)

E_δ(MeV)	Wave	$D^{V3}_{1/2}$	$D^{V3}_{3/2}$	$D^{p}_{1/2}$	$D^{p}_{3/2}$	$D^{N}_{1/2}$	$D^{N}_{3/2}$
			Part d[c]				
1950	f_{35}	281	131	X	X	X	X
		294	217	X	X	X	X
		283	240	X	X	X	X
1950	f_{37}	551	-426	X	X	X	X
		549	-447	X	X	X	X
		677	-450	X	X	X	X
2125	g_{17}	X	X	178	1300	729	-899
		X	X	-294	1568	984	-745
		X	X	-148	1529	973	-780

a. Parts a) and b) list the fitted K-mitrix parameters for isospin 3/2 and 1/2 partial waves. Results are quoted for those K-matrix poles which have been coupled to the γN-channel in at least one fit, successive rows corresponding to fits I-III respectively. X marks those parameters which have not been varied in a particular fit; brackets indicate that this number has been kept constant at the value of Table I. The index r refers to the pole sequence within a partial wave as given in Table I, the pole position being E_r. The couplings γ' are defined in section 2.4. The photon couplings $\gamma^{V3}_{1/2}$ etc. are multiplied by 10^4.

b. Part c) contains the fitted results for the parameters C defined in Eq. (2.30), which compensate for the possible nonconvergence of the partial-wave amplitudes in the unphysical region. Again for each parameter, successive rows correspond to the results of fits I-III, the units being defined by Eq. (2.30).

c. Results for parameters D of Eq. (2.31) are listed in part d). E_δ denotes the position of the energy δ-function and D^I_λ their strengths, where λ = 1/2, 3/2 refers to the total helicity in the γN-system and I = V3, P, N to our isospin convention.

TABLE IV. X^2/data point for the three best fits I-III.

Reaction	Type[a]	Number of data points	X^2/Data point Fit I	Fit II	Fit III
$\gamma p \to \pi^+ n$	σ	1846	2.44	2.59	2.38
	P	13	6.03	6.76	7.11
	Σ	116	2.81	2.81	2.57
	T	27	1.50	1.50	1.62
$\gamma p \to \pi^0 p$	σ	1393	5.64	5.91	5.19
	P	129	2.83	2.92	2.79
	Σ	37	2.78	3.66	3.02
$\gamma n \to \pi^- p$	σ	541	5.11	4.96	4.32
	P	1	0.65	0.65	0.99
	Σ	45	4.22	5.03	4.97
Number of variable parameters			56	68	74

[a] σ = differential cross section, P = recoil nucleon polarization, Σ = linearly polarized photon asymmetry and T = polarized target asymmetry.

TABLE V. Average resonance couplings compared with quark model predictions.[a]

{SU6} L	N*(mass) [SU3, $2S_q+1$] J^P	$A^{P(V3)}_{1/2}$	$A^{P(V3)}_{3/2}$	$A^{N}_{1/2}$	$A^{N}_{3/2}$
			Part a[a]		
$\{56\}_0$ L = 0^+	$p_{33}(1230)$	-142 ± 6	-259 ± 16		
	[10,4]3/2$^+$	-108 *	-187 *		
$\{70\}_1$ L = 1^-	$s_{11}(1545)$	53 ± 20		- 48 ± 21	
	[8,2]1/2$^-$	156		-108	
	$d_{13}(1512)$	- 26 ± 15	194 ± 31	85 ± 14	-124 ± 13
	[8,2]3/2$^-$	- 34	109 *	- 31	-109 *
	$s_{31}(1610)$	90 ± 76			
	[10,2]1/2$^-$	47			
	$d_{33}(1660)$	68 ± 42	22 ± 52		
	[10,2]3/2$^-$	88	84 *		
	$s_{11}(1690)$	66 ± 42		- 72 ± 66	
	[8,4]1/2$^-$	0		30	
	$d_{13}(1700)$	3 ± ?	20 ± ?	- 28 ± ?	27 ± ?
	[8,4]3/2$^-$	0 *	0 *	- 10 *	- 40 *
	$d_{15}(1670)$	11 ± 12	21 ± 20	10 ± 40	- 35 ± 14
	[8,4]5/2$^-$	0 *	0 *	- 38 *	- 53 *

TABLE V. (cont.)

{SU6} L	N*(mass) $[SU3, 2S_q+1]J^P$	$A^{P(V3)}_{1/2}$	$A^{P(V3)}_{3/2}$	$A^{N}_{1/2}$	$A^{N}_{3/2}$
			Part b[a]		
$\{56\}_2$ L = 2^+	$f_{15}(1690)$	- 8 ± 4	100 ± 12	17 ± 14	- 5 ± 18
	$[8,2]5/2^+$	- 10	60 *	30 *	0 *
	$f_{35}(1870)$	- 60 ± ?	-100 ± ?		
	$[10,4]5/2^-$	- 20	- 90		
	$f_{37}(1950)$	-133 ± 46	-100 ± 41		
	$[10,4]7/2^+$	- 50 *	- 70 *		
$\{56\}_2$ L = 0^+	$p_{11}(1470)$	- 55 ± 28		2 ± 25	
	$[8,2]1/2^+$	27		-18	
$\{70\}_2$ L = 0^+	$p_{11}(1750)$	26 ± 28		27 ± 22	
	$[8,2]1/2^+$	- 40		10	

TABLE V. (cont.)

{SU6} L	N*(mass) $[SU3, 2S_q+1]J^P$	$A^{P(V3)}_{1/2}$	$A^{P(V3)}_{1/2}$	$A^{N}_{1/2}$	$A^{N}_{3/2}$
			Part c [a]		
$\{56\}_0$ L = 0^+	$p_{33}(1230)$	-142 ± 1	-261 ± 1		
	$[10,4]3/2^+$	-108 *	-187 *		
$\{70\}_1$ L = 1^-	$s_{11}(1545)$	36 ± 2		- 27 ± 9	
	$[8,2]1/2^-$	156		-108	
	$d_{13}(1512)$	0 ± 6	174 ± 6	- 88 ± 7	-119 ± 25
	$[8,2]3/2^-$	- 34	109 *	- 31	-109 *
	$s_{31}(1610)$	78 ± 6			
	$[10,2]1/2^-$	47			
	$d_{33}(1660)$	41 ± 28	21 ± 20		
	$[10,2]3/2^-$	88	84 *		
	$s_{11}(1690)$	54 ± 5		- 82 ± 19	
	$[8,4]1/2^-$	0		30	
	$d_{13}(1700)$	23 ± ?	35 ± ?	- 15 ± ?	28 ± ?
	$[8,4]3/2^-$	0 *	0 *	- 10 *	- 40 *
	$d_{15}(1670)$	19 ± 7	16 ± 2	- 17 ± 4	- 49 ± 4
	$[8,4]5/2^-$	0 *	0 *	- 38 *	- 53 *

TABLE V. (cont.)

{SU6} L	N^*(mass) $[SU3, 2S_q+1]J^P$	$A^{P(V3)}_{1/2}$	$A^{P(V3)}_{3/2}$	$A^{N}_{1/2}$	$A^{N}_{3/2}$
			Part d[a]		
$\{56\}_2 L = 2^+$	$f_{15}(1690)$	-14 ± 3	147 ± 6	23 ± 3	-41 ± 4
	$[8,2]5/2^+$	-10	60 *	30 *	0 *
	$f_{35}(1870)$	?[b]	?[b]		
	$[10,4]5/2^-$	-20	- 90		
	$f_{37}(1950)$	-80[c]	-180[c]		
	$[10,4]7/2^+$	-50 *	- 70 *		
$\{56\}_2 L=0^+$	$p_{11}(1470)$	-87 ± 2		33 ± 13	
	$[8,2]1/2^+$	27		-18	
$\{70\}_2 L=0^+$	$p_{11}(1750)$	16 ± 25		57 ± 22	
	$[8,2]1/2^+$	-40		10	

a. *Part a and b* list the previously published [5] results from an average over seven fits where the error is the spread over the seven fits, which part c and d are taken as an average over the three best fits I-III with the errors now being the spread over these three fits.

In parts c and d, the errors probably do not represent a realistic estimate of the uncertainties of the couplings due to the relatively small number of fits

TABLE V. (cont.)

of good quality and the appreciable uncertainties in the estimation of the πN resonance parameters.

$A_\lambda^{P,N}$ denotes decays of $N_{1/2}^{*+,0}$ (I=1/2) and A_λ^{V3} $N_{3/2}^*$ (I=3/2) through helicity λ=1/2, 3/2 respectively. Units are $GeV^{-1/2}\times10^{-3}$. Directly underneath the partial-wave analysis result we give the quark model result for the usual assignment of the resonance to an {SU6}, [SU3, $2S_Q + 1$] multiplet, where S_Q denotes the spin of the quark state. An asterisk labels quark model results which do not involve a difference of two terms. Tables Va and Vc comprise resonances assigned to the $\{56\}_0 L = 0^+$ and $\{70\}_1$ $L = 1^-$ multiplets and Tables Vb and d the $\{56\}_2$ $L = 2^+$, $\{56\}_2$ $L = 0^+$ and $\{70\}_2$ $L = 0^+$ multiplets where the suffix indicates the equivalent harmonic oscillator energy level, n.

b. See comment in section 6.

c. Estimate from real part (see text).

TABLE VI. Partial-wave amplitudes of fit III as a function of photon laboratory energy.[a]

PROTON	S1/2				P1/2			
EG(MEV)	REAL A	IMAG	REAL B	IMAG	REAL A	IMAG	REAL B	IMAG
			Part a					
250	1.366	.067	C.OCC	0.000	.196	-.017	0.000	0.000
270	1.384	.084	C.OCO	0.000	.231	-.017	C.000	0.000
290	1.397	.102	C.OCC	0.000	.271	-.016	0.000	0.000
310	1.405	.122	C.OCC	0.000	.317	-.011	0.000	0.000
330	1.411	.144	C.OCC	0.000	.372	-.001	0.000	0.000
350	1.416	.169	C.OCC	0.000	.434	.023	0.000	0.000
370	1.419	.195	C.OCC	0.000	.501	.059	0.000	0.000
390	1.423	.224	C.CCC	0.000	.568	.111	0.000	0.000
410	1.425	.256	C.OCC	0.000	.634	.178	C.000	0.000
430	1.428	.290	C.CCC	0.000	.695	.263	0.000	0.000
450	1.430	.327	C.OCO	0.000	.744	.365	0.000	0.000
470	1.432	.368	C.OCC	0.000	.777	.482	0.000	0.000
490	1.432	.412	C.OCC	0.000	.787	.609	0.000	0.000
510	1.431	.459	C.OCC	0.000	.772	.739	C.000	0.000
530	1.429	.510	C.OCC	0.000	.729	.864	0.000	0.000
550	1.423	.564	C.CCC	0.000	.662	.976	0.000	0.000
570	1.415	.622	C.OCC	0.000	.577	1.068	0.000	0.000
590	1.402	.683	C.OCC	0.000	.480	1.136	0.000	0.000
610	1.384	.748	C.OCO	0.000	.379	1.181	0.000	0.000
630	1.360	.815	C.OCC	0.000	.278	1.205	0.000	0.000
650	1.329	.885	C.OCC	0.000	.185	1.209	0.000	0.000
670	1.291	.959	C.OCO	0.000	.097	1.203	0.000	0.000
690	1.246	1.036	C.OCC	0.000	.015	1.184	0.000	0.000
710	1.191	1.129	0.OCC	0.000	-.059	1.154	0.000	0.000
730	1.073	1.262	C.CCC	0.000	-.124	1.116	0.000	0.000
750	.876	1.321	C.OCC	0.000	-.181	1.071	C.000	0.000
770	.669	1.287	C.CCC	0.000	-.230	1.022	0.000	C.000
790	.509	1.165	C.OCC	0.000	-.272	.970	0.000	0.000
810	.432	1.012	C.OCC	0.000	-.309	.915	0.000	0.000
830	.423	.881	C.OCC	0.000	-.339	.859	0.000	0.000
850	.448	.788	C.OCO	0.000	-.365	.800	0.000	0.000
870	.483	.729	C.OCC	0.000	-.388	.740	0.000	0.000
890	.515	.692	C.OCC	0.000	-.406	.678	0.000	0.000
910	.541	.670	C.OOC	0.000	-.420	.614	0.000	0.000
930	.561	.657	C.OCO	0.000	-.431	.547	0.000	0.000
950	.574	.647	C.CCC	0.000	-.437	.479	0.000	0.000
970	.583	.640	C.OCO	0.000	-.438	.409	0.000	0.000
990	.589	.633	C.OCC	0.000	-.435	.336	C.000	0.000
1010	.592	.625	C.OCC	0.000	-.426	.262	0.000	0.000
1030	.594	.616	C.OCC	0.000	-.411	.187	0.000	0.000
1050	.596	.607	C.OCO	0.000	-.389	.111	0.000	0.000
1070	.599	.596	C.OCC	0.000	-.362	.038	0.000	0.000
1090	.604	.585	C.OCO	0.000	-.326	-.034	0.000	0.000
1110	.612	.572	C.OCC	0.000	-.286	-.101	0.000	0.000
1130	.625	.559	C.OCC	0.000	-.243	-.163	0.000	0.000
1150	.647	.545	C.OCC	0.000	-.200	-.218	0.000	0.000
1170	.685	.531	C.OCC	0.000	-.164	-.267	0.000	0.000
1190	.753	.516	C.OCC	0.000	-.150	-.309	C.000	0.000
1210	.902	.501	C.OCC	0.000	-.201	-.345	0.000	0.000

TABLE VI. (cont.)

PROTON	P3/2				D3/2			
EG(MEV)	REAL A	IMAG	REAL B	IMAG	REAL A	IMAG	REAL B	IMAG
			Part a (cont.)					
250	.224	-.003	.500	-.009	-.069	.000	.389	-.001
270	.240	-.005	.542	-.012	-.077	.000	.458	-.001
290	.253	-.006	.576	-.016	-.083	.000	.526	-.001
310	.264	-.008	.604	-.020	-.089	.000	.592	-.002
330	.274	-.009	.626	-.024	-.094	.000	.659	-.002
350	.283	-.011	.644	-.029	-.098	.000	.727	-.002
370	.291	-.012	.658	-.033	-.101	.000	.798	-.002
390	.298	-.014	.668	-.037	-.105	.000	.874	.000
410	.304	-.016	.676	-.041	-.108	.000	.955	.004
430	.310	-.017	.681	-.045	-.111	.001	1.043	.013
450	.315	-.018	.684	-.049	-.113	.001	1.140	.026
470	.319	-.020	.685	-.053	-.115	.002	1.247	.047
490	.323	-.021	.684	-.056	-.117	.003	1.365	.078
510	.326	-.022	.683	-.059	-.119	.004	1.497	.122
530	.329	-.024	.680	-.062	-.121	.006	1.642	.186
550	.331	-.025	.677	-.065	-.122	.008	1.803	.277
570	.333	-.026	.673	-.068	-.124	.011	1.977	.403
590	.334	-.027	.668	-.070	-.125	.014	2.161	.578
610	.334	-.027	.663	-.072	-.126	.019	2.342	.816
630	.334	-.028	.657	-.074	-.128	.025	2.500	1.133
650	.334	-.029	.652	-.076	-.132	.032	2.599	1.538
670	.333	-.030	.646	-.078	-.137	.040	2.589	2.023
690	.332	-.031	.641	-.080	-.145	.048	2.419	2.544
710	.330	-.032	.635	-.085	-.155	.055	2.064	3.017
730	.333	-.037	.647	-.098	-.169	.059	1.561	3.347
750	.333	-.025	.648	-.063	-.183	.059	.999	3.479
770	.325	-.025	.627	-.062	-.198	.056	.488	3.425
790	.319	-.024	.616	-.060	-.212	.051	.058	3.294
810	.313	-.024	.604	-.058	-.225	.043	-.293	3.071
830	.306	-.024	.589	-.058	-.238	.033	-.539	2.810
850	.299	-.025	.575	-.062	-.252	.022	-.691	2.551
870	.291	-.026	.563	-.067	-.268	.007	-.768	2.318
890	.283	-.028	.551	-.073	-.286	-.014	-.791	2.128
910	.275	-.030	.540	-.080	-.305	-.046	-.779	1.990
930	.267	-.033	.529	-.089	-.323	-.093	-.758	1.913
950	.259	-.036	.519	-.099	-.326	-.161	-.761	1.899
970	.250	-.039	.509	-.110	-.295	-.246	-.832	1.925
990	.241	-.043	.499	-.123	-.218	-.319	-.988	1.922
1010	.232	-.047	.490	-.137	-.114	-.343	-1.175	1.821
1030	.222	-.052	.481	-.153	-.022	-.318	-1.314	1.640
1050	.213	-.057	.472	-.171	.038	-.271	-1.376	1.444
1070	.204	-.063	.465	-.191	.071	-.225	-1.382	1.271
1090	.194	-.070	.458	-.212	.088	-.188	-1.363	1.130
1110	.184	-.076	.450	-.235	.096	-.158	-1.330	1.017
1130	.173	-.084	.441	-.259	.099	-.135	1.292	.925
1150	.161	-.091	.429	-.284	.099	-.117	1.247	.849
1170	.145	-.099	.407	-.310	.096	-.103	-1.189	.786
1190	.122	-.107	.362	-.337	.088	-.092	-1.098	.732
1210	.078	-.115	.252	-.363	.067	.083	-.909	.686

TABLE VI. (cont.)

PROTON	D5/2				F5/2			
EG(MEV)	REAL A	IMAG	REAL B	IMAG	REAL A	IMAG	REAL B	IMAG
				Part a (cont.)				
250	.077	.000	.095	.000	-.037	.000	.069	.000
270	.088	.000	.111	.000	-.044	.000	.086	.000
290	.096	.000	.125	.000	-.052	.000	.103	.000
310	.104	.000	.138	.000	-.058	.000	.120	.000
330	.112	.000	.150	.000	-.065	.000	.136	.000
350	.118	.000	.161	.000	-.071	.000	.152	.000
370	.124	.000	.170	.000	-.077	.000	.168	.000
390	.130	.000	.179	.000	-.082	.000	.184	.000
410	.136	.000	.186	.000	-.087	.000	.200	.000
430	.141	.000	.193	.000	-.093	.000	.216	.000
450	.147	.000	.198	.000	-.098	.000	.232	.000
470	.152	.000	.203	.000	-.103	.000	.249	.000
490	.158	.000	.206	.000	-.108	.000	.265	.000
510	.164	.000	.209	.000	-.112	.000	.283	.000
530	.169	.000	.211	.000	-.117	.000	.301	.000
550	.175	.001	.212	-.001	-.122	.000	.320	.000
570	.181	.001	.213	-.001	-.127	.000	.340	.000
590	.188	.001	.212	-.001	-.131	.000	.361	.000
610	.194	.001	.211	-.001	-.136	.000	.383	.001
630	.201	.002	.209	-.002	-.141	.000	.408	.001
650	.208	.002	.206	-.002	-.145	.000	.434	.002
670	.216	.003	.203	-.003	-.149	.000	.463	.003
690	.224	.004	.199	-.004	-.154	.001	.494	.006
710	.232	.005	.194	-.005	-.157	.001	.528	.009
730	.240	.007	.188	-.007	-.161	.001	.566	.013
750	.250	.009	.181	-.008	-.164	.002	.608	.019
770	.259	.011	.174	-.011	-.167	.003	.655	.027
790	.270	.014	.166	-.014	-.170	.004	.708	.039
810	.281	.019	.157	-.018	-.172	.006	.767	.055
830	.293	.024	.147	-.024	-.173	.008	.833	.078
850	.306	.032	.136	-.032	-.173	.012	.907	.110
870	.319	.042	.125	-.042	-.173	.017	.991	.155
890	.332	.057	.114	-.056	-.171	.024	1.082	.218
910	.343	.076	.104	-.075	-.169	.033	1.180	.307
930	.348	.102	.100	-.100	-.167	.047	1.276	.432
950	.345	.132	.106	-.130	-.167	.065	1.356	.602
970	.327	.161	.125	-.159	-.171	.089	1.394	.822
990	.296	.179	.158	-.177	-.184	.117	1.356	1.076
1010	.261	.178	.194	-.176	-.207	.143	1.216	1.319
1030	.234	.163	.224	-.161	-.240	.162	.988	1.489
1050	.218	.140	.242	-.138	-.277	.168	.726	1.543
1070	.213	.117	.250	-.115	-.310	.162	.502	1.494
1090	.215	.096	.251	-.095	-.336	.153	.331	1.409
1110	.222	.080	.248	-.079	-.357	.139	.208	1.278
1130	.232	.067	.243	-.066	-.371	.123	.149	1.134
1150	.243	.056	.237	-.056	-.378	.108	.147	.996
1170	.256	.048	.230	-.048	-.380	.095	.196	.873
1190	.270	.042	.222	-.041	-.374	.084	.304	.769
1210	.290	.037	.209	-.036	-.357	.074	.521	.682

TABLE VI. (cont.)

NEUTRON	S1/2				P1/2			
EG(MEV)	REAL A	IMAG	REAL B	IMAG	REAL A	IMAG	REAL B	IMAG
			Part b					
250	-2.022	-.147	C.OCC	0.000	-.357	.034	0.000	0.000
270	-2.088	-.182	C.OCC	0.000	-.406	.034	0.000	0.000
290	-2.141	-.219	C.COO	0.000	-.452	.030	0.000	0.000
310	-2.182	-.26C	C.CCC	0.000	-.496	.020	0.000	0.000
330	-2.213	-.3C4	C.OCO	0.000	-.539	.003	0.000	0.000
350	-2.236	-.351	C.CCC	0.000	-.579	-.023	0.000	0.000
370	-2.250	-.402	C.OCC	0.000	-.614	-.059	0.000	0.000
390	-2.256	-.456	C.OCC	0.000	-.642	-.104	0.000	0.000
410	-2.255	-.513	C.OCC	0.000	-.661	-.159	0.000	0.000
430	-2.245	-.575	C.OCO	0.000	-.668	-.222	0.000	0.000
450	-2.227	-.64C	C.OCC	0.000	-.661	-.291	0.000	0.000
470	-2.201	-.7C8	C.OCO	0.000	-.638	-.362	0.000	0.000
490	-2.166	-.78C	C.OCC	0.000	-.598	-.431	0.000	0.000
510	-2.121	-.855	C.OCO	0.000	-.541	-.493	0.000	0.000
530	-2.066	-.933	C.OCC	0.000	-.472	-.542	0.000	0.000
550	-2.001	-1.012	C.OCC	0.000	-.394	-.575	0.000	0.000
570	-1.923	-1.093	C.OCC	0.000	-.314	-.591	0.000	0.000
590	-1.832	-1.174	C.OCO	0.000	-.237	-.592	0.000	0.000
610	-1.729	-1.254	C.CCC	0.000	-.168	-.580	0.000	0.000
630	-1.611	-1.332	C.OCC	0.000	-.109	-.558	0.000	0.000
650	-1.478	-1.4C5	C.OCC	0.000	-.060	-.531	0.000	0.000
670	-1.333	-1.472	C.OCC	0.000	-.021	-.501	0.000	0.000
690	-1.177	-1.537	C.OCO	0.000	.007	-.469	0.000	0.000
710	-1.007	-1.616	C.OCC	0.000	.025	-.439	0.000	0.000
730	-.724	-1.754	C.OCO	0.000	.034	-.411	0.000	0.000
750	-.321	-1.721	C.OCC	0.000	.036	-.388	0.000	0.000
770	.053	-1.507	C.OCO	0.000	.032	-.370	0.000	0.000
790	.291	-1.157	C.CCC	0.000	.022	-.358	0.000	0.000
810	.354	-.798	C.OCO	0.000	.009	-.351	0.000	0.000
830	.297	-.518	C.OCC	0.000	-.007	-.352	0.000	0.000
850	.193	-.332	C.OCC	0.000	-.025	-.359	0.000	0.000
870	.086	-.219	C.OCC	0.000	-.044	-.374	0.000	0.000
890	-.004	-.153	C.OCC	0.000	-.061	-.394	0.000	0.000
910	-.076	-.115	C.OCC	0.000	-.077	-.422	0.000	0.000
930	-.129	-.094	C.OCO	0.000	-.089	-.456	0.000	0.000
950	-.167	-.082	C.OOC	0.000	-.097	-.495	0.000	0.000
970	-.195	-.075	C.OCC	0.000	-.100	-.539	0.000	0.000
990	-.213	-.07C	C.OCO	0.000	-.095	-.586	0.000	0.000
1010	-.225	-.066	C.OCO	0.000	-.081	-.635	0.000	0.000
1030	-.231	-.062	C.OCC	0.000	-.058	-.684	0.000	0.000
1050	-.234	-.057	C.OCC	0.000	-.027	-.730	0.000	0.000
1070	-.235	-.052	C.OCC	0.000	.013	-.770	0.000	0.000
1090	-.234	-.045	C.OOC	0.000	.057	-.803	0.000	0.000
1110	-.232	-.038	C.OCC	0.000	.104	-.825	0.000	0.000
1130	-.230	-.03C	C.OCC	0.000	.148	-.836	0.000	0.000
1150	-.227	-.021	C.CCC	0.000	.182	-.835	0.000	0.000
1170	-.223	-.012	C.OOC	0.000	.193	-.822	0.000	0.000
1190	-.219	-.002	C.OCC	0.000	.155	-.799	0.000	0.000
1210	-.210	.008	C.000	0.000	-.008	-.767	0.000	0.000

TABLE VI. (cont.)

NEUTRON	P3/2				D3/2			
EG(MEV)	REAL A	IMAG	REAL B	IMAG	REAL A	IMAG	REAL B	IMAG
				Part b (cont)				
250	-.129	.001	-.716	.002	.152	-.000	-.528	.000
270	-.130	.002	-.798	.002	.179	-.000	-.625	.000
290	-.129	.002	-.871	.003	.206	-.001	-.717	.001
310	-.127	.003	-.936	.003	.234	-.001	-.807	.001
330	-.124	.004	-.996	.004	.263	-.001	-.894	.001
350	-.121	.004	-1.049	.004	.293	-.001	-.980	.001
370	-.118	.005	-1.097	.005	.325	-.001	-1.066	.001
390	-.115	.006	-1.140	.005	.359	.000	-1.151	.000
410	-.113	.007	-1.179	.005	.397	.002	-1.239	-.003
430	-.110	.008	-1.213	.005	.438	.005	-1.328	-.009
450	-.107	.009	-1.244	.004	.483	.011	-1.421	-.018
470	-.105	.009	-1.271	.004	.533	.019	-1.518	-.032
490	-.102	.010	-1.294	.003	.589	.032	-1.620	-.053
510	-.099	.011	-1.314	.003	.650	.050	-1.727	-.084
530	-.097	.012	-1.332	.002	.718	.077	-1.842	-.126
550	-.094	.013	-1.346	.001	.793	.114	-1.964	-.186
570	-.092	.014	-1.358	.000	.874	.165	-2.092	-.269
590	-.089	.015	-1.367	-.002	.959	.237	-2.224	-.383
610	-.086	.016	-1.374	-.003	1.044	.334	-2.351	-.537
630	-.082	.016	-1.378	-.004	1.119	.464	-2.461	-.742
650	-.079	.017	-1.381	-.006	1.172	.631	-2.530	-1.004
670	-.076	.018	-1.381	-.007	1.180	.829	-2.526	-1.315
690	-.071	.018	-1.379	-.007	1.122	1.043	-2.417	-1.648
710	-.067	.019	-1.374	-.005	.990	1.236	-2.188	-1.949
730	-.060	.017	-1.388	.008	.797	1.371	-1.861	-2.157
750	-.054	.024	-1.388	-.034	.580	1.425	-1.494	-2.238
770	-.051	.024	-1.360	-.038	.384	1.403	-1.156	-2.199
790	-.046	.025	-1.340	-.042	.223	1.349	-.866	-2.105
810	-.042	.026	-1.317	-.046	.093	1.258	-.624	-1.953
830	-.038	.026	-1.287	-.046	.007	1.151	-.443	-1.773
850	-.035	.024	-1.256	-.038	-.040	1.044	-.314	-1.589
870	-.030	.022	-1.226	-.026	-.056	.948	-.226	-1.412
890	-.024	.018	-1.196	-.012	-.051	.869	-.162	-1.246
910	-.017	.015	-1.167	.006	-.031	.811	-.114	-1.087
930	-.010	.010	-1.137	.026	-.006	.777	-.076	-.925
950	-.002	.004	-1.108	.050	.009	.768	-.057	-.750
970	.006	-.002	-1.078	.077	-.001	.774	-.079	-.559
990	.016	-.009	-1.049	.108	-.043	.769	-.162	-.380
1010	.026	-.017	-1.020	.143	-.096	.727	-.290	-.261
1030	.036	-.026	-.992	.182	-.130	.654	-.418	-.214
1050	.047	-.035	-.966	.225	-.136	.576	-.514	-.209
1070	.059	-.046	-.942	.272	-.121	.508	-.576	-.216
1090	.071	-.058	-.918	.322	-.094	.452	-.615	-.224
1110	.084	-.070	-.896	.376	-.063	.407	-.640	-.228
1130	.097	-.083	-.872	.433	-.029	.371	-.658	-.228
1150	.109	-.096	-.843	.493	.007	.341	-.674	-.226
1170	.118	-.110	-.798	.554	.048	.316	-.690	-.222
1190	.118	-.124	-.712	.615	.103	.294	-.716	-.216
1210	.092	-.138	-.501	.677	.197	.276	-.772	-.210

TABLE VI. (cont.)

NEUTRON	D5/2				F5/2			
EG(MEV)	REAL A	IMAG	REAL B	IMAG	REAL A	IMAG	REAL B	IMAG
				Part b (cont.)				
250	-.084	.000	-.090	.000	.031	.000	-.063	.000
270	-.095	.000	-.105	.000	.036	.000	-.078	.000
290	-.106	.000	-.117	.000	.041	.000	-.092	.000
310	-.116	.000	-.129	.000	.045	.000	-.106	.000
330	-.126	.000	-.139	.000	.048	.000	-.119	.000
350	-.135	.000	-.148	.000	.051	.000	-.131	.000
370	-.144	.000	-.156	.000	.053	.000	-.143	.000
390	-.152	.000	-.163	.000	.054	.000	-.154	.000
410	-.161	.000	-.168	.000	.055	.000	-.165	.000
430	-.169	.000	-.173	.000	.056	.000	-.175	.000
450	-.178	.000	-.177	.000	.056	.000	-.185	.000
470	-.187	.000	-.179	.000	.056	.000	-.194	.000
490	-.196	.000	-.181	.000	.056	.000	-.204	.000
510	-.205	.000	-.182	.001	.055	.000	-.213	.000
530	-.215	-.000	-.182	.001	.054	.000	-.222	.000
550	-.225	-.001	-.181	.001	.053	.000	-.231	.000
570	-.235	-.001	-.179	.002	.052	.000	-.240	.000
590	-.246	-.001	-.176	.003	.050	.000	-.249	.000
610	-.257	-.001	-.172	.004	.048	.000	-.258	.000
630	-.268	-.002	-.167	.005	.046	.000	-.267	.000
650	-.281	-.003	-.160	.006	.044	-.001	-.277	-.001
670	-.293	-.003	-.153	.008	.041	-.001	-.288	-.001
690	-.306	-.004	-.145	.011	.037	-.002	-.299	-.002
710	-.319	-.006	-.135	.014	.033	-.002	-.311	-.003
730	-.334	-.007	-.124	.018	.029	-.004	-.324	-.004
750	-.348	-.009	-.111	.023	.024	-.005	-.338	-.006
770	-.364	-.012	-.097	.030	.018	-.007	-.353	-.008
790	-.380	-.015	-.080	.039	.010	-.011	-.370	-.012
810	-.397	-.020	-.062	.050	.002	-.015	-.390	-.017
830	-.415	-.026	-.041	.065	-.008	-.021	-.411	-.024
850	-.434	-.034	-.019	.086	-.019	-.030	-.435	-.034
870	-.453	-.045	.005	.114	-.032	-.042	-.461	-.047
890	-.472	-.060	.028	.153	-.046	-.060	-.490	-.067
910	-.489	-.080	.045	.205	-.062	-.084	-.521	-.094
930	-.501	-.107	.050	.274	-.076	-.119	-.551	-.132
950	-.502	-.138	.028	.355	-.085	-.165	-.577	-.184
970	-.488	-.169	-.032	.433	-.082	-.226	-.590	-.251
990	-.461	-.188	-.126	.481	-.057	-.295	-.580	-.329
1010	-.430	-.187	-.231	.481	-.003	-.362	-.539	-.403
1030	-.405	-.171	-.318	.438	.076	-.409	-.471	-.455
1050	-.393	-.147	-.372	.377	.165	-.424	-.393	-.472
1070	-.391	-.123	-.399	.315	.246	-.410	-.327	-.457
1090	-.397	-.101	-.405	.260	.312	-.387	-.277	-.431
1110	-.408	-.084	-.399	.215	.367	-.351	-.242	-.391
1130	-.421	-.070	-.386	.179	.405	-.311	-.227	-.347
1150	-.435	-.059	-.370	.152	.429	-.273	-.230	-.304
1170	-.450	-.051	-.350	.130	.440	-.240	-.249	-.267
1190	-.466	-.044	-.326	.113	.436	-.211	-.286	-.235
1210	-.487	-.039	-.289	.099	.404	-.187	-.357	-.209

TABLE VI. (cont.)

V3	S1/2				P1/2			
EG(MEV)	REAL A	IMAG	REAL B	IMAG	REAL A	IMAG	REAL B	IMAG
			Part c					
250	-1.469	.175	C.OCC	0.000	-.585	.019	0.000	0.000
270	-1.504	.21C	C.OCC	0.000	-.645	.025	0.000	0.000
290	-1.534	.247	C.CCC	0.000	-.695	.031	0.000	0.000
310	-1.560	.284	C.OCC	0.000	-.736	.037	0.000	0.000
330	-1.577	.322	C.OCC	0.000	-.770	.042	0.000	0.000
350	-1.590	.36C	C.OCC	0.000	-.796	.047	0.000	0.000
370	-1.604	.398	C.OCC	0.000	-.815	.052	0.000	0.000
390	-1.619	.435	C.OCC	0.000	-.829	.057	C.000	0.000
410	-1.637	.468	C.OCC	0.000	-.837	.061	0.000	C.000
430	-1.648	.494	C.OCC	0.000	-.840	.065	C.000	0.000
450	-1.656	.532	C.OCC	0.000	-.839	.069	0.000	0.000
470	-1.671	.568	C.OCC	0.000	-.834	.073	0.000	0.000
490	-1.690	.603	C.OCC	0.000	-.827	.077	0.000	0.000
510	-1.712	.636	C.OCC	0.000	-.816	.080	0.000	0.000
530	-1.739	.667	C.CCC	0.000	-.804	.083	0.000	0.000
550	-1.771	.694	C.OCC	0.000	-.790	.087	C.000	0.000
570	-1.808	.719	C.OCC	0.000	-.774	.090	0.000	0.000
590	-1.851	.739	C.OCC	0.000	-.759	.092	0.000	0.000
610	-1.901	.753	C.OCC	0.000	-.743	.094	0.000	0.000
630	-1.957	.761	C.OCC	0.000	-.730	.092	0.000	0.000
650	-2.022	.761	C.OCC	0.000	-.695	.072	0.000	0.000
670	-2.092	.75C	C.OCC	0.000	-.664	.109	0.000	0.000
690	-2.169	.728	C.OCC	0.000	-.658	.113	0.000	0.000
710	-2.252	.69C	C.OCC	0.000	-.645	.117	0.000	0.000
730	-2.339	.634	C.OCC	0.000	-.632	.121	0.000	0.000
750	-2.428	.558	C.CCC	0.000	-.622	.126	0.000	0.000
770	-2.514	.457	C.OCC	0.000	-.613	.128	C.000	0.000
790	-2.592	.329	C.OCC	0.000	-.605	.127	0.000	0.000
810	-2.653	.172	C.OCC	0.000	-.597	.127	0.000	0.000
830	-2.688	-.011	C.OOC	0.000	-.590	.125	0.000	0.000
850	-2.690	-.217	C.CCC	0.000	-.586	.124	0.000	0.000
870	-2.642	-.435	C.OCC	0.000	-.580	.122	0.000	0.000
890	-2.541	-.651	C.CCC	0.000	-.576	.120	0.000	0.000
910	-2.387	-.847	C.OCC	0.000	-.573	.118	0.000	0.000
930	-2.186	-1.005	0.OCC	0.000	-.572	.115	0.000	0.000
950	-1.954	-1.111	C.CCC	0.000	-.571	.111	0.000	0.000
970	-1.708	-1.161	C.OCC	0.000	-.571	.108	0.000	0.000
990	-1.466	-1.154	C.OCC	0.000	-.572	.103	0.000	0.000
1010	-1.244	-1.101	C.OCC	0.000	-.574	.098	0.000	0.000
1030	-1.049	-1.011	0.00C	0.000	-.577	.092	0.000	0.000
1050	-.886	-.897	C.CCC	0.000	-.581	.085	0.000	0.000
1070	-.753	-.769	C.OCC	0.000	-.585	.076	0.000	0.000
1090	-.651	-.635	C.OCC	0.000	-.589	.067	0.000	0.000
1110	-.571	-.501	C.OCC	0.000	-.592	.055	0.000	0.000
1130	-.510	-.37C	C.CCC	0.000	-.595	.042	0.000	0.000
1150	-.463	-.245	C.OCC	0.000	-.597	.027	0.000	0.000
1170	-.424	-.128	C.OCC	0.000	-.601	.009	0.000	0.000
1190	-.381	-.019	C.OCC	0.000	-.607	-.012	0.000	0.000
1210	-.305	.083	C.OCC	0.000	-.624	-.036	0.000	0.000

TABLE VI. (cont.)

V3	P3/2				D3/2			
EG(MEV)	REAL A	IMAG	REAL B	IMAG	REAL A	IMAG	REAL B	IMAG
				Part c (cont)				
250	.883	.466	-2.696	-1.085	.118	.000	-.427	.000
270	1.106	.914	-3.184	-2.085	.136	.000	-.498	.000
290	1.109	1.550	-3.154	-3.463	.153	.000	-.565	.000
310	.761	2.170	-2.349	-4.748	.170	.000	-.626	.000
330	.161	2.495	-1.028	-5.345	.185	.000	-.682	.000
350	-.434	2.487	.232	-5.215	.200	.000	-.734	.000
370	-.879	2.297	1.133	-4.715	.214	.000	-.781	.000
390	-1.162	2.028	1.672	-4.074	.229	.000	-.825	.000
410	-1.311	1.761	1.925	-3.461	.243	.000	-.864	.000
430	-1.373	1.527	1.997	-2.935	.258	-.001	-.900	.000
450	-1.382	1.333	1.968	-2.504	.273	-.001	-.932	.000
470	-1.362	1.173	1.883	-2.155	.288	-.001	-.961	.000
490	-1.325	1.043	1.771	-1.871	.305	-.001	-.987	.000
510	-1.279	.936	1.646	-1.640	.322	-.001	-1.011	.001
530	-1.229	.847	1.517	-1.448	.340	-.002	-1.032	.001
550	-1.177	.772	1.389	-1.287	.359	-.002	-1.050	.001
570	-1.124	.708	1.262	-1.151	.380	-.002	-1.066	.001
590	-1.072	.653	1.140	-1.035	.402	-.001	-1.081	.001
610	-1.021	.605	1.022	-.934	.426	-.001	-1.093	.000
630	-.971	.564	.908	-.845	.452	.001	-1.104	.000
650	-.922	.526	.799	-.766	.480	.004	-1.114	-.002
670	-.875	.493	.694	-.696	.510	.007	-1.122	-.003
690	-.831	.462	.592	-.633	.542	.013	-1.129	-.006
710	-.788	.434	.495	-.575	.576	.021	-1.134	-.009
730	-.748	.408	.400	-.521	.613	.032	-1.139	-.014
750	-.711	.383	.308	-.471	.650	.048	-1.142	-.020
770	-.678	.359	.217	-.424	.688	.067	-1.144	-.029
790	-.649	.335	.127	-.377	.725	.093	-1.144	-.040
810	-.635	.310	.026	-.328	.760	.124	-1.141	-.053
830	-.611	.249	-.083	-.305	.789	.160	-1.134	-.068
850	-.563	.206	-.176	-.301	.809	.200	-1.123	-.085
870	-.520	.170	-.254	-.296	.822	.241	-1.107	-.103
890	-.479	.137	-.326	-.291	.826	.279	-1.085	-.119
910	-.439	.106	-.393	-.287	.823	.312	-1.059	-.133
930	-.401	.076	-.456	-.286	.814	.336	-1.030	-.143
950	-.365	.047	-.514	-.286	.804	.352	-.999	-.150
970	-.331	.019	-.567	-.287	.795	.359	-.967	-.153
990	-.299	-.008	-.617	-.291	.789	.360	-.936	-.154
1010	-.269	-.035	-.662	-.296	.788	.357	-.906	-.152
1030	-.241	-.061	-.703	-.302	.796	.351	-.879	-.150
1050	-.215	-.087	-.740	-.310	.806	.355	-.852	-.151
1070	-.193	-.112	-.773	-.319	.813	.357	-.823	-.152
1090	-.174	-.137	-.803	-.329	.819	.358	-.794	-.153
1110	-.161	-.161	-.831	-.340	.827	.357	-.764	-.152
1130	-.152	-.185	-.857	-.353	.838	.355	-.735	-.152
1150	-.152	-.208	-.884	-.366	.853	.353	-.708	-.151
1170	-.161	-.231	-.919	-.380	.879	.350	-.685	-.149
1190	-.193	-.252	-.975	-.395	.926	.347	-.669	-.148
1210	-.281	-.275	-1.099	-.411	1.027	.345	-.678	-.147

TABLE VI. (cont.)

V3	D5/2				F5/2			
EG(MEV)	REAL A	IMAG	REAL B	IMAG	REAL A	IMAG	REAL B	IMAG
				Part c (cont.)				
250	-.083	C.00C	-.067	.000	.027	.000	-.055	.000
270	-.096	.00C	-.076	.000	.031	.000	-.068	.000
290	-.109	.00C	-.084	.000	.035	.000	-.080	.000
310	-.121	.00C	-.091	.000	.039	.000	-.091	.000
330	-.132	.00C	-.096	.000	.042	.000	-.102	.000
350	-.143	.00C	-.101	.000	.044	.000	-.113	.000
370	-.153	.00C	-.104	.000	.046	.000	-.122	.000
390	-.163	.00C	-.107	.000	.047	.000	-.131	.000
410	-.173	.00C	-.109	.000	.048	.000	-.140	.000
430	-.182	.00C	-.110	.000	.049	.000	-.147	.000
450	-.191	.00C	-.111	.000	.049	.000	-.155	.000
470	-.200	.000	-.111	.000	.050	.000	-.161	.000
490	-.208	.00C	-.111	.000	.050	.000	-.167	.000
510	-.216	.000	-.111	.000	.049	.000	-.173	.000
530	-.223	.00C	-.110	.000	.049	.000	-.178	.000
550	-.229	.00C	-.110	.000	.049	.000	-.182	.000
570	-.235	-.001	-.109	.000	.048	.000	-.186	.000
590	-.241	-.001	-.108	.000	.048	.000	-.190	.000
610	-.245	-.001	-.108	.000	.048	.000	-.192	.000
630	-.249	-.001	-.107	.000	.047	.000	-.195	.000
650	-.251	-.001	-.107	.000	.047	.000	-.197	.000
670	-.253	-.001	-.106	.000	.047	.000	-.198	.000
690	-.254	-.001	-.106	.000	.048	.000	-.199	.000
710	-.254	-.001	-.107	.000	.048	.000	-.199	.000
730	-.253	-.002	-.107	.000	.049	.000	-.199	.000
750	-.251	-.002	-.109	.000	.050	.000	-.198	.000
770	-.247	-.002	-.110	.000	.052	.000	-.197	.000
790	-.241	-.001	-.112	.000	.055	.001	-.195	.000
810	-.234	-.001	-.115	.000	.058	.001	-.193	.000
830	-.226	.000	-.118	.000	.062	.001	-.190	.000
850	-.214	.001	-.122	.000	.066	.001	-.186	.000
870	-.202	.003	-.127	-.001	.071	.002	-.182	.001
890	-.189	.005	-.132	-.001	.077	.003	-.177	.001
910	-.175	.008	-.138	-.002	.085	.003	-.172	.001
930	-.159	.011	-.144	-.002	.094	.005	-.166	.001
950	-.141	.014	-.152	-.003	.103	.006	-.159	.002
970	-.122	.018	-.160	-.003	.115	.007	-.151	.002
990	-.100	.022	-.169	-.004	.128	.010	-.142	.003
1010	-.077	.027	-.179	-.005	.144	.012	-.132	.004
1030	-.053	.032	-.189	-.006	.161	.015	-.121	.005
1050	-.026	.037	-.201	-.007	.180	.019	-.109	.006
1070	.002	.043	-.213	-.008	.202	.024	-.096	.008
1090	.034	.049	-.227	-.009	.227	.030	-.081	.010
1110	.068	.055	-.242	-.011	.255	.038	-.064	.012
1130	.103	.062	-.257	-.012	.286	.047	-.046	.015
1150	.144	.069	-.274	-.013	.323	.058	-.025	.019
1170	.187	.077	-.293	-.015	.365	.072	-.001	.023
1190	.239	.085	-.314	-.016	.417	.088	.028	.029
1210	.311	.093	-.339	-.018	.495	.106	.065	.034

TABLE VI. (cont.)

V3		F7/2		
EG(MEV)	REAL A	IMAG	REAL B	IMAG
			Part c (cont.)	
250	-.024	.000	-.022	.000
270	-.028	.000	-.028	.000
290	-.032	.000	-.033	.000
310	-.035	.000	-.039	.000
330	-.038	.000	-.044	.000
350	-.040	.000	-.050	.000
370	-.042	.000	-.055	.000
390	-.043	.000	-.061	.000
410	-.043	.000	-.066	.000
430	-.044	.000	-.071	.000
450	-.043	.000	-.077	.000
470	-.043	.000	-.082	.000
490	-.042	.000	-.087	.000
510	-.040	.000	-.092	.000
530	-.039	.000	-.098	.000
550	-.037	.000	-.103	.000
570	-.034	.000	-.109	.000
590	-.031	.000	-.114	.000
610	-.028	.000	-.120	.000
630	-.024	.000	-.126	.000
650	-.020	.000	-.132	.000
670	-.015	.000	-.138	.000
690	-.010	.000	-.145	.000
710	-.004	.000	-.151	.000
730	.002	.000	-.158	.000
750	.009	.000	-.166	.000
770	.017	.000	-.173	.000
790	.025	.000	-.181	.000
810	.034	.001	-.190	.000
830	.044	.001	-.199	.000
850	.055	.001	-.208	.000
870	.067	.001	-.219	.000
890	.080	.002	-.229	.000
910	.094	.002	-.241	.000
930	.110	.003	-.253	.000
950	.127	.004	-.267	.000
970	.146	.004	-.281	.000
990	.167	.006	-.297	.000
1010	.189	.007	-.314	.000
1030	.215	.008	-.333	.000
1050	.243	.010	-.353	.000
1070	.274	.012	-.375	.000
1090	.308	.015	-.400	-.001
1110	.346	.018	-.427	-.001
1130	.389	.021	-.457	-.001
1150	.437	.025	-.490	-.001
1170	.493	.030	-.528	-.001
1190	.559	.035	-.570	-.001
1210	.641	.042	-.619	-.002

[a]The symbols PROTON (Table VIa), NEUTRON (Table VIb), and V3 (Table VIc) refer to our usual isospin labels P, N, V3, while A, B denote amplitudes of total γN-helicity λ= 1/2, 3/2 respectively. EG denotes the photon laboratory energy. These amplitudes are introduced in Appendix B and related to the helicity elements $T_{\ell\pm}$ by 100 $(\sqrt{qk})^{1/2} T_{\ell\pm}$ where q, k are the c.m. momenta in the πN, γN systems.

FIGURE CAPTIONS

Fig. 1) Kinematical environment for this analysis in the grid variable t and E_γ the photon laboratory energy. Indicated are lines of constant t along which the imaginary parts of the invariant amplitudes are calculated in steps of ΔE_γ = 20 MeV. The solid parts of such lines indicate the energy range for which the fixed-t dispersion integral is calculated in the same energy steps, circles marking the two ends of the energy range. The two arrows mark the threshold for $\gamma N \rightarrow \pi N$ and the energy Λ up to which the dispersion integral is determined by K-matrix parameters. The physical boundary for backward scattering is indicated, as well as the energy positions of the δ-functions for the C-parameters (compensating for possible nonconvergence of the partial wave expansion in the unphysical region) and for that part of the D-parameters which represent the f_{37} partial wave (used in the parameterization of the high-energy part of the dispersion integral). The dotted lines indicate constant $u = (M_\Delta)^2$ and $u = (M_N + m)^2$ where m, M_N and M_Δ refer to the masses of pion, nucleon and p_{33} (1230) respectively.

Fig. 2) Angular distributions of differential cross-section measurements for positive pion photoproduction from protons, compared with fit B III.

Fig. 3) Angular distributions of differential cross-section measurements for neutral pion pnotoproduction from protons, compared with fit B III.

Fig. 4) Angular distributions of differential cross-section measurements for negative pion photoproduction from neutrons, compared with fit B III.

Fig. 5) Differential cross-section excitation curves for photoproduction of positive pions from protons, compared with fit B III.

Fig. 6) Differential cross-section excitation curves for photoproduction of neutral pions from protons, compared with fit B III.

Fig. 7) Differential cross-section excitation curves for photoproduction of negative pions from neutrons, compared with fit B III.

Fig. 8) Angular distribution of polarized photon asymmetry for photoproduction of position pion from protons, compared with fits B I-III.

Fig. 9) Angular distribution of polarized photon asymmetry for photoproduction of neutral pions from protons, compared with fits B I-III.

Fig. 10) Angular distribution of polarized photon asymmetry for photoproduction of negative pions from neutrons, compared with fits B I-III.

Fig. 11) Polarized photon asymmetry of positive and negative pions from protons and neutrons as a function of energy at fixed angles from experimental measurements and from fits B I-III.

Fig. 12) Polarized photon asymmetry and recoil nucleon polarization of neutral pions from protons as a function of energy at fixed angles from experimental measurements and from fits B I-III.

Fig. 13) Polarized target asymmetry of positive and neutral pions from protons as a function of energy at fixed angles from experimental measurements and from fits B I-III.

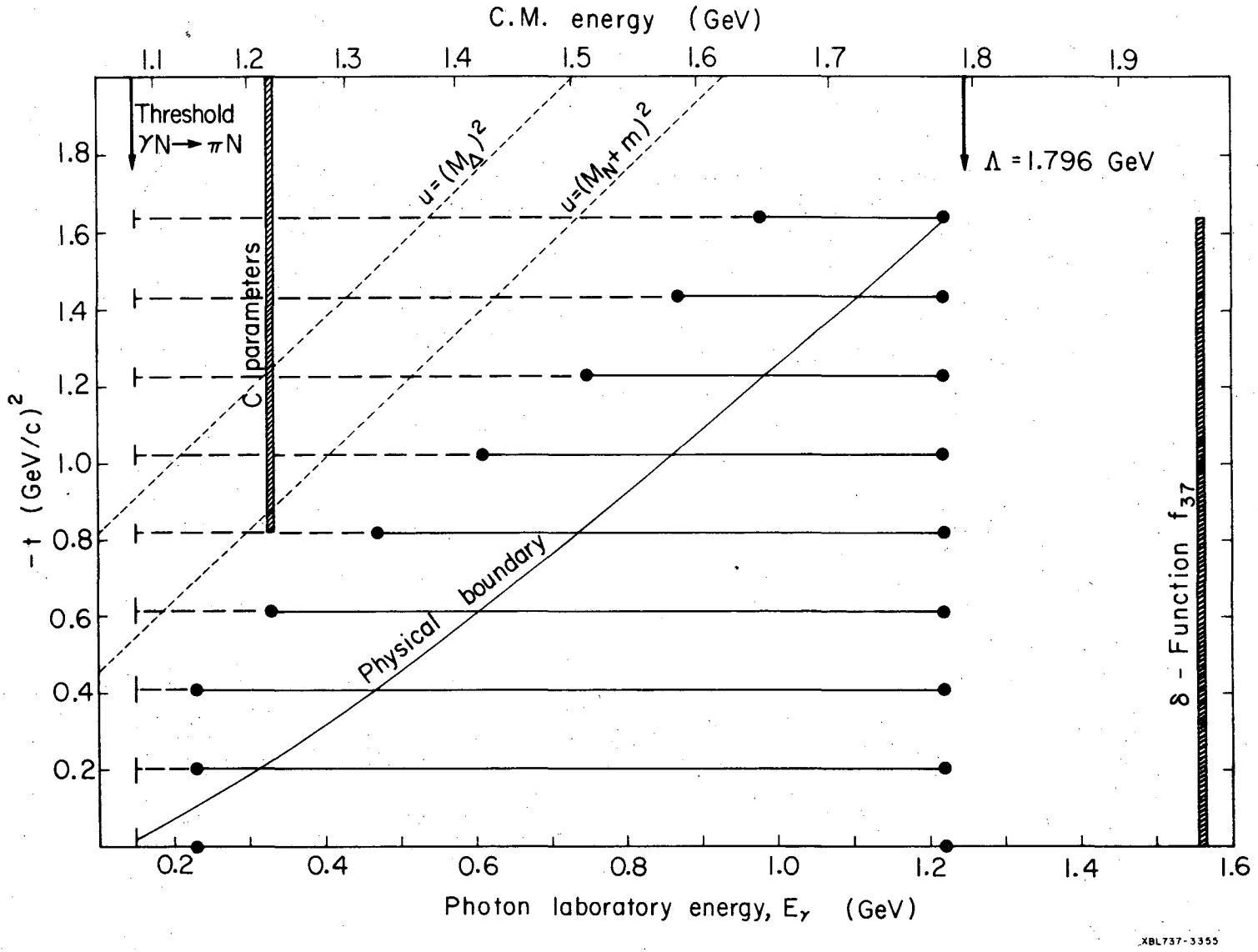
C.M. energy (GeV)
1.1
1.2
1.3
1.4
1.5
1.6
1.7
1.8
1.9
Threshold
γN→πN
u=(M_Δ)²
u=(M_N+m)²
Λ = 1.796 GeV
C parameters
δ - Function f37
Physical boundary
-t (GeV/c)²
0.2
0.4
0.6
0.8
1.0
1.2
1.4
1.6
1.8
Photon laboratory energy, Eγ (GeV)
XBL737-3355

Fig. 1

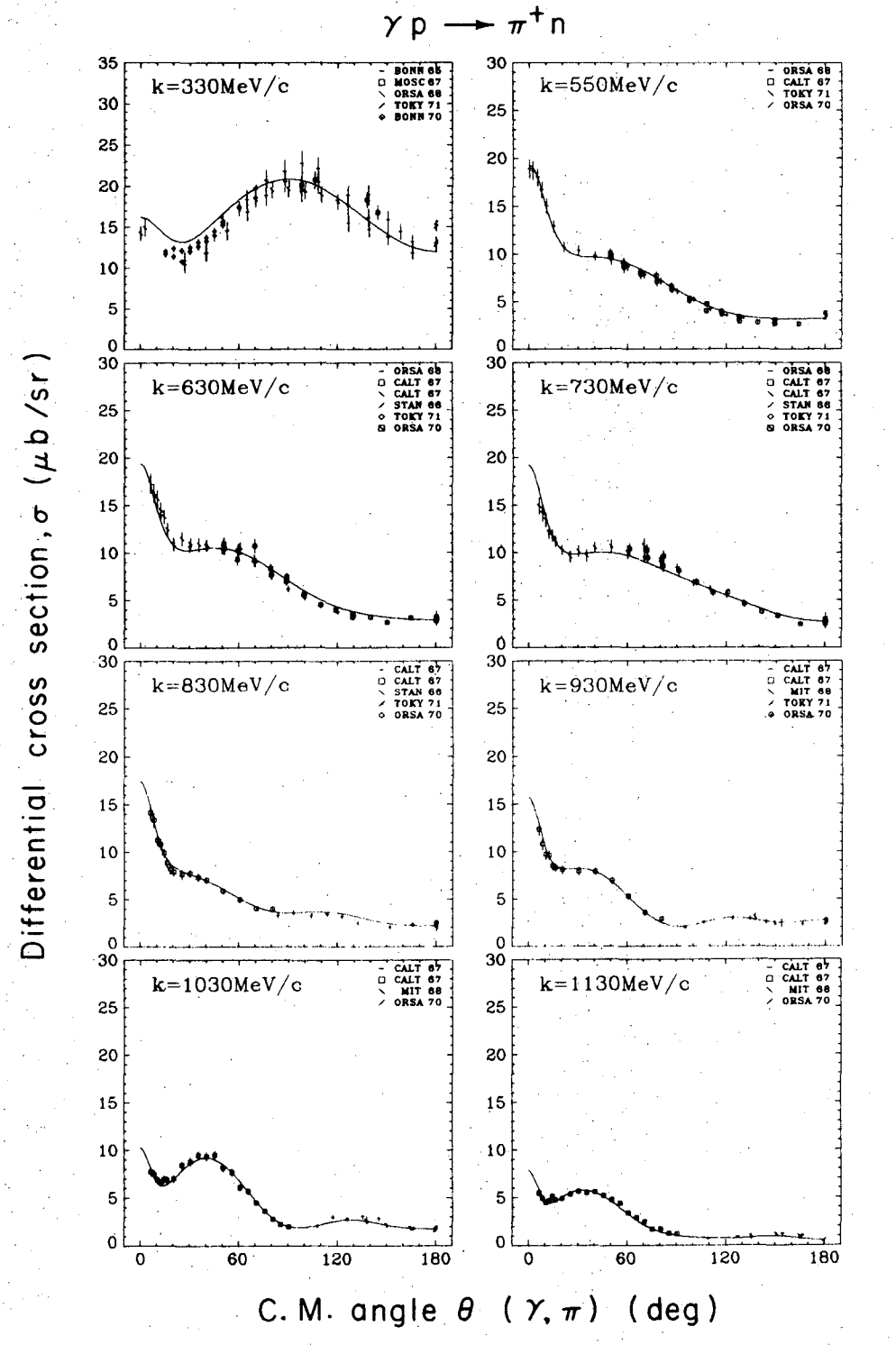
γ p ⟶ π⁺ n
k=330MeV/c
BONN 65
MOSC 67
ORSA 68
TOKY 71
BONN 70
k=550MeV/c
ORSA 68
CALT 67
TOKY 71
ORSA 70
k=630MeV/c
ORSA 68
CALT 67
CALT 67
STAN 66
TOKY 71
ORSA 70
k=730MeV/c
ORSA 68
CALT 67
CALT 67
STAN 66
TOKY 71
ORSA 70
k=830MeV/c
CALT 67
CALT 67
STAN 66
TOKY 71
ORSA 70
k=930MeV/c
CALT 67
CALT 67
MIT 68
TOKY 71
ORSA 70
k=1030MeV/c
CALT 67
CALT 67
MIT 68
ORSA 70
k=1130MeV/c
CALT 67
CALT 67
MIT 68
ORSA 70
Differential cross section, σ (μb/sr)
C. M. angle θ (γ, π) (deg)
0
60
120
180
XBL737-3304

Fig. 2

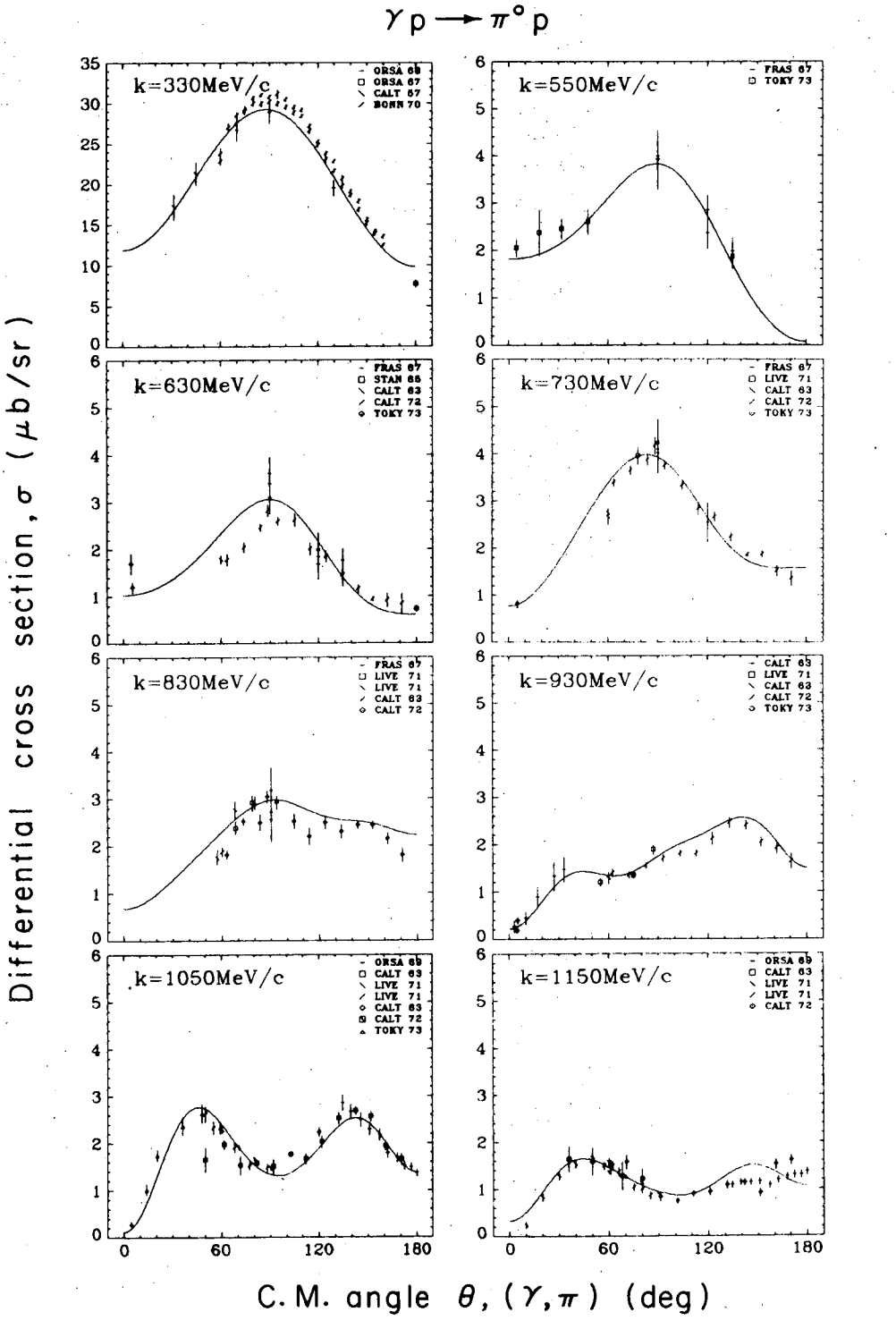

XBL737-3305

Fig. 3

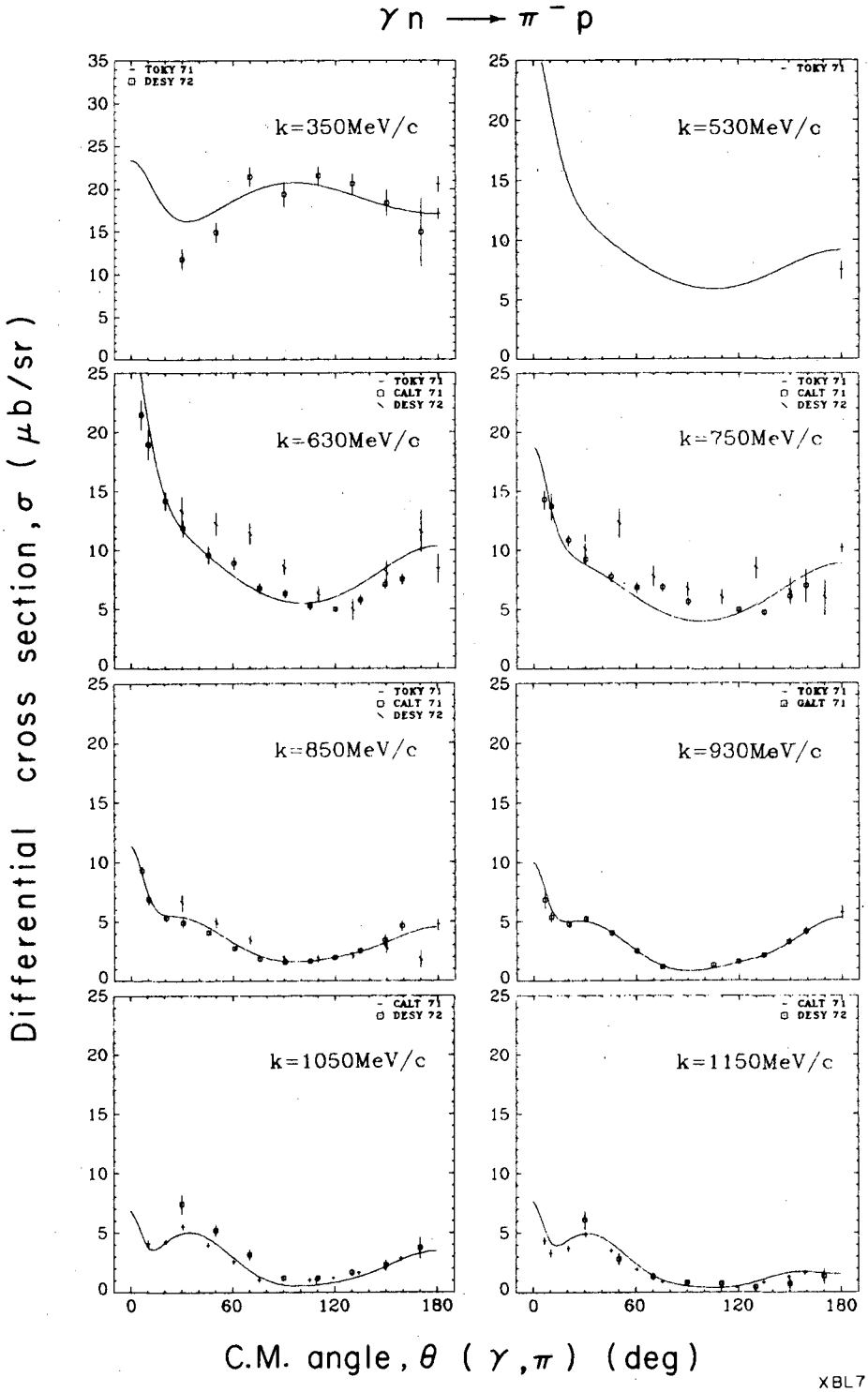
γ n ⟶ π⁻ p
TOKY 71
DESY 72
k=350MeV/c
k=530MeV/c
CALT 71
k=630MeV/c
k=750MeV/c
k=850MeV/c
k=930MeV/c
k=1050MeV/c
k=1150MeV/c
Differential cross section, σ (μb/sr)
C.M. angle, θ (γ, π) (deg)
XBL737-3300

Fig. 4

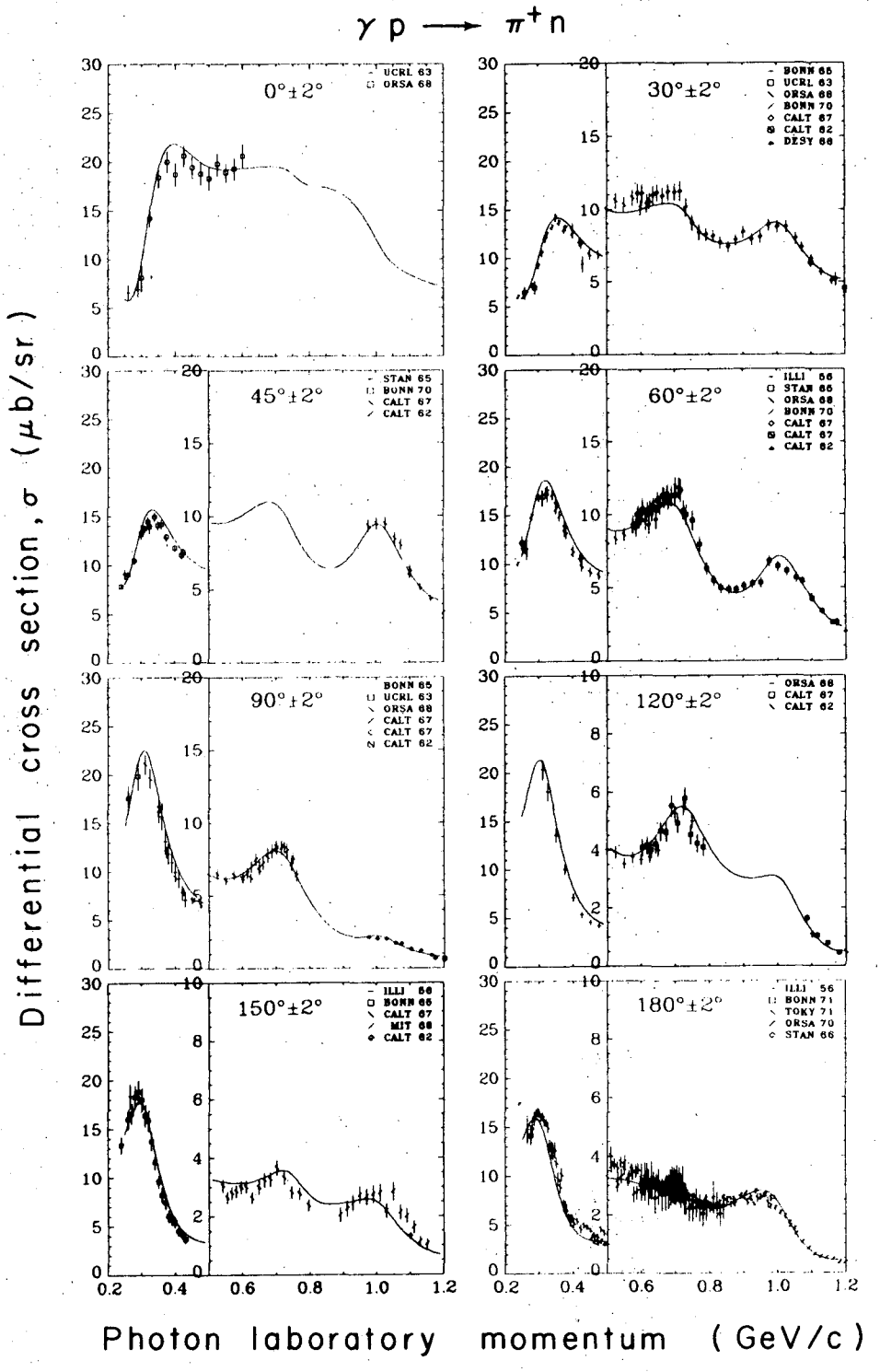
γ p ⟶ π⁺ n
0°±2°
UCRL 63
ORSA 68
30°±2°
BONN 65
UCRL 63
ORSA 68
BONN 70
CALT 67
CALT 62
DESY 66
45°±2°
STAN 65
BONN 70
CALT 67
CALT 62
60°±2°
ILLI 66
STAN 65
ORSA 68
BONN 70
CALT 67
CALT 67
CALT 62
90°±2°
BONN 65
UCRL 63
ORSA 68
CALT 67
CALT 67
CALT 62
120°±2°
ORSA 68
CALT 67
CALT 62
150°±2°
ILLI 66
BONN 65
CALT 67
MIT 68
CALT 62
180°±2°
ILLI 56
BONN 71
TOKY 71
ORSA 70
STAN 66
Differential cross section, σ (μb/sr)
Photon laboratory momentum (GeV/c)
XBL737-3296

Fig. 5

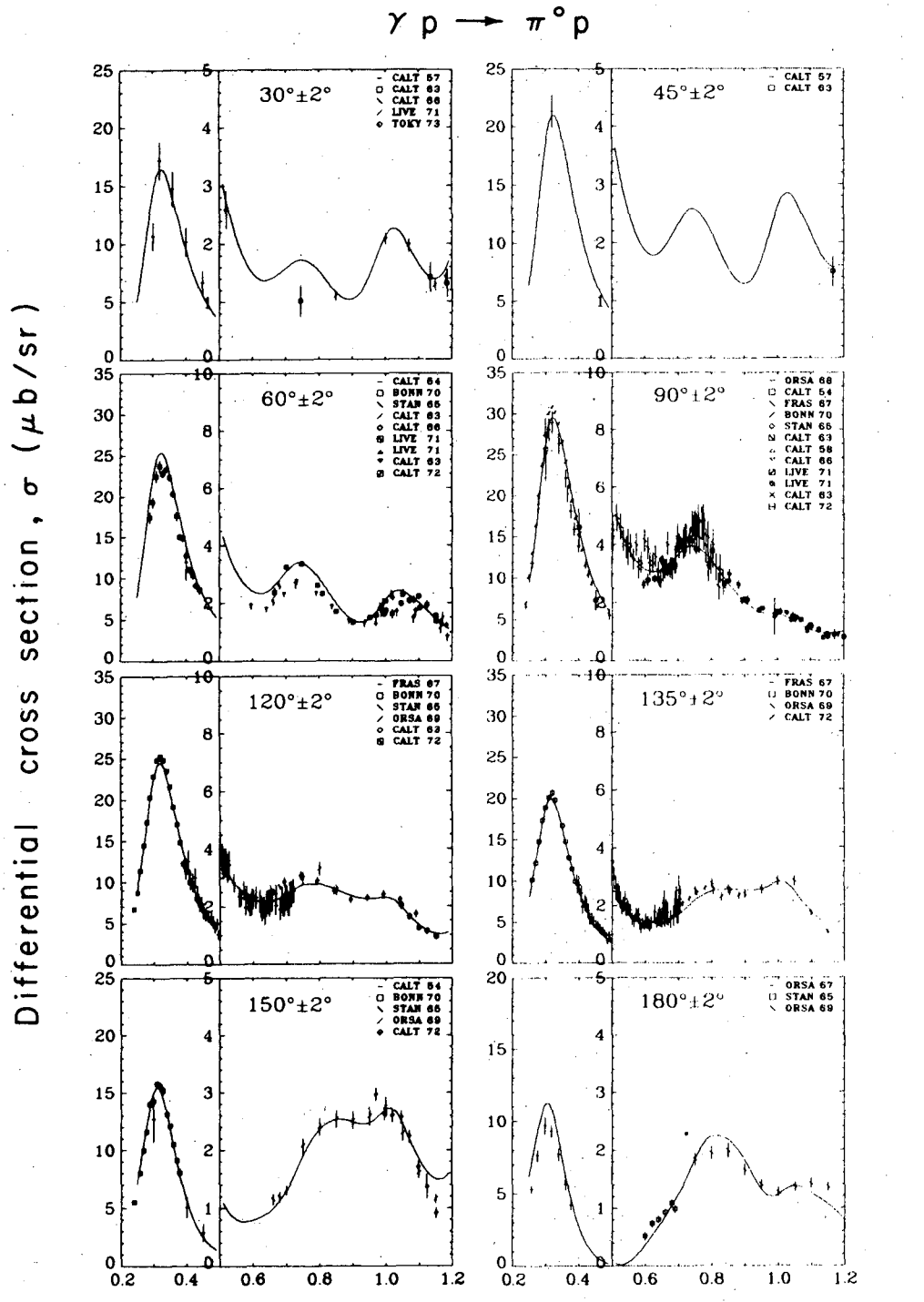
γ p → π° p
30°±2°
45°±2°
60°±2°
90°±2°
120°±2°
135°±2°
150°±2°
180°±2°
Differential cross section, σ (μb/sr)
Photon laboratory momentum (GeV/c)
XBL737-3298

Fig. 6

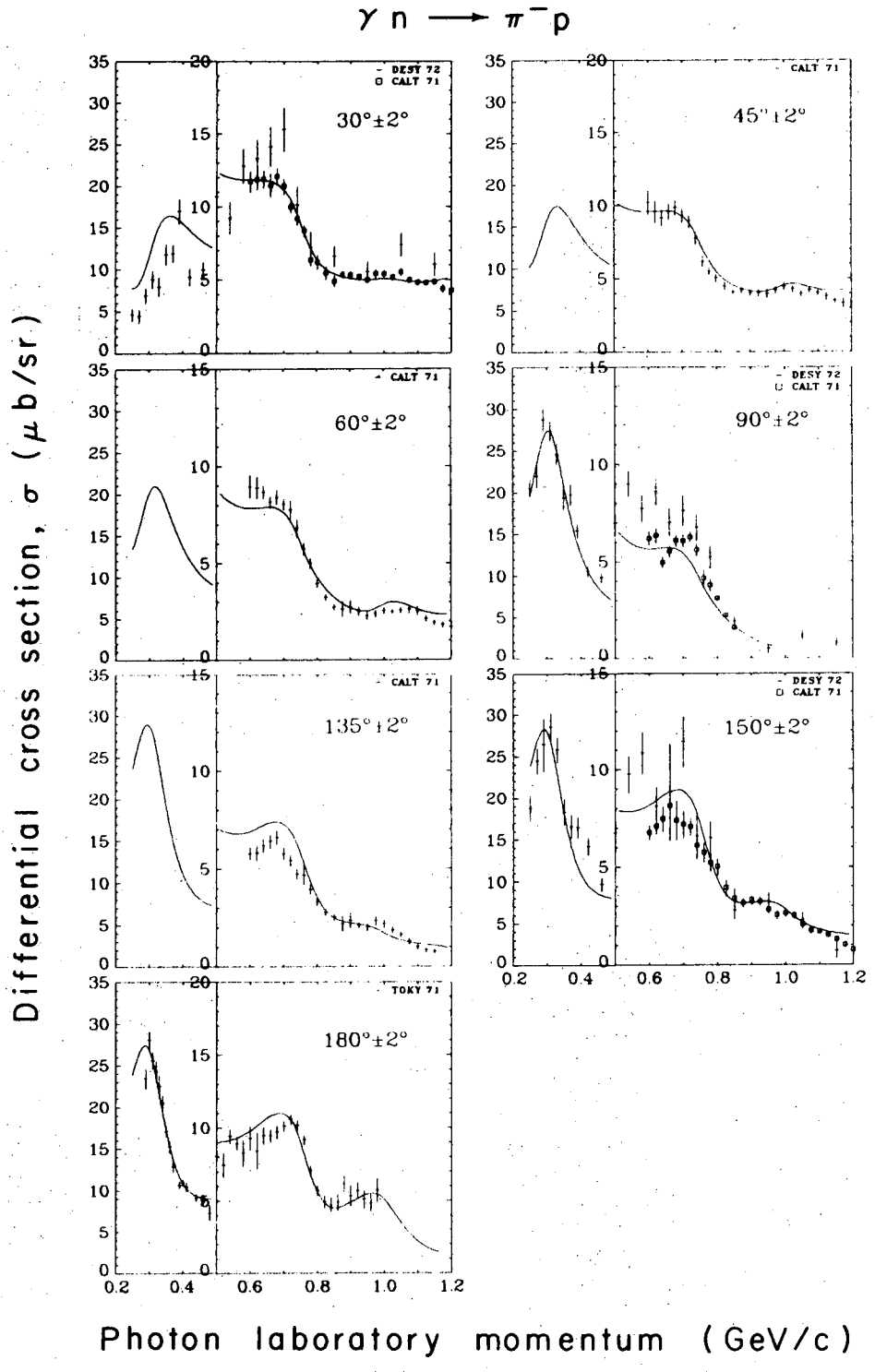

XBL737-3297

Fig. 7

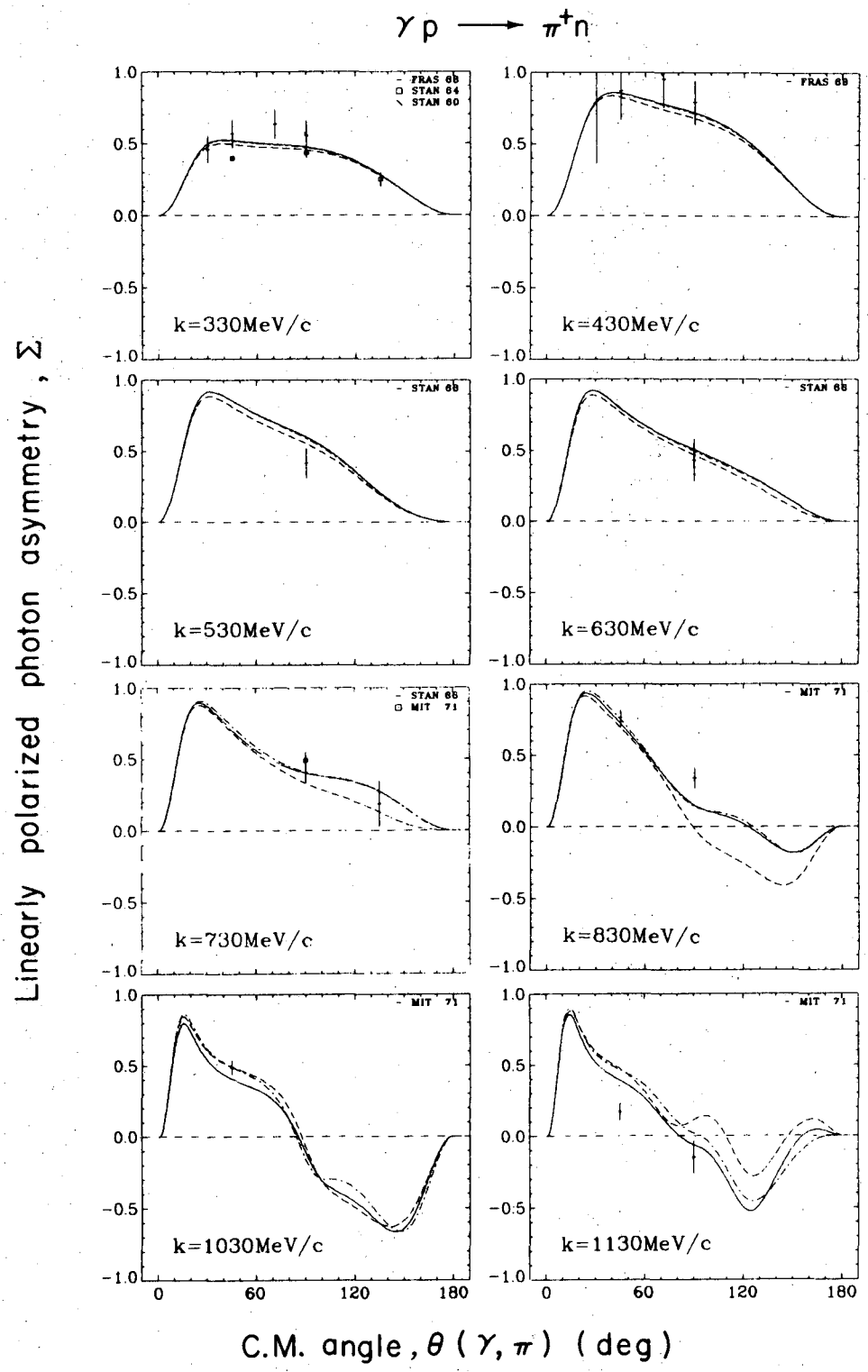

XBL737 - 3303

Fig. 8

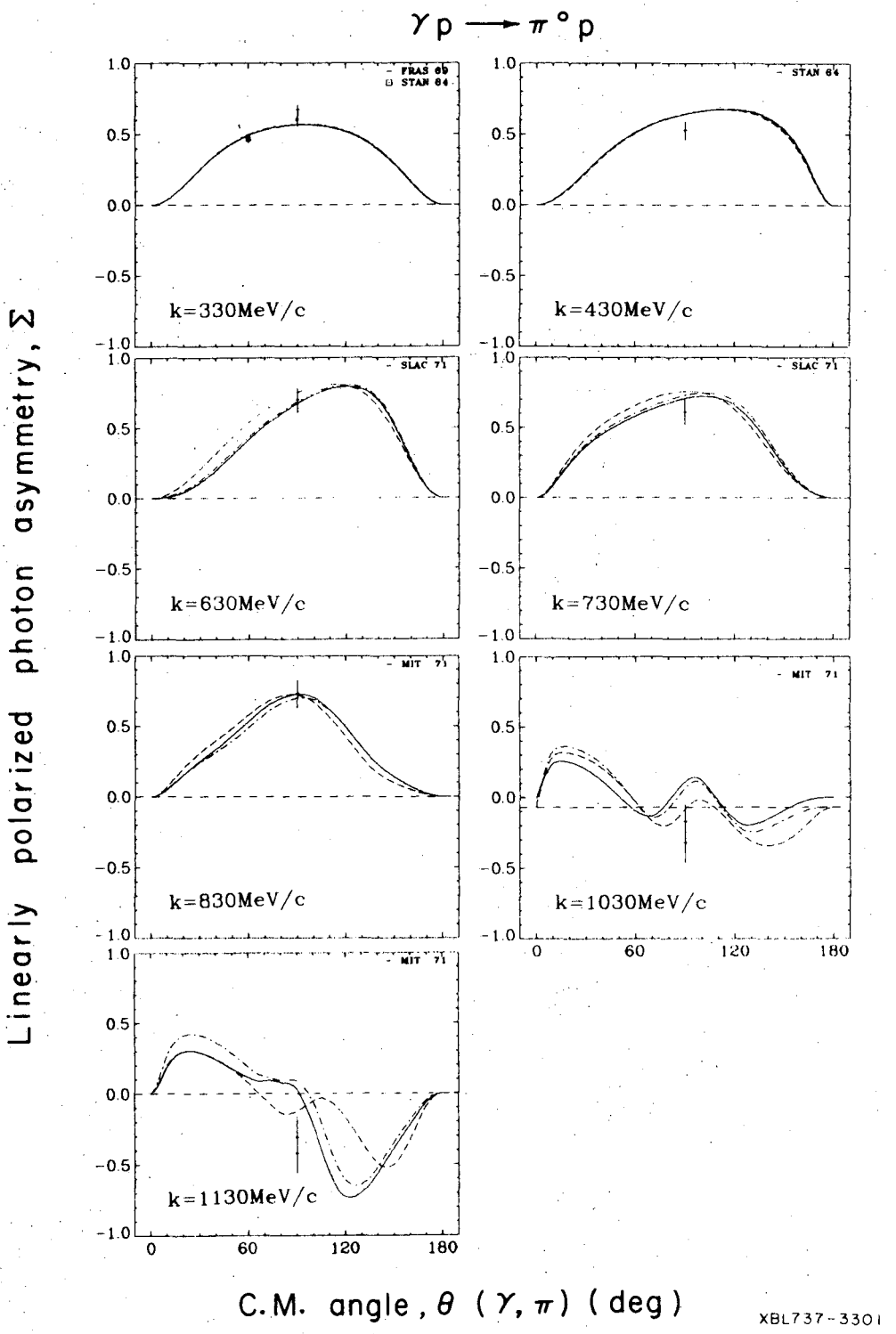
γp → π°p
Linearly polarized photon asymmetry, Σ
C.M. angle, θ (γ, π) (deg)
FRAS 66
STAN 64
SLAC 71
MIT 71
k=330MeV/c
k=430MeV/c
k=630MeV/c
k=730MeV/c
k=830MeV/c
k=1030MeV/c
k=1130MeV/c
XBL737-3301

Fig. 9

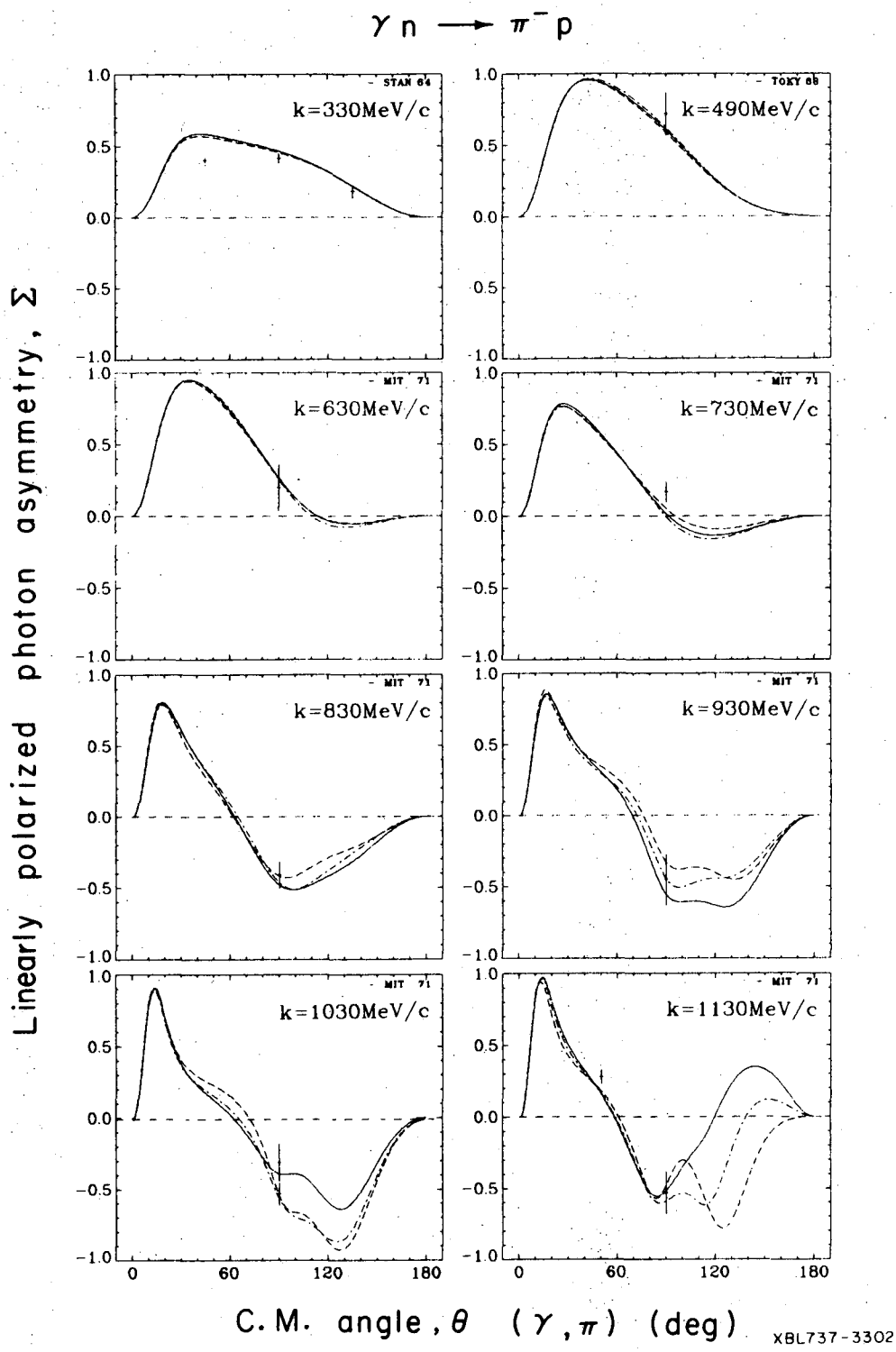
γ n ⟶ π⁻ p
k=330MeV/c
k=490MeV/c
k=630MeV/c
k=730MeV/c
k=830MeV/c
k=930MeV/c
k=1030MeV/c
k=1130MeV/c
Linearly polarized photon asymmetry, Σ
C.M. angle, θ (γ,π) (deg)
XBL737-3302

Fig. 10

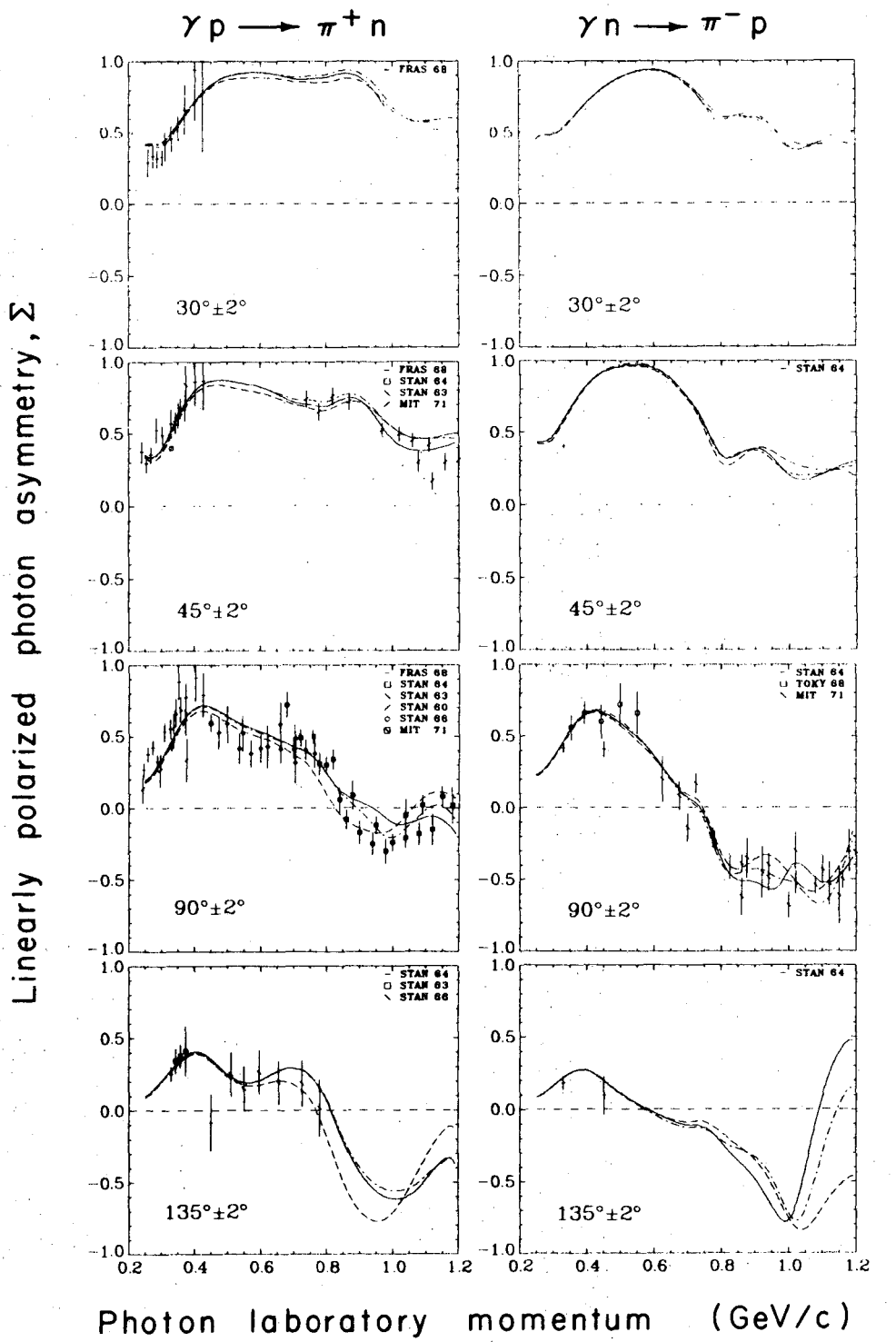

XBL 737-3299

Fig. 11

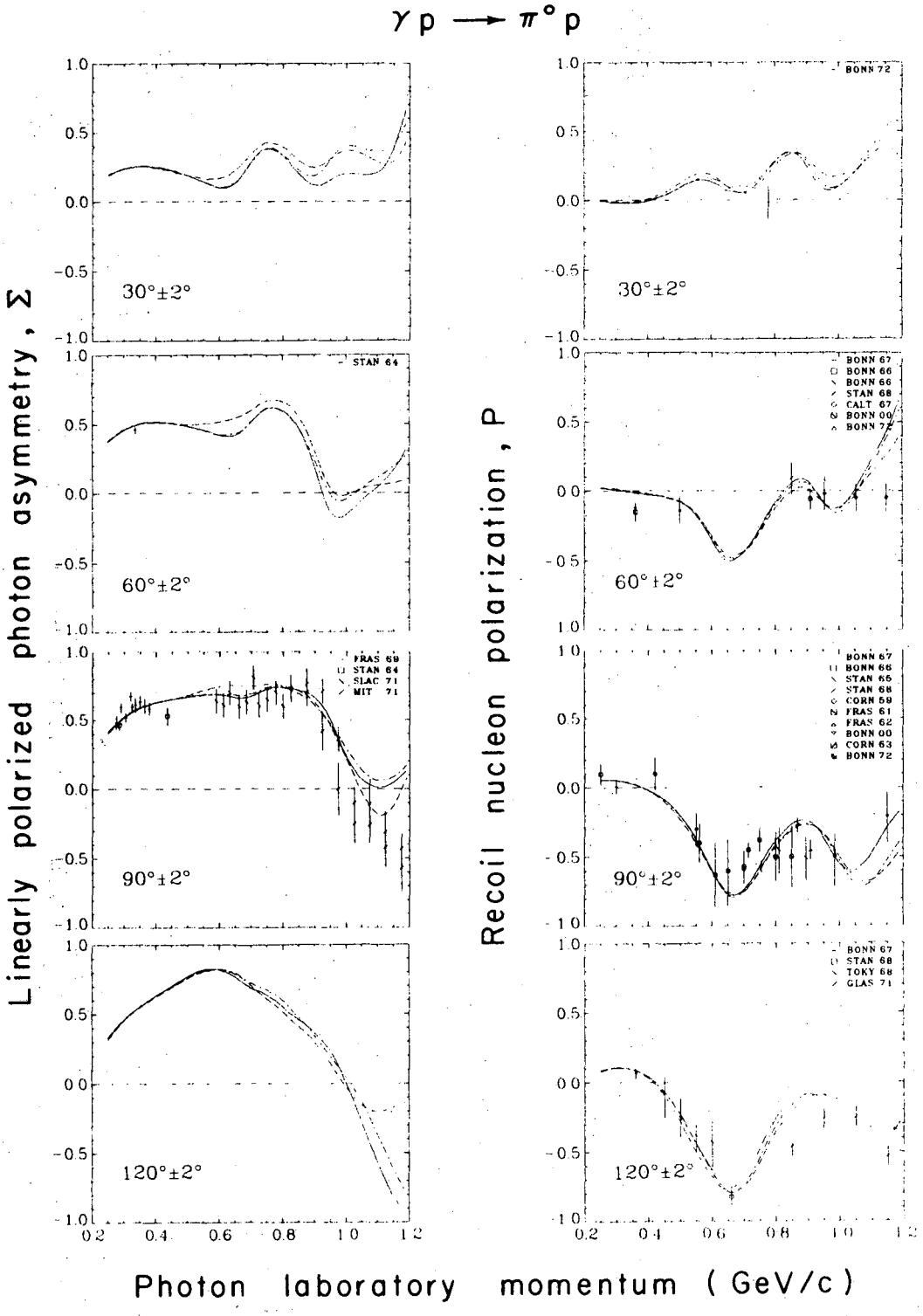
γ p → π° p
Linearly polarized photon asymmetry, Σ
Recoil nucleon polarization, P
30°±2°
60°±2°
90°±2°
120°±2°
STAN 64
FRAS 69
STAN 64
SLAC 71
MIT 71
BONN 72
BONN 67
BONN 66
BONN 66
STAN 68
CALT 67
BONN 00
BONN 72
BONN 67
BONN 66
STAN 65
STAN 68
CORN 59
FRAS 61
FRAS 62
BONN 00
CORN 63
BONN 72
BONN 67
STAN 68
TOKY 68
GLAS 71
Photon laboratory momentum (GeV/c)
XBL 737-3295

Fig. 12

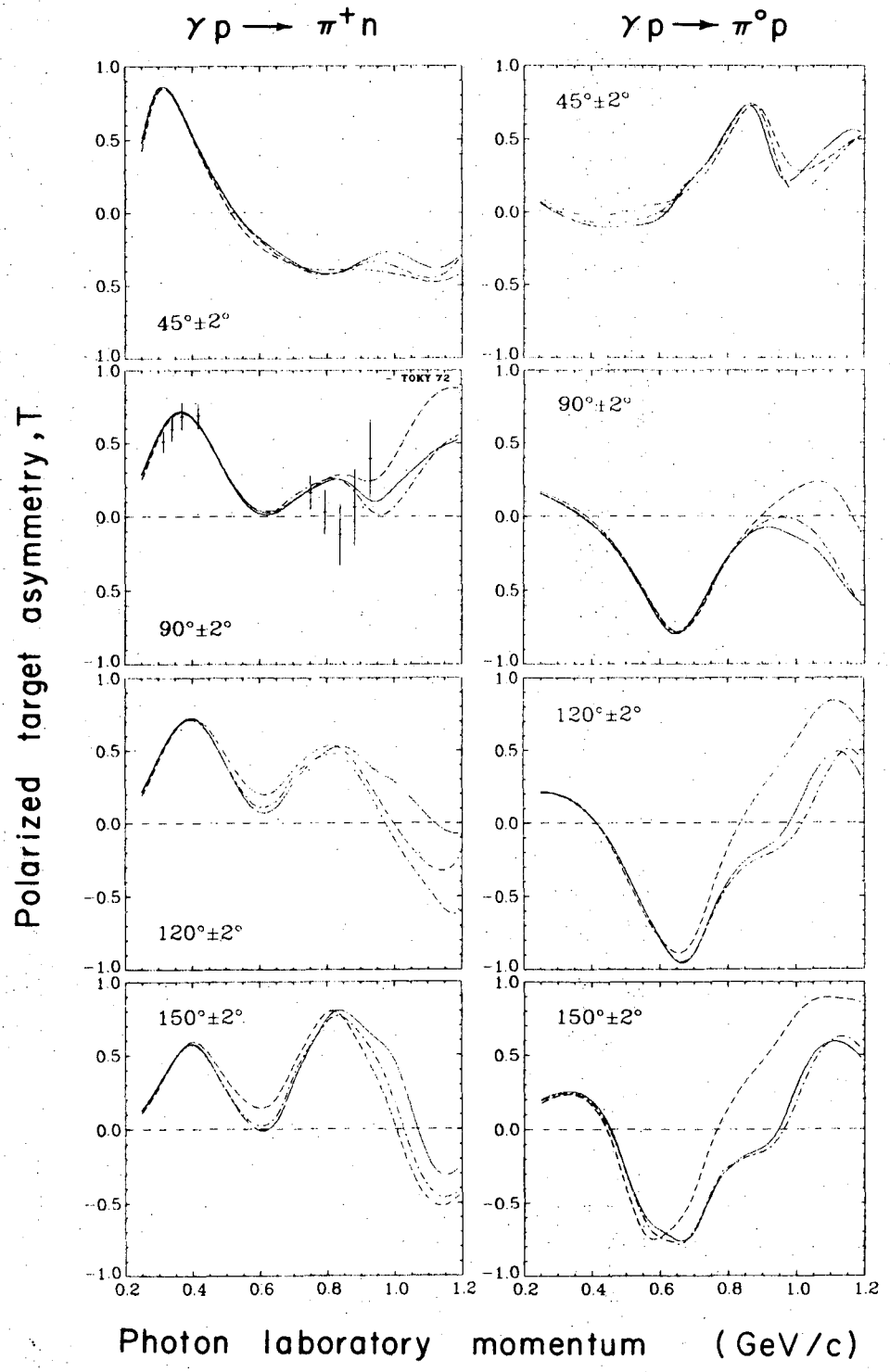

XBL737-3306

Fig. 13

TECHNICAL INFORMATION DIVISION
LAWRENCE BERKELEY LABORATORY
UNIVERSITY OF CALIFORNIA
BERKELEY, CALIFORNIA 94720